**Master Thesis, Department of Geosciences**

# Reservoir quality, diagenesis and depositional environments of Early Jurassic sandstone reservoirs located in the northern North Sea, Knarr area

A sedimentological, mineralogical and petrographic approach

**Christopher Kjølstad**

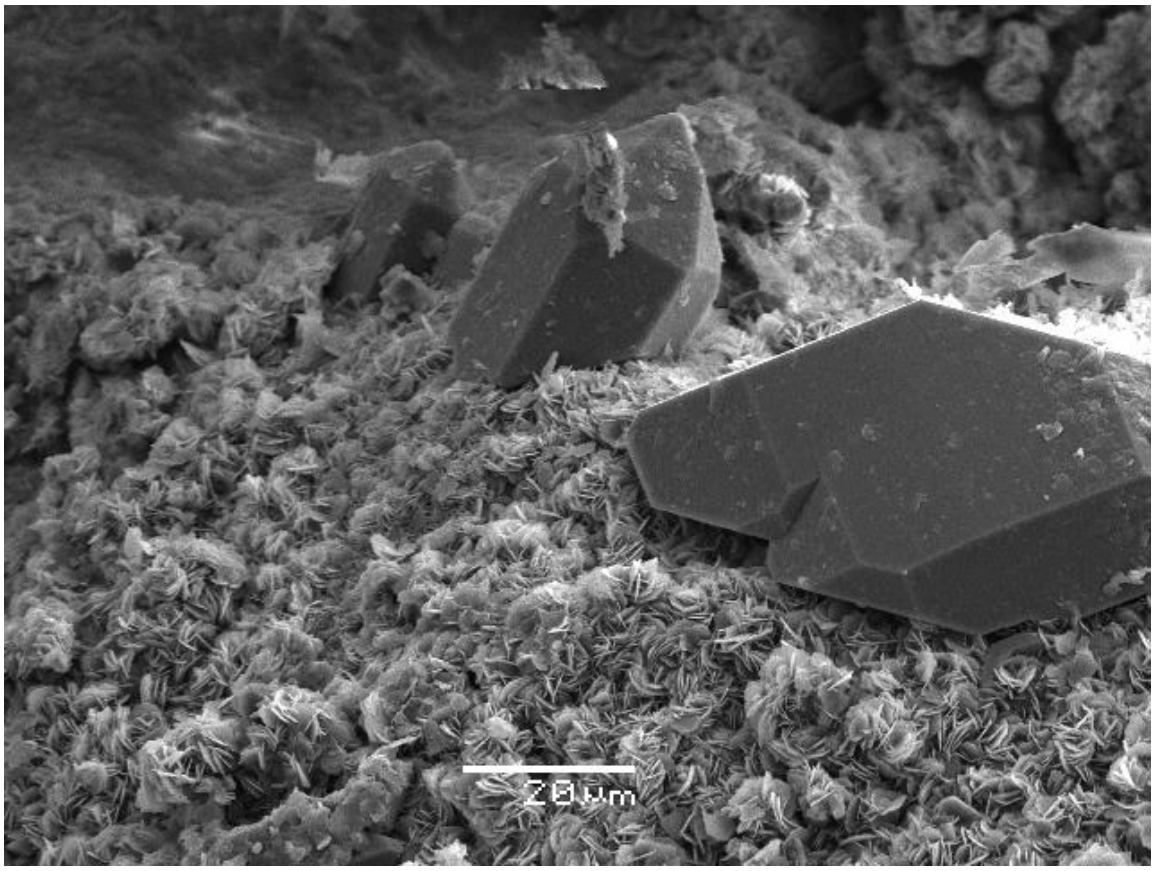


UNIVERSITY OF OSLO

FACULTY OF MATHEMATICS AND NATURAL SCIENCES

# Reservoir quality, diagenesis and depositional environments of Early Jurassic sandstone reservoirs located in the northern North Sea, Knarr area

A sedimentological, mineralogical and petrographic approach

Christopher Kjølstad

Master Thesis in Geosciences

Discipline: Sedimentology

Department of Geosciences

Faculty of Mathematics and Natural Sciences

University of Oslo

02.06.2014

# *Acknowledgements*

I would like to specially thank my supervisors Associate Professor Jens Jahren and Dr. Audun Vestheim Kjemeperud for guidance and support throughout the master thesis. Thanks to Knut Bjørlykke and Johan Petter Nystuen for good and valuable comments and feedback. Thanks to fellow students Jenny Torsæter and Sanne Lorentzen for cooperation, feedback and discussion.

Several days were used in the SEM lab; thank you Berit Løken for guidance and support.

A special thanks to friends for reviewing the English language, even if you didn't understand all the technical terms, Margrethe Lia, Andreas Nebdal, Thomas Ness Eriksen, Philip Øverby and Jon Martin Trondalen.

Special thanks to BG and Idemitsu Petroleum Norge for supplying of data and samples to the project.

Thanks to room 210 for discussions, support and just being awesome.

Last but not least I would like to thank my family: Grete, Svein-Erik, Maria, Sophie and my wife Zsófia Kjølstad for encouragement and support through the whole thesis.

And thank you God for Your support and peace.

2014

Christopher Kjølstad

# *Abstract*

The Early Jurassic Cook sandstones from the northern North Sea, Knarr area have been investigated to provide information of the reservoir quality. Four cored wells, 34/3-2 S, 34/3-1 S, 34/3-3 S and 34/5-1 S, have been analyzed and observed in the manner of sedimentology, mineralogy and petrography. The main focus has been on the relation between the formation of the precursor of chlorite coating and the depositional environment.

Four Facies associations have been interpreted from the five sandstones, C1, C2, C3, C4 and C5, in the cored intervals from the four wells; Nearshore delta slope deposits, Tidal compound dunes, Tidal bars and Offshore deposits.

All the deeply buried sandstones in the Knarr area, which is situated around 3500 m bsf show anomalously high porosities. There are observed minor amounts of quartz cement, due to retardation by the chlorite coating.

Chlorite, kaolinite and illite are the three dominant clay minerals in the sediments. Much of the fine-grained constituents were deposited as detrital mud drapes and subaquatic infiltrated mud clogs. The detrital clay minerals also formed the precursor (i.g. berthierine) of the iron rich chlorite coating (i.g. chamosite).

The Cook sandstones in the Knarr area are interpreted to have been deposited in a pro delta-delta slope environment as tidal bars and compound dunes. The sandstones have experienced reworking in different stages by the tidal dominated environment.

Subaerial exposure of the tidal bars and compound dunes are interpreted to have created a vadose zone. The formations of the precursor to the chlorite coating on the detrital grains are suggested to have occurred in a vadose zone. Subaquatic infiltration of fine-grained constituents has also been suggested as a reason for the formation of the precursor. The origin of the precursor is of great importance because the precursor is the link between the chlorite coating and the depositional environment.

# *Table of contents*

# *Chapter 1 - Introduction*

## 1.1 Introduction

This master thesis is part of a collaboration project between the University of Oslo, IPN (Idemitsu Petroleum Norway) and BG Norway. Two master students, Torsæter (in press) and Kjølstad (this thesis), focus on the reservoir characteristics from different perspectives. Torsæter (in press) focuses on the reservoir characteristics from a petrophysicist point of view. This master thesis has the purpose to understand the reservoir characteristics with respect to depositional environment, porosity, coating and cement in deeply buried, Lower Jurassic, Cook sandstone.

The oil field Knarr is situated in the northern North Sea, block 34/3. The production license, PL 373 S, was awarded to BG in 2006. The production is expected to start in May 2014 (NPD, 2013b).

In this study of deeply buried sandstones found down to 3600 meters below sea floor, it is important to understand how the porosity is reduced. The primary cause for porosity reduction is quartz cementation in deeply buried sandstones containing a great amount of quartz. Dissolution of quartz occurs mainly at stylolites, but can also be dissolved by a grain-to-grain contact, as well as released in a chemical transition from e.g. K-feldspar to Kaolinite. The dissolved quartz will start to precipitate on quartz grains with a free surface. However coating of the detrital grains can retard cementation of quartz (Walderhaug, 1996).

## 1.2 Purpose and method

The main purpose of this thesis is to provide sufficient information of the relation between depositional environment and the development of chlorite coating in the deeply buried sandstones. The reason for this is to understand the reservoir quality in the Knarr area. Four cores (34/3-2 S, 34/3-3 S, 34/3-1 S and 34/5-1 S) have been studied through the methods of sedimentological core description, point counting, scanning electron microscopy (SEM) and x-ray diffraction (XRD).

## 1.3 The study area

The study area is located in Tampen area in the northern North Sea in block 34/3, about 120 km from the west coast of Norway (Figure 1.3.1). The water depth is about 400

meters and the depth of the reservoir is located around 3500 meters bsf. The Cook Formation is one out of five Formations in the Dunlin Group. The Formation ranges from earliest to youngest in this order: Nansen, Amundsen, Johansen, Cook and Drake. Cook Formation consists of five sandstones in the study area. For simplicity the sandstones are referred to as C1, C2, C3, C4 and C5, where C1 is the deepest and C5 the most shallow.

The North Sea is a good example of a development of a rift system due to thinning of the lithosphere. The area was tectonically active for a long time before the Jurassic sandstone was deposited. Badley et al. (1988) suggest that the earliest rifting episode of importance for this area occurred during the late Permian to early Triassic. There have been three major rifting episodes in the North Sea (Glennie and Underhill, 1998). The late Permian to early Triassic episode of rifting and subsidence had not reached equilibrium before the next episode took place (BADLEY et al., 1988, Gabrielsen et al., 1990) (See table 2.2.1).

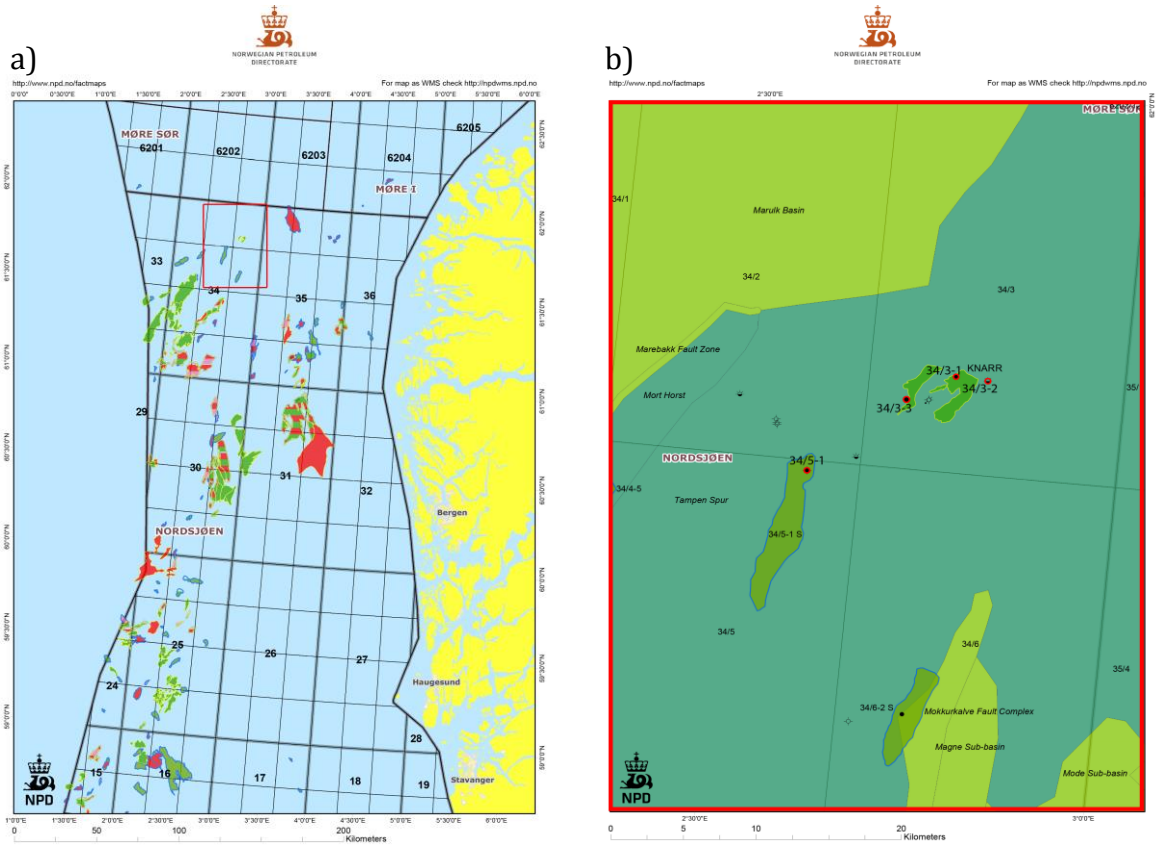


*Figure. 1.3.1. a) Northern North Sea*
*b) Zoom of the Knarr field, including the selected wells in red.*
*Source: (NPD, 2013a)*

# *Chapter 2 – Geological background of the northern North Sea*

## 2.1 Introduction

The northern North Sea is a prominent area for hydrocarbon exploration. The excellent Late Jurassic Kimmeridge Clay Formation is the primary source rock in the area. The reservoir rocks are thick widespread sandstone units containing good permeability and porosity, in an area that experienced minor uplift and erosion in the Early to Middle Jurassic. These sandstones experienced the Late Jurassic to Early cretaceous extensional tectonics, which resulted in tilted fault block traps where the hydrocarbons could migrate into (Hay, 1978). In total, a recoverable resource has been estimated in the order of $9200*10^6$ $Sm^3$ of oil-equivalents (NPD, 2012). Most of the hydrocarbons located in the northern North Sea are found in the Early – Middle Jurassic sandstones (Nøttvedt and Johannessen, 2007b), and about 70 % of the hydrocarbons are found in fault block traps (Spencer and Larsen, 1990).

## 2.2 Structural setting

The geological history of the North Sea is quite complex. It is suggested that as much as three main rifting stages and five intra plate deformation stages have occurred. (Glennie and Underhill, 1998). See Table 2.2.1.

| Nr | Event | Age |
|---|---|---|
| 1 | Precambrian events | Precambrian |
| 2 | The Caledonian plate cycle | Ordovician – Devonian |
| 3 | The Variscan plate cycle | Devonian - Carboniferous |
| **4** | **Permo-Triassic rifting and thermal subsidence** | **Perm – Triassic** |
| **5** | **Middle Jurassic domal uplift** | **Jurassic** |
| **6** | **Late Jurassic to early cretaceous extensional tectonics** | **Jurassic – Cretaceous** |
| 7 | Development of the Iceland hot spot and North Atlantic rifting | Cretaceous |
| 8 | Tectonic inversion of Mesozoic basin | Cretaceous |

*Table 2.2.1. Structural events in the North Sea*
*Source: (Glennie and Underhill, 1998)*

When introducing these events (Table 2.2.1), it is important to take a look at the big scale geology, because the rifting in the northern North Sea is related to the structural

geology on a global scale as well. The structural development of interest for this thesis is the fourth to sixth stage in Table 2.2.1. The fourth stage was the start of what today is known as the Central and Viking Graben (Glennie and Underhill, 1998).

The Viking Graben is a part of a triple junction (Figure 2.2.2), together with the Central Graben and Moray Firth Graben. The rifting started in the south and propagated up north. The trigger for the rifting was thinning of the lithosphere beneath the North Sea due to a mantle head plume in stage five (Glennie and Underhill, 1998). The orientation of the rift system (stage six) was east–west and followed the old Perm – Triassic rift (Table 2.2.1) along the Norwegian shelf (Nøttvedt and Johannessen, 2007a). The crustal failure of the Late Permian into Early Triassic opened up for the Later Jurassic, Cretaceous and Early Cenozoic time to separate the super continent of Pangea from each other. The subsidence after the Perm-Triassic rifting started a complex rift system in a large area at the time of separation of Pangea, from Triassic to Cretaceous (Ziegler, 1982). Figure 2.2.1 shows the Triassic rift system of the Arctic-North Atlantic area.

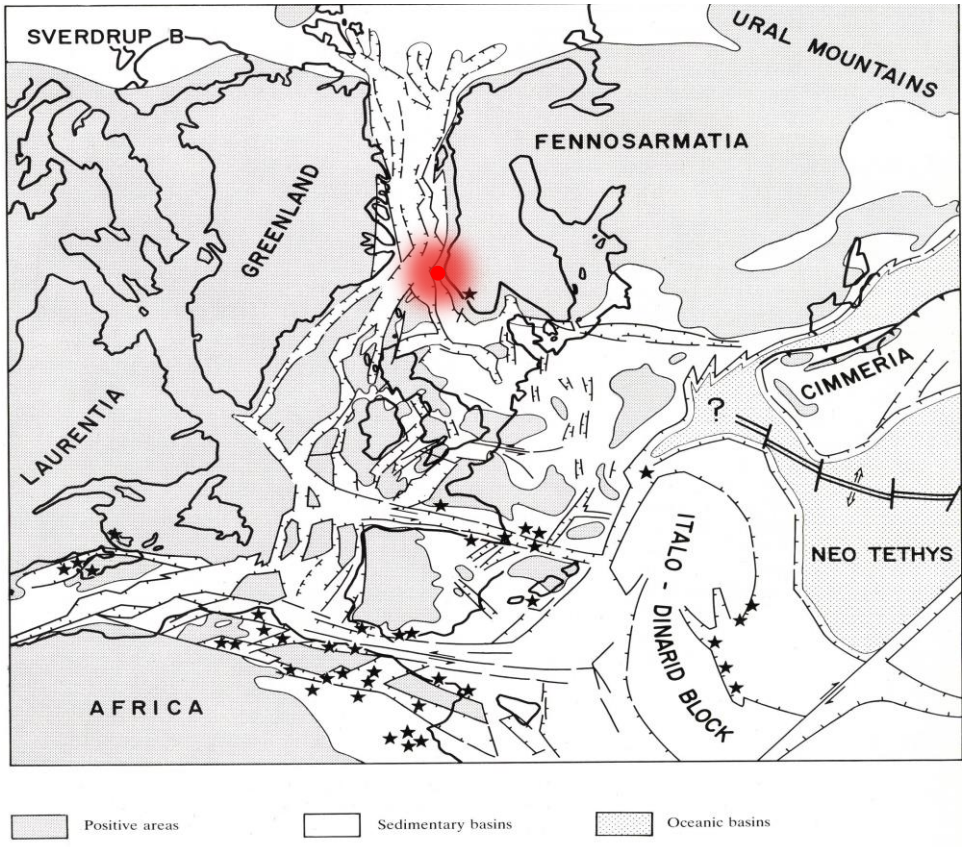

*Figure 2.2.1. The Triassic rift system of the Arctic-North Atlantic area. It is a distinct orientation in the separation of Pangea, North - South between Africa and Laurentia, and East – West between Greenland and Fennosarmatia. The red circle is the study area. After (Ziegler, 1982).*

The Central Graben and the Viking Graben are important geological structures that evolved in the Late Jurassic time (Nøttvedt and Johannessen, 2007a). Today the Horda platform and the Shetland platform, have a structural low in between the structural high platforms (Figure 2.2.3). In this structural low, the Knarr field is located.

The thermal subsidence that followed the early rifting episode in Triassic – Early Jurassic, trapped all the sediments produced for the Brent and Dunlin Group. The overlain Viking group was deposited in the subsidence after the sixth stage rift, in Middle Jurassic – Early Cretaceous (BADLEY et al., 1988) (Table 2.2.1). Throughout the sixth stage, the formation of rotated fault-blocks and structural traps developed (Glennie and Underhill, 1998).

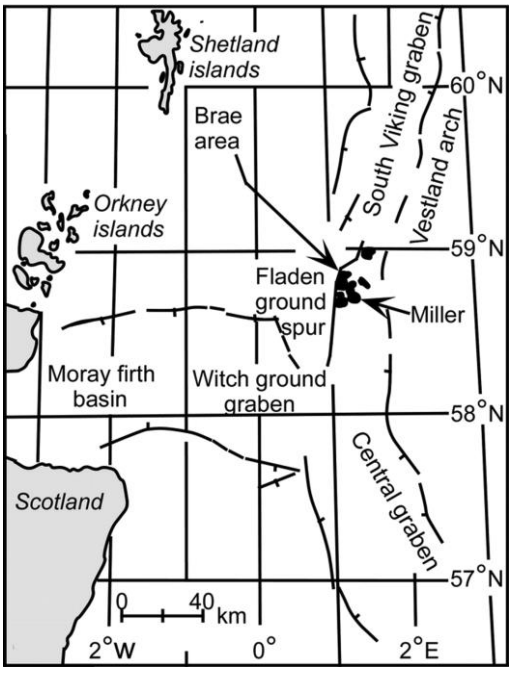


*Figure 2.2.2: Triple junction of the three rift arms: Central-, Viking- and Moray Firth Graben. (Marchand et al., 2001)*

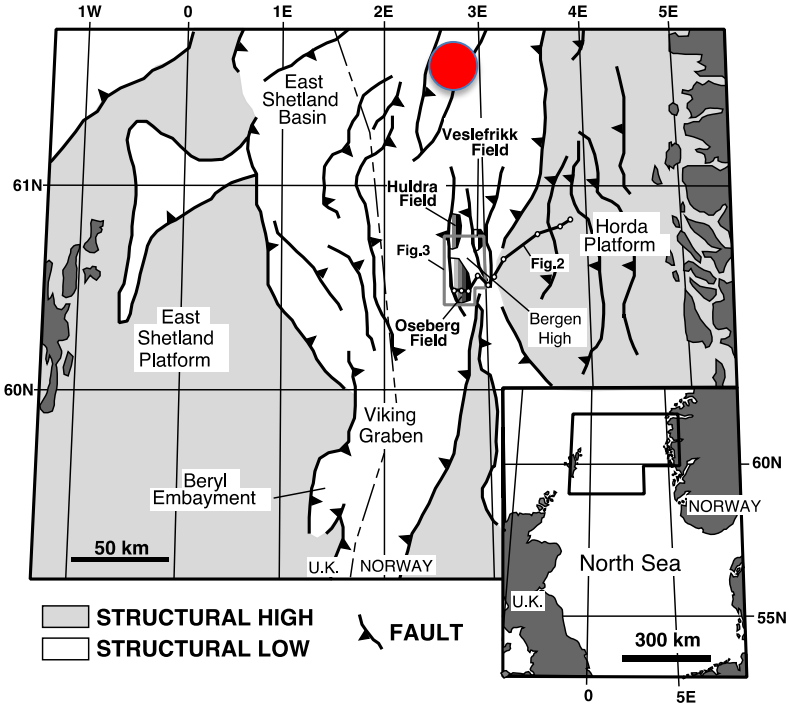


*Figure 2.2.3: Location of the Horda Platform and the Shetland platform. The red circle is the study area. (Muto and Steel, 1997)*

## 2.3 Stratigraphical Framework

A steady sea level rise established marine conditions in the transition from Late Triassic to Early Jurassic. Erosion of the Early Jurassic sediments was a result of the volcanic updoming in the beginning of the Middle Jurassic. From the updomed areas, deltaic systems started to build out. The huge Brent delta was deposited in the Middle Jurassic. Into the late Middle Jurassic, the updomed areas collapsed and the marine conditions entered due to rise of the sea level. Throughout the Late Jurassic time structural evolution of rotated fault blocks developed. The structural rifting and rotating of fault blocks resulted in erosion, and periods of lack of deposition created an unconformity (BCU – Base Cretaceous Unconformity). The erosion and lack of deposition were different from locality to locality, both in time and magnitude (Vollset and Doré, 1984). Kyrkjebø et al. (2004) suggest that the term; Northern North Sea Unconformity complex, is used due to the several stages and complexity of the unconformity.

In the early Jurassic, there was a distinct change in climate from dry to humid. This increased the transport of eroded and weathered sediments into the sea and deposited several of the most important reservoir rocks for hydrocarbons on the Norwegian continental shelf (Nøttvedt and Johannessen, 2007b). About 50% of the hydrocarbons on the Norwegian Continental Shelf are situated in Jurassic sediments (Underhill, 1998).

The Cook Formation within the Dunlin Group is well documented, but the diversity of opinions of the Formation is great. Core and well data of the Cook Formation are interpreted from several oil fields (Statfjord, Gullfaks, Oseberg, Veslefrikk, Valemon and The Kvitebjørn Field (NPD, 2014a)), but the depositional environment differs between the areas where the Cook Formation is a reservoir (e.g. Vollset and Doré, 1984, Livbjerg and Mjøs, 1989, Folkestad et al., 2012).

## 2.4 Depositional development of the Dunlin Group and Cook Formation

The Dunlin Group was deposited when the northern North Sea was located at some 40° north of equator (Nøttvedt and Johannessen, 2007b). An epicontinental sea gave the opportunity for the sediments to extend far from the coastline (Ziegler, 1982).

An epicontinental sea is a shallow sea, generally not deeper than 200 meters. In average there is a slope gradient of 0,001 – 1°. Due to this slope gradient, the epicontinental sea is very exposed to fluctuation of relative sea level changes. If there is a drop in relative sea level, the rivers have the possibility to transport material for longer distance basinward. If there is uplift in the relative sea level, the sea has the possibility to wash over great distances landward.

*The Dunlin Group* consists of five different formations (Figure 2.4.1), the Amundsen, Johansen, Burton, Cook and Drake formations. It stretches from the Hettangian (201 Ma) to the Bajocian (170) time, in Early to Middle Jurassic.

a)

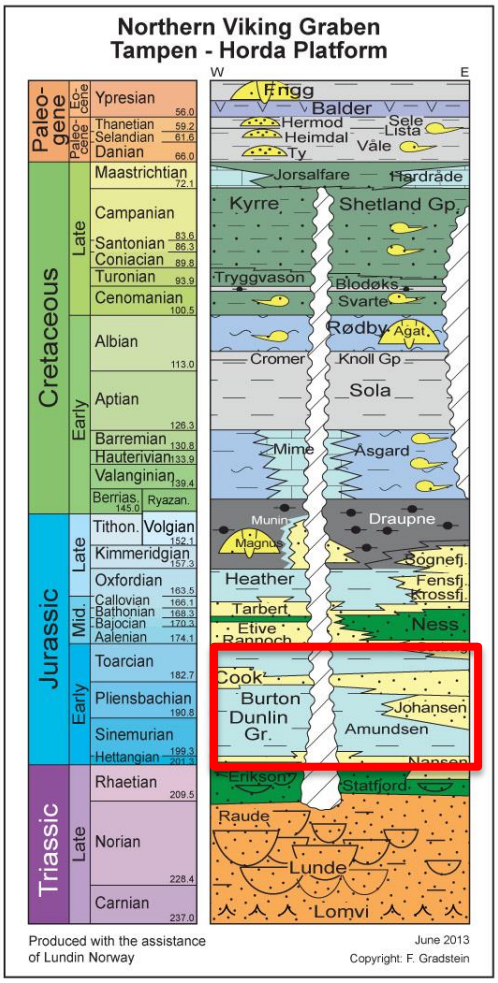


b)

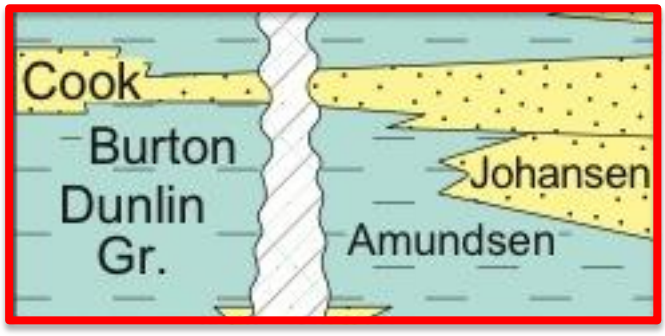


*Figure 2.4.1.*
*a) Lithostratigraphical chart of the Northern Viking Graben, from Late Triassic to Early Eocene time. The red square represents the Dunlin Group.*
*b) Lithostratigraphical chart over the Dunlin group*
*Source: (Gradstein, 2013)*

*The Amundsen* Formation stretches out into the East Shetland Basin from the Norwegian coast. The lithology is mainly light to dark gray silt and shale. In the marginal locations of the basin, there are fine to coarse, thin sandstone beds, consisting of glauconite and carbonate. The Formation is located above the Statfjord Formation in the Hegre Group. The depositional environment is interpreted as shallow marine (Vollset and Doré, 1984, Underhill, 1998).

*The Johansen Formation* is limited in distribution only to the Horda Platform. The lithology consists mostly of sandstones in sequences. The sandstone contains thin calcite cemented bands throughout the Formation. The lower most part goes from a silty claystone to a medium – fine sandstone. The middle section consists of medium sandstone, and the top consists of a medium – fine-grained sandstone. The depositional environment is interpreted as shallow marine shelf with high energy (Vollset and Doré, 1984, Marjanac and Steel, 1997, Underhill, 1998).

*The Burton Formation* is found in a wide area in the Northern North Sea except the Horda Platform. The lithology consists of claystone and shale. The color ranges from dark gray to reddish gray. The depositional environment is interpreted as a calm open marine basin, with little bioturbation (Vollset and Doré, 1984, Underhill, 1998).

*The Cook Formation* stretches out into the East Shetland Basin and on the northern part of the Horda Platform. The lithology is commonly a marine siltstone with some thin layers of claystone in between. On the Horda Platform and its western margin there are sandstones that constitute the lithology. The Formation is build up by several sequences depending on the locality (i.g. Livbjerg and Mjøs, 1989, Marjanac and Steel, 1997, Underhill, 1998, Charnock et al., 2001). The decrease in gamma ray and increase in velocity separate the sandstones from the adjacent lithology (Vollset and Doré, 1984, Livbjerg and Mjøs, 1989). The most common cement is quartz cement (Vollset and Doré, 1984). The Formation has good porosity and permeability due to chlorite coating.

The Cook formation has no impressive thickness regionally, but locally great thickness has been achieved. Figure 2.4.4 shows that where the deposition has a growth fault

beneath, the thickness is greater. This has kept the accommodation space in balance with respect to incoming sediments (Folkestad et al., 2012).

The depositional environment is interpreted as marine sand deposits in different depositional environments due to the extension of the Formation. The Statfjord Field area is interpreted to be marine shoal sands. Prograding shelf sand is interpreted for the Horda platform and its westward margins. The thinner sandstones in the Graben area are interpreted as redeposited sands from the shelf edges (Vollset and Doré, 1984, Steel, 1993, Marjanac and Steel, 1997, Underhill, 1998, Charnock et al., 2001). In the Knarr Field the upward coarsening sandstone sequences are interpreted as tidal sand deposits.

*The Drake Formation* stretches out into the East Shetland Basin. The lithology, in the lowermost part, consists of sandy calcareous claystone, and the color is gray. The upper part of the Formation consists of micaceous shale, and the color ranges from dark gray to black. Fine to coarse sandstones are found on the Horda Platform and the western margin of the Horda Platform. An upward coarsening is seen in the gamma ray log of the sandstones. The depositional environment of the Drake Formation is interpreted as delta front and prodelta. The Formation is commonly erupted by the erosion-base of the Brent Group (Vollset and Doré, 1984, Steel, 1993, Marjanac and Steel, 1997, Underhill, 1998, Charnock et al., 2001).

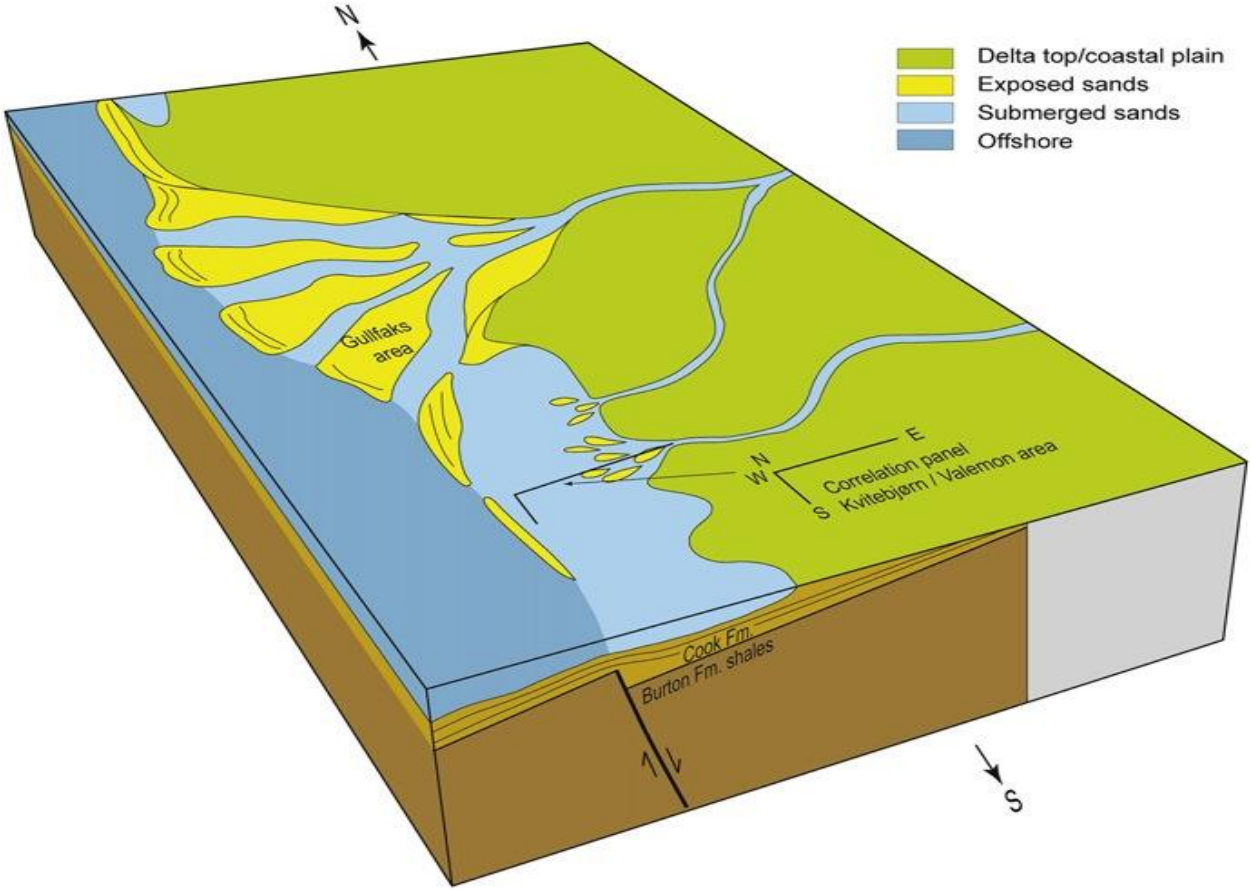


*Figure 2.4.4. Deposition of sediments above a growth fault, results in great sediment thicknesses.*
*(Folkestad et al., 2012)*

# *Chapter 3 – Theoretical background*

## 3.1 Geological influence on the quality of a reservoir

### 3.1.1 Introduction

Sandstones consist mostly of sand, but also smaller particles as silt, mud and clay. Sand grains ranging between 63 μm to 2,0 mm, constitute the framework, while silt, mud and clay forms the matrix. Classification of sandstones can be based on the mineralogy, grain size, and percentage of detrital matrix < 30μm (Dott, 1964).

The geological influence on the quality of a reservoir is both from primary depositional and post depositional processes. The porosity and permeability are closely related to the textural composition of the sediments with respect to grain size and sorting, while the post depositional processes are related to burial diagenesis. Burial diagenesis contains both mechanical and chemical compaction, which control packing and reorientation of the grains, porosity reduction, and cementation rates (Slatt, 2006).

Precipitated quartz cement strengthens the framework that holds up the overburden (Walderhaug, 1994b). Grain coatings decrease the surface area available for precipitation of quartz cement. A thin film of coating occupies the surface of the grains and the cement cannot precipitate. With increasing depth increasing pressure from the overburden may fracture uncemented grains. The quartz cement will in such cases precipitate on the fresh new surfaces and the pore space will eventually be filled up (Chuhan et al., 2002).

Permeability is like a bottleneck; it is the connection between the voids between the grains. If the fluid (viscous fluid) flow easily trough the connections, the permeability is higher than if the fluid have difficulties to flow trough. In some cases it is not the pore throats between the grains that gives the best permeability, but cracks in the rock unit, like in the Ekofisk field (Warren and Smalley, 1994).

### 3.1.2 Mechanical Compaction

Every grain that is deposited will eventually go through the process of diagenesis. The grains will be reoriented to denser packing, and crushed due to the weight of the

overburden and lithostatic pressure. This is called Mechanical Compaction (MC) and the main thermodynamic is effective stress.

The grain size is of big importance. If the grains are fine, there will be more contact points between the grains per cubic cm than coarser grains. This implies that the porosity in fine-grained sandstones is not so easily affected as coarse-grained sandstones. The initial porosity can be higher in coarse-grained sandstones, but the porosity is more rapidly lost than in small-grain sandstones (Chuhan et al., 2002, Fawad et al., 2011).

Mechanical compaction affects the sediments as long as they are loose. When cement start to precipitate on the sediments, the mechanical compaction decreases rapidly. Sediments buried deeper than 2-2,5 km (>80°C), experience little or no influence of the weight of the overburden.

The cementation will increase the velocity and density of the sediments. Figure 3.1.2.1, shows the transition zone between mechanical and chemical compaction in a schematic porosity vs. depth cross plot.

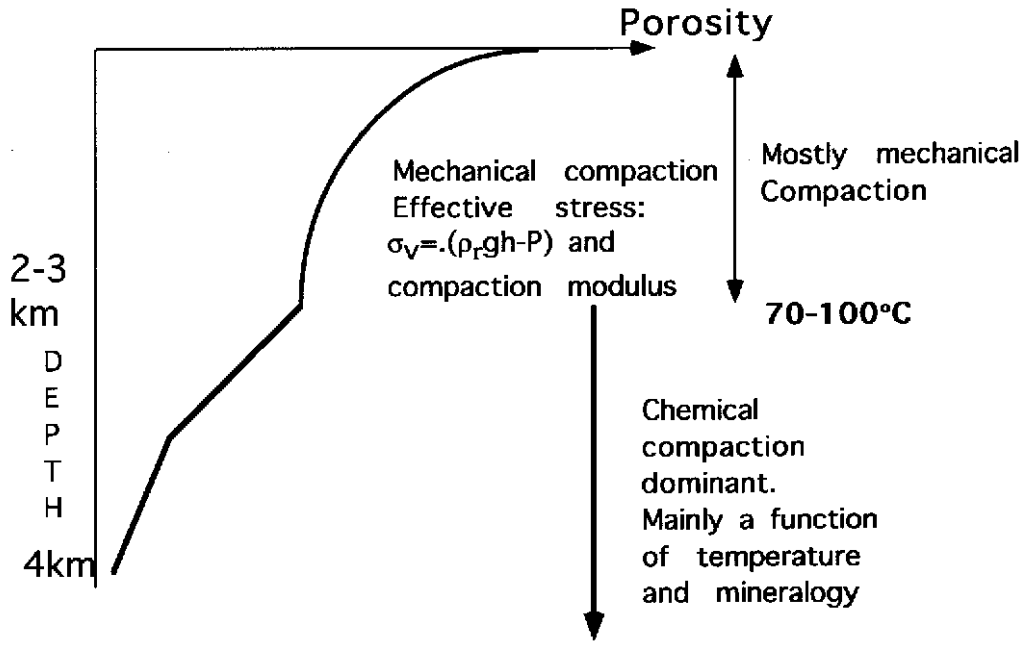


*Figure 3.1.2.1. This chart shows porosity vs. depth in a normal geothermal basin with some 30°C/km. The transition between Mechanical and Chemical Compaction are dependent on the relation between textural and mineralogy (Bjørlykke, 1998)*

However, if the geothermal gradient is around 20°C/km (Hitchon, 1984), loose sand can experience about 3-4 km of overburden before cementation starts. This means that about 30-40 MPa of overburden crushes the grain-to-grain contacts, fractures the grains and destroying the porosity by packing them together (Bjørlykke, 1998).

### 3.1.3 Chemical Compaction

When the temperature increases, the entire chemical compound starts to behave differently. Dissolution and precipitation increases with the temperature, and gravity are no longer a factor of importance (Bjørlykke, 1998). When the temperature exceed 70-80°C silica starts to dissolve at adjacent stylolites and grain-to-grain contacts, to further precipitate as cement on quartz grains. As mention above, the velocity and the density will increase drastically when quartz cementation enters the system. The prior loose sediments, is no longer influenced by the overburden due to the strengthened framework. Only 2-4% of cement is needed to bear the weight of the overburden. The cementation will continue until the void is filled up, unless the temperature gets below 70-80°C (Walderhaug, 1994b, Bjørlykke, 2014).

### 3.1.4 Intergranular Volume (IGV)

Intergranular Volume (IGV) is the total volume of the intergranular void space, matrix and cement at the base of mechanical compaction (Paxton et al., 2002). Figure 3.1.4.1 show how the IGV is lost with increased depth down to chemical compaction starts. With the IGV it is possible to calculate the initial porosity, and at the same time see how the sedimentary basin is transformed through burial. The results of IGV calculated from point counting, are presented in chapter 7.

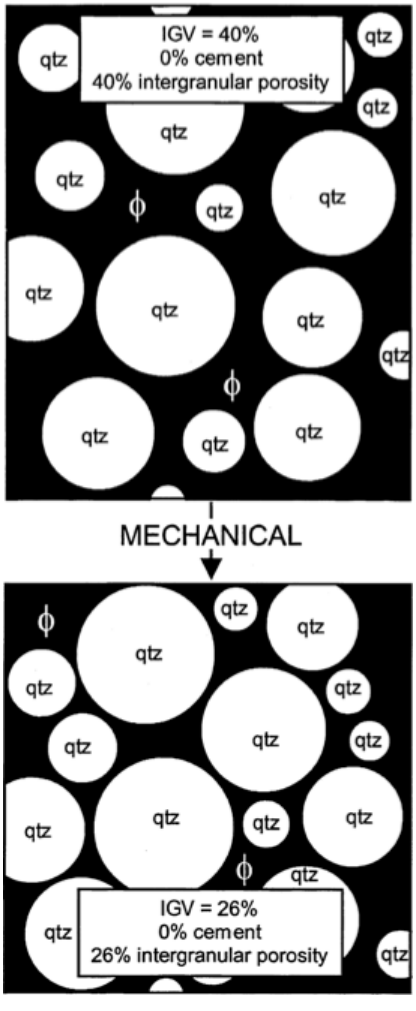


Figure 3.1.4.1: Illustration of compaction and decreasing IGV with increased depth down to chemical compaction starts. (Paxton et al., 2002).

### 3.1.5 Shallow burial (<2,0-2,5 km, <50-70°C)

In shallow burial, the composition of the sediment pays an enormous role to what extend will happen trough burial. Just after deposition the sediments are exposed to percolating meteoric water and to some extent air due to diffusion.

The texture of the grains is of importance. Carbonate grains behave more ductile under pressure than quartz do. This enlarges the grain contacts and the overburden stress is distributed over a bigger area on each grain. Early strengthening of the framework is introduced already under the redox boundary. (Shinn and Robbin, 1983). When biogenic carbonates reaches under the redox boundary, it gets unstable, dissolves and precipitates as cement (Saigal and Bjørlykke, 1987). This will increase the velocity and density of the rock, which is also reflected in the seismic and electric logs. Carbonate cement can also enter the system at later stages, due to dissolution of detrital carbonate grains. (Morad, 2009).

Meteoric water has the ability to reach great distances; up to 100 km from the shore (Manheim and Paull, 1981). The composition of meteoric water is different from seawater. Meteoric water becomes, in most cases, saturated with silica, due to leaching from e.g. the transition between feldspar and kaolinite (see Eq. 3.1.5.1 and Eq. 3.1.5.2). Seawater, on the other hand, is normally undersaturated with respect to silica, due to all the organisms that have taken the silica out of the water.

The flow of groundwater through a porous rock, is the main drive for precipitation of kaolinite due to leaching of minerals like mica and feldspar (Bjørlykke, 1994). The reactions can be written like this:

Eq. 3.1.5.1 $2K(Na)AlSi_3O_8 + 2H^+ + 9H_2O = Al_2Si_2O_5(OH)_4 + 4H_4SiO_4^{4+} + 2K^+(2Na^+)$

K-Feldspar Kaolinite dissolved silica + cations

Eq. 3.1.5.2 $2KAl_3Si_3O_{10}(OH)_2 + 2H^+ + 9H_2O = Al_2Si_2O_5(OH)_4 + 4H_4SiO_4^{4+} + 2K^+(2Na^+)$

Mica Kaolinite dissolved silica + cations

(Bjørlykke, 1994)

The $K^+/H^+$ ratio will move the reaction to the right, if the supply of freshwater continually removes $Na^+$, $K^+$ and silica out of the system. This requires undersaturated freshwater with respect to mica and feldspar (Bjørlykke, 1994).

### 3.1.6 Intermediate to deep burial (>2,0-2,5 km, >50-70°C)

Paxton et al. (2002) show, through data reconstruction, that initial porosity, about 42%, are quickly reduced to 28% at 1500 meters burial depth. But at 1500 to 2500 meters burial depth, the rearranging and packing of the sediments is slower.

Albitization is also common in the intermediate depth. Down to about 3 km, there is normal to see patchy albite that has replaced K-feldspar. In deeper sediments (>3,5 km, 120°C) the albite have almost finished the replacement (Saigal et al., 1988). The reaction can be written like this:

$$KAlSi_3O_8 + Na^+ \rightarrow NaAlSi_3O_8 + K^+$$

Eq. 3.1.6.1 K-feldspar + Sodium → Albite + Potassium

The albitization starts at some 65°C and finish at some 105°C. One of the controlling factors in the formation of albite is sodium. Sodium can be derived from oceanic pore water or the chemical transition between smectite to illite (Saigal et al., 1988).

A strong reduction of the permeability and porosity in a sandstone reservoir, takes place at about 3-4.5 km depth, where the temperature is about 120-160°C. The reason for this is precipitation of quartz cement. The quartz cement will fill up the porosity. Autogenic kaolinite and illite (see Eq. 3.1.5.1, Eq. 3.1.5.2 and Eq. 3.1.7.1) can retard the permeability much more than the porosity. Figure 3.1.7.1 show a typical illustration of the main diagenetic processes.

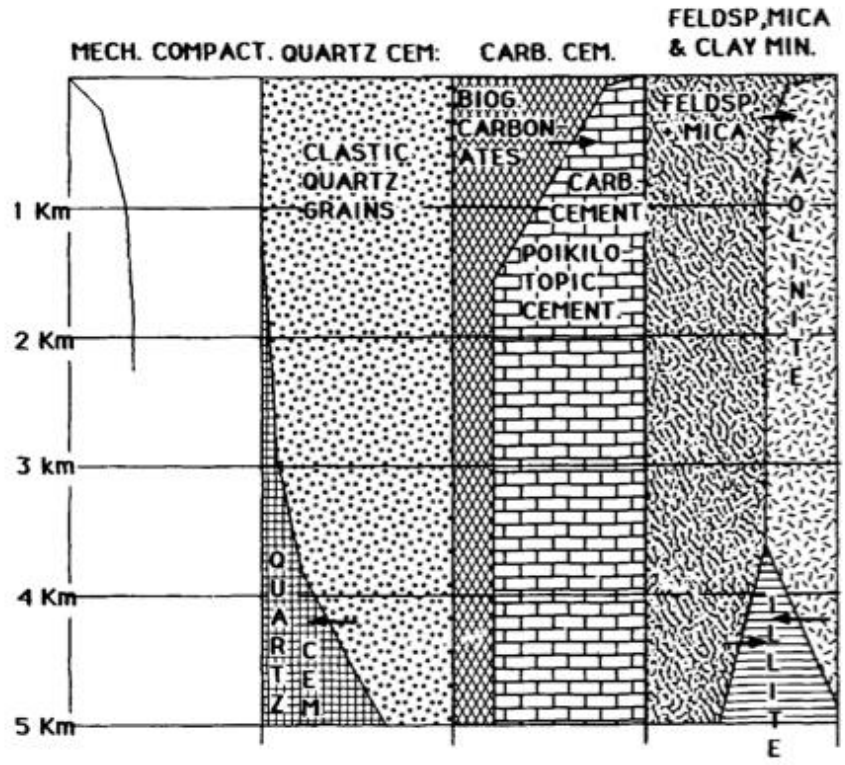


*Figure 3.1.7.1. Illustration of the main diagenetic processes that can change the properties of a sandstone. Modified after Bjørlykke et al. (1992)*

Potassium ($K^+$) is one of the components to form authigenic illite. Leaching of K-feldspar together with kaolinite can source the formation of authigenic illite, but there is needed around 140°C (Bjørlykke, 1994). The reaction can be written like this:

Eq. 3.1.7.1 $KAlSi_3O_8 + Al_2Si_2O_5(OH)_4 = KAL_3Si_3O_{10}(OH)_2 + 2SiO_2 + H_2O$

K-feldspar + Kaolinite = Illite + Quartz + Water

(Bjørlykke, 1994)

## 3.2 Quartz cement

Quartz cement is one of the dominantly porosity destroying mechanisms (Walderhaug, 1994b). In almost every sedimentary basin there will be quartz cement precipitated in some order. The thermodynamics control the driving mechanism for the precipitation of quartz cement, one of the important factors are temperature. The source of quartz cement was debated for a long time, but the introduction of the I-MID (Illite – Mica Induced Dissolution) (Figure 3.2.1) stated, with strong evidences that this was the main source (Walderhaug, 1994b, Bjørkum, 1996, Walderhaug, 1996, Oelkers et al., 2000).

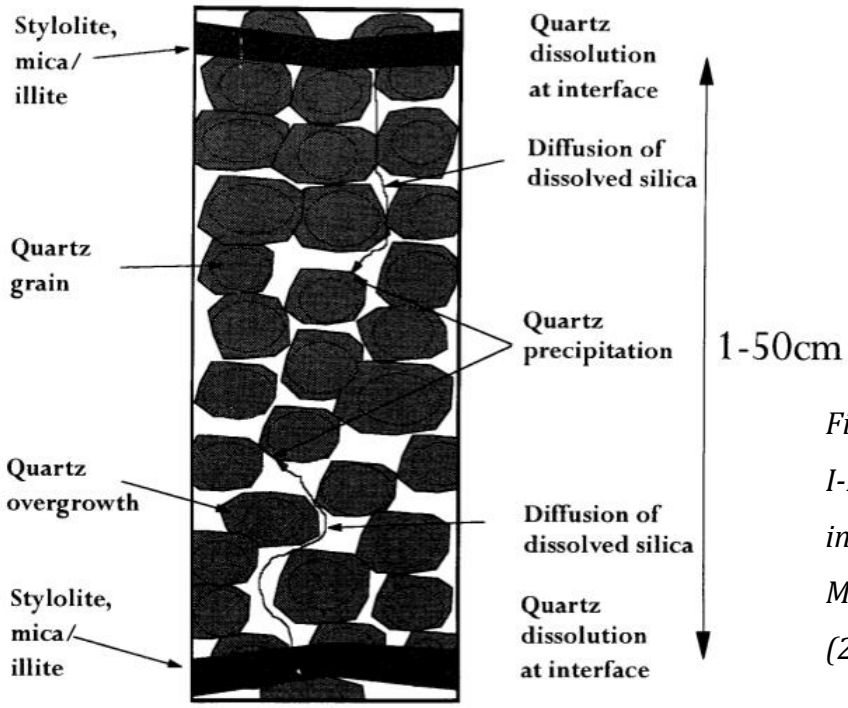


*Figure 3.2.1. Illustration of the I-MID model (Illite – Mica induced dissolution). Modified after Oelkers et al. (2000)*

Quartz cementation starts to precipitate when the temperature reach around 70 – 80°C. In the North Sea it is not common to see quartz cement before 2.5 km of burial depth (Bjørlykke and Egeberg, 1993).

## 3.3 Porosity preserving mechanisms in deeply buried sandstones

### 3.3.1 Introduction

There are different kinds of porosity preserving mechanisms. Different coatings can occupy the grain surface from precipitating cement (Bloch et al., 2002). Early hydrocarbon emplacement have the ability to surround grains and make them oil-wet (Walderhaug, 1994a). However, this is rare and often in collaboration with other preserving mechanisms. In both cases cement is prohibited to precipitate on the surface of grains. As mention above, grains will be packed and crushed together due to the weight of the overburden. Grain coating is a good porosity preserving mechanism (Figure 3.3.2.1). The most common is: chlorite coating, Illite coating (chlorite and illite can often occur together) and micro quartz coating. For more info see; (Heald and Larese, 1974, Jahren and Aagaard, 1992, Pittman et al., 1992, Ehrenberg, 1993, Aase et al., 1996, Aagaard et al., 2000, Bloch et al., 2002). Early hydrocarbon emplacement can

also preserve the porosity. If the cementation is retarded or even prevented in a reservoir that is oil filled, is debated (Saigal et al., 1992, Marchand et al., 2002, Aase and Walderhaug, 2005). If the grains are oil wet, the formation water will not be in contact with the grains and not be able to precipitate. Another important factor for the preservation of the porosity is the rigidity of the sediment. Since quartz grains are rigid grains, the framework is held up, and the porosity preserved. In the cases of more ductile grains, the coating on the grains is of no help, the weight of the overburden will deform the grains and the porosity will be lost (Paxton et al., 2002). Fluid overpressure can be a mechanism that prevents porosity loss, due to the delay of the chemical compaction realm.

### 3.3.2 Chlorite coating

Chlorite coating is an important porosity-preserving component in quartz rich sandstones (Aagaard et al., 2000). The existence of iron-rich chlorite (i.g. chamosite) coatings are well documented, but Aagaard et al. (2000) suggest two necessary conditions for the coating to develop; an iron rich precursor e.g. berthierine, and temperatures between 90 and 120°C.

The effect of the coating is preservation of the porosity from precipitating quartz cement. When these sandstones maintain their porosity at greater depths, mechanical compaction can still encounter. This can fracture the grains and create new, fresh surfaces where there is no coating. Quartz cement now has the opportunity to start to grow on the fresh surface, and the pore space will eventually be filled up.

# *Chapter 4 – Methods*

## 4.1 Introduction

The focus of this thesis has been on sedimentology and petrography. The study has been in the order of core description, point counting of thin sections and SEM analysis of thin sections and stubs. XRD results where kindly supplied by BG. The different levels of methods gave different resolution to obtain data and results. This was of importance to understand the reservoir quality, diagenesis of the sandstones and to interpret the depositional environment.

## 4.2 Core description

Five days was used to manually describe about 250 meters of core material from four wells (34/3-1 S, 34/3-2 S, 34/3-3 S and 34/5-1 S). Grain size, structures and textures, as well as bioturbation where used to predict the depositional environment. The logging has been digitalized and is presented simple in chapter 5 and more detailed in appendix V.

## 4.3 Well information

This master thesis had four wells to its disposal, as well as their electric logs. Samples from all the wells have been given, and put into interpretation through different procedures. In total 125 thins ection has been given, where 45 was selected. Later, slabs and stubs was provided and made out of these 45 samples. The reason for selecting a fewer amount of samples, is due to the interest of sand and not shale, as well as the amount of time consumed of each sample. The list of selected samples is presented below in table 4.2.1, and 4.2.2 for corresponding sands.

| 34-5-1 S | 34-3-3 S | 34-3-1 S | 34-3-2 S |
|---|---|---|---|
| 3638,00 | 3921,12 | 3868,79 | 4053,00 |
| 3640,00 | 3925,12 | 3868,87 | 4053,75 |
| 3645,75 | 3929,12 | 3870,35 | 4057,75 |
| 3646,50 | 3933,12 | 3873,30 | 4059,50 |
| 3649,25 | 3946,06 | 3874,18 | 4061,75 |
| 3650,25 | 3949,06 | 3880,56 | 4069,25 |
| 3677,73 | 3952,06 | 3885,70 | 4071,00 |
| 3678,50 | 3975,06 | 3886,27 | 4073,25 |
| 3679,25 | 3984,06 | 3887,35 | 4079,50 |
| 3684,90 | | 3899,97 | 4086,00 |
| 3686,32 | | 3900,01 | |
| 3688,50 | | 3901,13 | |

*Table 4.3.1: Total table of selected samples in all of the four wells in MD*

| |
|---|
| 3915,60 |
| 3927,81 |

| Corresponding depth - MD | | | | Sands |
|---|---|---|---|---|
| 34-5-1 S | 34-3-3 S | 34-3-1 S | 34-3-2 S | C5 |
| | | 3868,79 | | C4 |
| | | 3868,87 | | C3 |
| | | 3870,35 | | C2 |
| 3638,00 | 3921,12 | 3873,30 | | C1 |
| 3640,00 | 3925,12 | 3874,18 | | |
| | 3929,12 | 3880,56 | | |
| | 3933,12 | 3885,70 | | |
| | | 3886,27 | | |
| | | 3887,35 | | |
| 3645,75 | 3946,06 | 3899,97 | | |
| 3646,50 | 3949,06 | 3900,01 | | |
| 3649,25 | 3952,06 | 3901,13 | | |
| 3650,25 | | | | |
| 3677,73 | 3975,06 | 3915,60 | 4053,00 | |
| | | 3927,81 | 4053,75 | |
| | | | 4057,75 | |
| 3678,50 | | | 4059,50 | |
| | | | 4061,75 | |
| | | | 4069,25 | |
| | | | 4071,00 | |
| | | | 4073,25 | |
| 3679,25 | 3984,06 | | 4079,50 | |
| 3684,90 | | | 4086,00 | |
| 3686,32 | | | | |
| 3688,50 | | | | |

*Table 4.3.2a: Table of all the selected samples in corresponding sands*
*Table 4.3.2b: Color code for the five cook sands in the wells.*

## 4.4 Scanning Electron Microscope (SEM)

Type JEOL JSM-6460L V Scanning Electron Microscope, with LINK INCA Energy 300 (EDS) from Oxford Instruments was used to analyze 20 thin sections coated with carbon, and 20 stubs coated with gold. The list of samples is showed in table 4.4.1.

The carbon-coated *thin sections* were analyzed in backscattered (BEC). The *thin sections* were used to analyze chlorite coatings, and the distribution and effect of them. In

addition they were used to analyze pore filling clay and dissolution of feldspar. The gold-coated stubs where analyzed in secondary electron image (SEI). They were used to analyze the chlorite coatings and the effectiveness against quartz cement.

| Thin sections - MD | | | | Sands |
|---|---|---|---|---|
| 34-5-1 S | 34-3-3 S | 34-3-1 S2 | 34-3-2 S | C5 |
| | 3925,12 | 3885,70 | | C4 |
| 3645,75 | 3949,06 | 3901,13 | | C3 |
| | 3959,06 | | | C2 |
| 3677,73 | 3975,06 | 3911,76 | 4057,75 | C1 |
| | | 3915,60 | 4061,75 | |
| | | 3924,47 | 4067,25 | |
| | | 3927,81 | 4073,25 | |
| 3686,32 | 3984,06 | | 4079,50 | |
| 3688,50 | | | | |

*Table 4.4.1a: Selected samples to SEM in corresponding depth - MD*
*Table 4.4.1b: Color code for the five cook sands in the wells.*

## 4.5 Point counting

Optical microscopy has been used for the purpose of point counting and grain size analysis. As mention above, 45 thin sections were selected for analysis. To obtain a representative selection of the content and porosity in each thin section, 300 points per thin section was counted. A Swift automatic counter was mounted on the turning disk on the optical microscope. Each thin section was mounted on the Swift automatic counter and analyzed throughout the 300 points.

The analyzed minerals counted in the thin sections are illustrated in the legend of Figures 6.2.3.2, 6.2.3.4, 6.2.3.6 and 6.2.3.8 and appendix VI.

The limitation of this analyze is based upon the resolution of the microscope, the quality and thickness of the thin sections, as well as the skills of the operator which performed the point counting.

## 4.6 Grain size

The computer program Scope View was used to measure grain sizes. 50 grains in each thin section was measured by the long axis of the grain. All the results was collected and calculated in the excel program GRADISTAT (Blott and Pye, 2001).

The Geometric equations from Folk and Ward (1957) was selected from the GRADISTAT program.

Eq. 4.6.1 Mean

$$M_G = exp\frac{lnP16+lnP50+lnP84}{3}$$

Eq. 4.6.2 Standard deviation

$$\sigma_G = \exp(\frac{lnP16-lnP84}{4} + \frac{lnP5-lnP95}{6.6}$$

Eq. 4.6.3 Skewness

$$Sk_G = \frac{lnP16+lnP84-2(lnP50)}{2(lnP84-lnP16} + \frac{lnP5+lnP95-2(lnP50)}{2(lnP25-lnP5)}$$

Eq. 4.6.4 Kurtosis

$$K_G = \frac{lnP5-lnP95}{2.44(lnP25-lnP75}$$

Different plots and analysis where displayed in the program to give a better understanding of the deposition and distribution of the grains and grain sizes. It is important to emphasis a limitation of correctness; even though the 50 chosen grains where selected on a basis to be representative for each thin section; the interpreter chose the grains.

## 4.7 X-Ray Diffraction (XRD)

Bulk and clay fraction XRD results from three wells (34/3-1 S, 34/3-2 S and 34/3-3 S) where kindly distributed by BG. There were no available XRD results from well 34/5-1 S.

# *Chapter 5 – Core description and sedimentology*

## 5.1 Introduction

Lithological and sedimentological interpretation was done in the facilities of Weatherford in Stavanger. Five days was used to collect data of grain size, structures and texture, as well as bioturbation, to interpret the depositional environment. The core description has also been digitalized (Figure 5.2.1-5.1) and is illustrated in Appendix V. The cored intervals have been described and put into a facies table. Different facies have built up facies associations, which again have built up the interpreted depositional environment for the Cook Formation.

## 5.2 Facies and facies association (FA)

A sedimentary facies is a unit of rock that distinguish it self from adjacent lithology, with respect to e.g. grain size, texture and structure. A short interpretation of the different facies has been given in Table 5.2.1. A short presentation of the individual facies and the findings from their cores is presented in figure 5.2.1. The facies interpretation was used to interpret the facies association in table 5.2.2.

| Litho. | Code | Sub-code | Description | Structures | Grain size | Interpreted depositional environment |
|---|---|---|---|---|---|---|
| Sandstone | A | A1 | Clean sandstone without clay | Stratified | V. Fine – Coarse sand | Subtidal zone, upper and lower shoreface |
| | | A2 | Sandstone with mm-thick mud draping | Mud drapes | Fine – Medium sand | Subtidal zone, upper and lower shoreface |
| | | A3 | Sandstone with bioturbated mud draping | Mud drapes, Bioturbated | Fine – Medium sand | Subtidal zone, upper and lower shoreface |
| | | A4 | Sandstone | Ripples and cross lamination | Fine – Medium sand | Subtidal zone, upper and lower shoreface |
| | | A5 | Sandstone - From cm to several meter in thickness | Cross stratification and Dunes | Fine – Medium sand | Subtidal zone, upper and lower shoreface |
| | | A6 | Sandstone - The rip up clasts is scattered around | Bioturbation, rip up clasts of clay | V. Fine – Medium sand | Subtidal zone, upper and lower shoreface |
| Siltstone | B | B1 | Silty sandstone | Bioturbation | Silt – Medium sand | Transition zone, offshore |
| | | B2 | Silty mudstone | Heavy bioturbation | Mud – Silt | Transition zone, offshore |
| Shale | C | C1 | Mudstone | Bioturbation | Mud | Offshore |
| | | C2 | Sandy mudstone | Heavy bioturbation | Mud – Medium sand | Transition zone, offshore |
| | | C3 | Alternating mud and sand | Minor bioturbation, Double mud drapes | Mud – Medium sand | Transition zone, offshore |

*Table 5.2.1. Observed facies and interpreted depositional environment*

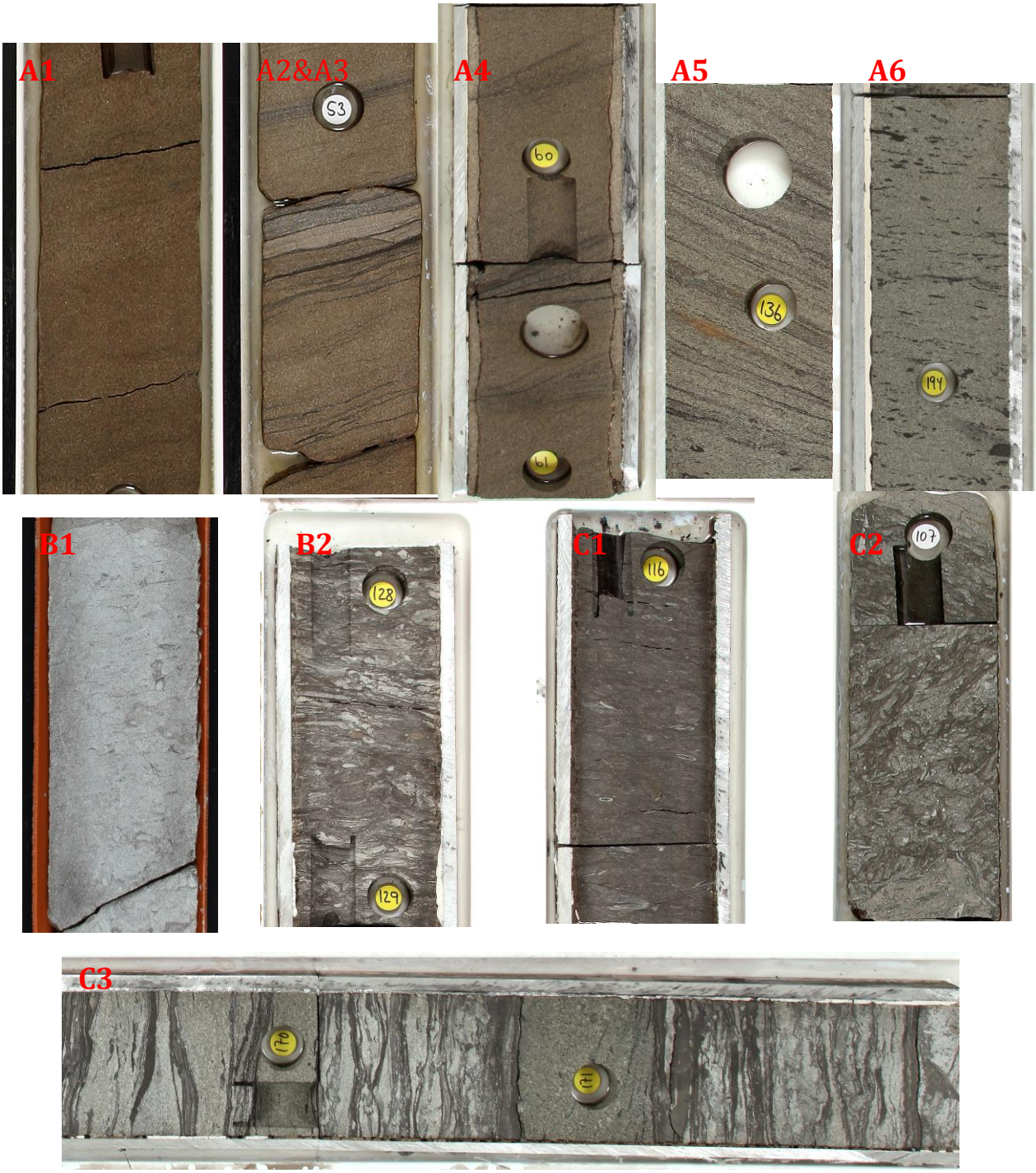


*Figure 5.2.3.* ***Facies A1*** *– Sandstone- Oil filled, 34/3-1 S, 3876,10 – 3876,35 MD.* ***Facies A2&A3*** *– Sandstone with mud drapes – Bioturbated or not - Oil filled, 34/3-1 S, 3885,30 – 3885,60 MD.* ***Facies A4*** *– Sandstone with ripples and cross lamination - Oil filled, 34/3-3 S, 3925,65 – 3926 MD.* ***Facies A5*** *– Sandstone with dunes, 34/3-3 S, 3946,12 – 3946,38 MD.* ***Facies A6*** *– Sandstone with rip up clasts of clay – Bioturbated or not, 34/3-3 S, 3960,30 – 3960,60 MD.* ***Facies B1*** *– Silty sandstone – Bioturbated, 34/3-3 S, 3912,43 – 3912,60 MD.* ***Facies B2*** *– Silty shale – Bioturbated, 34/3-3 S, 3941,00 – 3944,30 MD.* ***Facies C1*** *– Marine Shale – Bioturbation, 34/3-3 S, 3941,00 – 3941,30 m bsf.* ***Facies C2*** *– Sandy shale – Bioturbated, 34/3-1 S, 3906,00 – 3906,35 MD.* ***Facies C3*** *– Sandy shale – Bioturbated, 34/3-3 S, 3954,40 – 3955,00 MD.*

| Environment | Facies association | Sub units | Facies motif | Description | Interpretation of depositional setting |
|---|---|---|---|---|---|
| **Shallow marine - tidally influenced deltaic environment** | FA1 Nearshore delta slope deposits | FA1.1 Sand deposits | A1, A2, A3, A4, A5 | Constitute most of the cores (49,8% in total). Can occur both ways | Subtidal zone and shoreface |
| | | FA1.2 Silty and muddy sand deposits | B2, B1, C3, C2 | FA1.2 is more silty and muddy than FA1.1 and occur both ways | Shoreface and transition zone |
| | FA2 Tidal compound dune | FA2.1 Dune crest | A4, A5 | FA2.1 is observed all together in 37,25 m in well 34/3-3 S, minor or nothing in the other wells. | Subtidal zone and shoreface |
| | | FA2.2 Dune lee side | A3, A6, A2 | Upward coarsening muddy sand | Shoreface |
| | | FA2.3 Bottomsets | B2, C3, B1, C2 | Mudstone | Transition zone |
| | FA3 Tidal bar | | B2, C2, A6, A5, A4, A1 | Upward coarsening unit | Subtidal zone and shoreface |
| **Deep marine** | FA4 Offshore deposits | FA4.1 Silty and sandy mudstone | C3, C1, B2 | FA4.1 is mostly bioturbated mudstone. | Transition zone and offshore |
| | | FA4.2 Mudstone | C1 | FA4.2 is a offshore mudstone with bioturbation | Offshore |

*Table 5.2.2. Facies association with facies motif and the interpreted depositional environment*

## 5.3 Depositional environment

The facies and facies associations, which constitute the interpreted depositional environment, are recognized in the different cores.

From the sandstones in the wells there has been interpreted a depositional environment (Table 5.3.1). In some of the sandstones the interpretation differs between the cores, while others are the same.

| Sandstones | 34/5-1 S | 34/3-3 S | 34/3-1 S | 34/3-2 S |
|---|---|---|---|---|
| **C5** | - | - | Delta front | - |
| **C4** | - | Delta front | Pro delta - Prograding dune compound | - |
| **C3** | Pro delta | Delta front | Pro delta - Prograding Dune compound | - |
| **C2** | - | Pro delta – tidal bar | Delta front | Delta front |
| **C1** | Delta front | Pro delta – tidal bar | - | Delta front |

*Table 5.3.1. The interpreted depositional environments of the Cook sandstones. The interpretation is in a tidally influenced environment.*

## 5.4 Vertical and lateral trends

Inside the individual cores there are different FA upon each other, which can strengthen the understanding of the vertical deposition of the different Cook sandstones. In the same way as the different FA is deposited vertically, the lateral deposition can strengthen the understanding of the outbuilding processes of the different Cook sandstones and the Cook system.

The cores are described individually in the order of proximal to distal from shore. The digitalized core descriptions are simplified and contain only; grain size, bioturbation rate and lithology. As described in chapter 1, the Cook Formation contains five sandstones (C1-C5) in the Knarr area. Each core contains two or more of these sandstones.

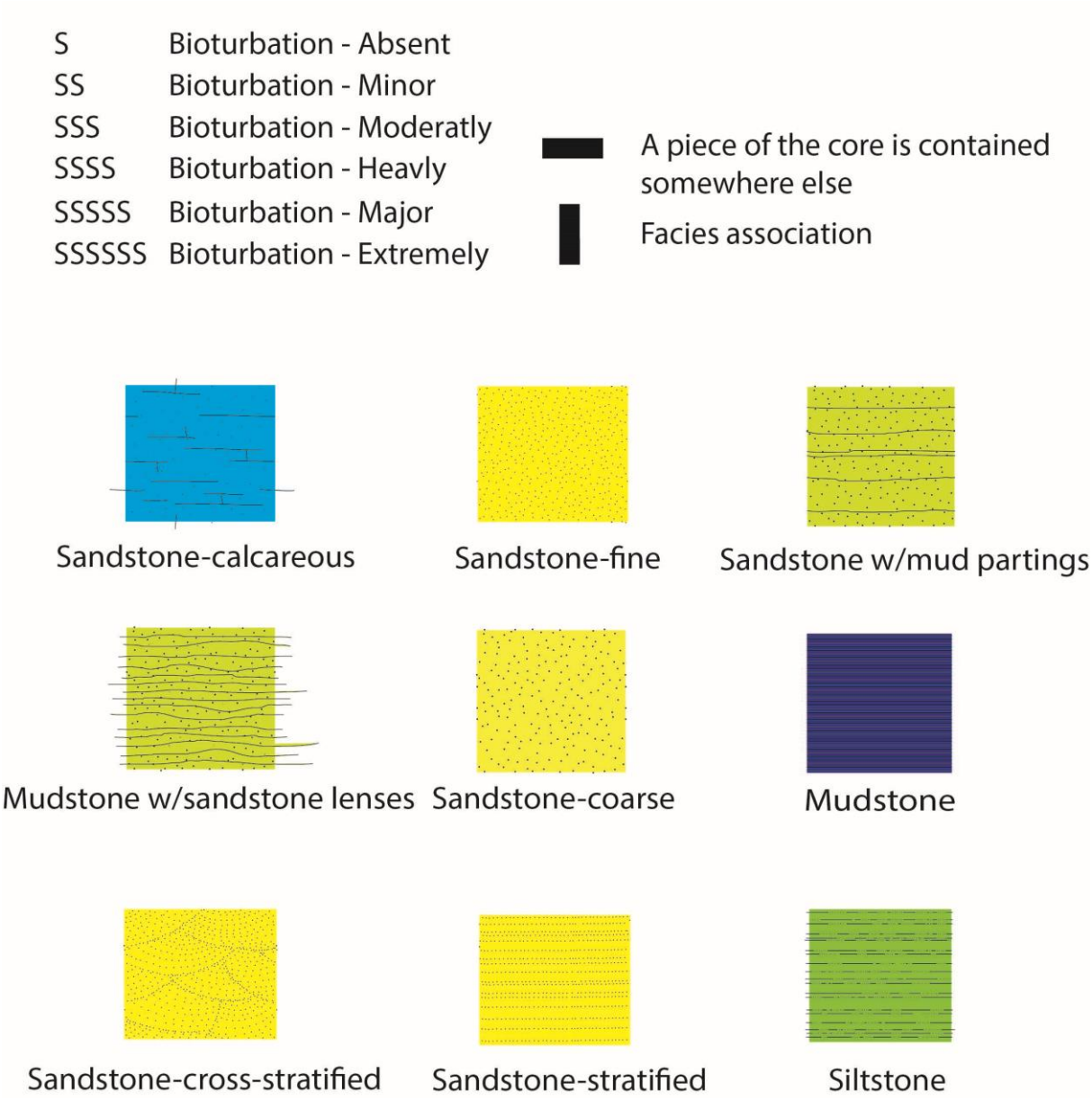


*Figure 5.4.1. Legend of the core descriptions*

### 5.4.1 – 34/3-2 S

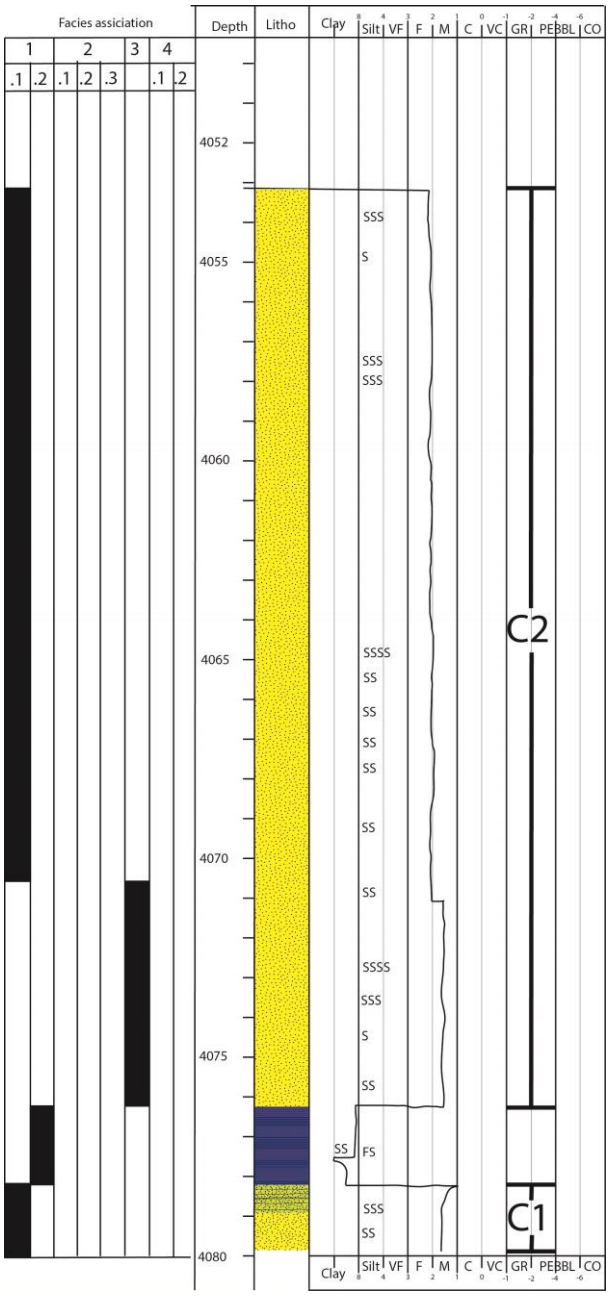


The cored interval ranges from 4079,85 – 4053,00 mMD. This core is the shortest of the four cores and contains only two out of the five sandstones, C1 and C2. The cored interval of the C1 sandstone only represents the two top meters of the sandstone. The C2 sandstone is about 25 meter and the top of the core is stopped before the top of the C2 sandstone (See Figure 5.4.10.1 for the whole sandstone).

The C1 sandstone starts with FA1.1 and transfer over to FA1.2. The C2 sandstone starts with FA3 on a sharp base and transfer over to FA1.1.

*Figure 5.4.1.1. Digitalized cored interval of well 34/3-2 S, with FA intervals.*

### 5.4.2 – 34/3-1 S

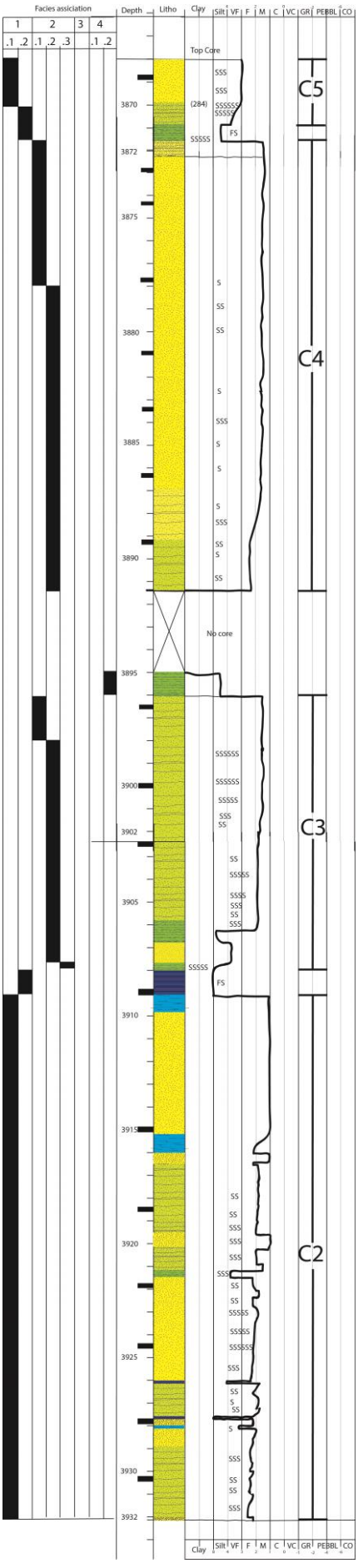


The cored interval ranges from 3932,25 – 3868,00 mMD and consists of two cores. The core contains the C2, C3, C4 and C5 sandstones. The sandstone package of C2 is a bit thinner (22 meter) than in 34/3-2 S.

The C2 sandstone starts with FA1.1 and transfer over to FA1.2 at the top. The C3 sandstone starts with FA2.3 and continues with FA2.2 and transfer to FA2.1, which is suddenly overlain by FA4.2. The core stops here (3895 mMD) and continues in the next C4 sandstone. The C4 sandstone in the core starts out with FA2.2 and continues with FA2.1. The top of C4 is sharply overlaid by FA1.2 and is smoothly transferred to FA1.1 in the C5 sandstone.

*Figure 5.4.2.1. Digitalized cored interval of well 34/3-1 S, with FA intervals.*

### 5.4.3 – 34/3-3 S

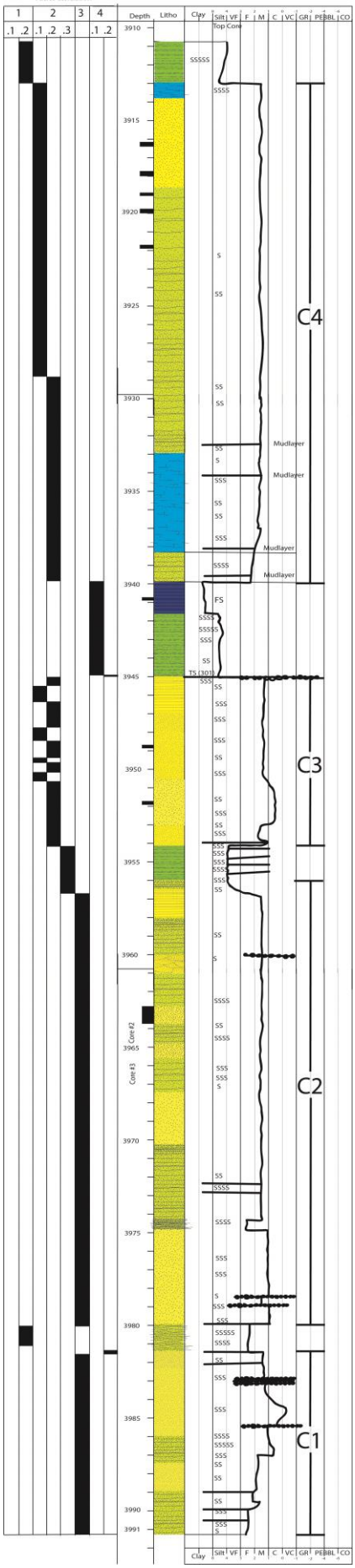


The cored interval ranges from 3989,00 – 3910,85 mMD and consists of three cores. The core contains the C1, C2, C3 and C4 sandstones. The C2 sandstone has about the same thickness as the C2 sandstone in the 34/3-1 S well.

The core starts with the C1 sandstone consisting of parasequences of FA3. The top of the C1 sandstone is sharply overlaid by a thin layer of FA4.2 followed by FA1.2. The C2 sandstone starts with FA3 and erosive surfaces divide FA3 in parasequences throughout the whole sandstone. The top of the C2 sandstone is quite quickly transferred to FA2.3. The C3 sandstone starts out with FA2.2 and continues into parasequences with alternating FA2.1 and FA2.2. The top of the C3 sandstone is overlaid by a sharp transition to a thin layer of FA4.2 followed by FA4.1. The C4 sandstone starts with FA2.2 with a sharp boundary at the base and continues with FA2.1 to the top. The top of the C3 sandstone is transferred to FA1.2.

*Figure 5.4.3.1. Digitalized cored interval of well 34/3-3 S, with FA intervals.*

### 5.4.4 – 34/5-1 S

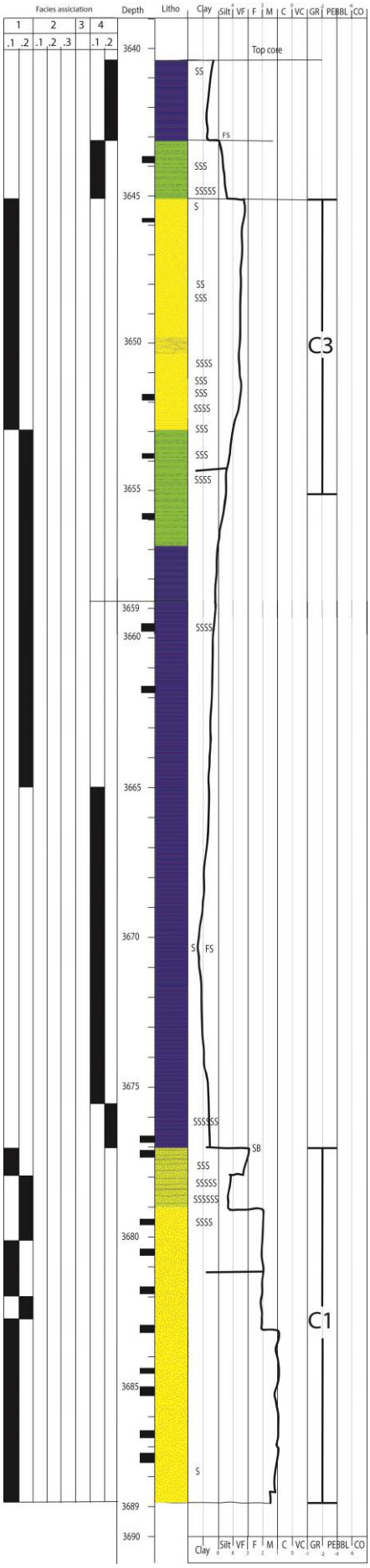


The cored interval ranges from 3689,00 – 3640,50 mMD and consists of two cores. The core contains the C1 and C3 sandstones.

The core starts with the C1 sandstone and FA1.1. The C1 sandstone fines upward and changes to FA1.2. A new parasequence of FA1.1 and FA1.2 with erosive base is deposited. FA1.2 transfers over to FA4.2. FA4.1 is deposited and FA1.2 is smoothly introduced. The C3 sandstone starts with FA1.1 and is quickly changed to FA4.1 and last FA4.2.

*Figure 5.4.4.1. Digitalized cored interval of well 34/5-1 S, with FA intervals.*

### 5.4.5 – C1

*Description*

The C1 sandstone is seen in three of the four cores (34/3-2 S, 34/3-3 S and 34/5-1 S). The vertical trends of FA seen in the C1 sandstone in the different wells differ from one another. In 34/3-2 S the sandstone consists of FA1.1 and transfer to FA1.2. In 34/3-3 S the sandstone consists of parasequences of FA3. In 34/5-1 S the sandstone consists of parasequences of FA1.1 and FA1.2.

*Interpretation*

All of the three different cores that contain the C1 sandstone are interpreted to be migrating tidal bars in a pro delta - delta front environment.

### 5.4.6 – C2

*Description*

The C2 sandstone is seen in three of the four cores (34/3-2 S, 34/3-1 S and 34/3-3 S). There are similarities in the C2 sandstone between the wells. In 34/3-2 S the C2 sandstone consists of FA3 and FA1.1. In 34/3-1 S the C2 sandstone consists of FA1.1 and FA1.2. In 34/3-3 S the C2 sandstone consists of FA3 and FA2.3.

*Interpretation*

All of the three different cores that contain the C2 sandstone are interpreted to be migrating tidal bars in a pro delta – delta front environment.

### 5.4.7 – C3

*Description*

The C3 sandstone is seen in three of the four cores (34/3-1 S, 34/3-3 S and 34/5-1 S). The sandstone has similarities and differences between the cores. In 34/3-1 S the sandstone consists of FA2.3, FA2.2, FA2.1 and FA4.2. In 34/3-3 S the sandstone consists of FA2.2, FA2.1 and FA4.2. In 34/5-1 S the sandstone consists of FA1.1, FA4.1 and FA4.2.

*Interpretation*

The three different cores that contain the C3 sandstone are interpreted to be migrating dune compounds and tidal bars in a pro delta – delta front environment.

### 5.4.8 – C4

*Description*

The C4 sandstone is only seen in two of the four cores (34/3-1 S and 34/3-3 S). The sandstone consists in both wells of FA2.2 and FA2.1.

*Interpretation*

Both of the cores that contain the C2 sandstone are interpreted to be migrating dune compounds in a pro delta – delta front environment.

### 5.4.9 – C5

*Description*

The C5 sandstone is only seen in 34/3-1 S and consists of FA1.1.

*Interpretation*

The C5 sandstone is interpreted to be a migrating tidal bar in a delta front environment.

### 5.4.10 Well correlation

Figure 5.4.10.1 illustrates the well correlation between the four wells. All of the Cook sandstones are correlated even if they are not in the cored interval. The cored intervals are represented with red lines in the figure (Figure 5.4.10.1). The log can also give a good impression of what the sandstones look like, with respect to grain size, porosity and the way they stack upon each other, both vertically and laterally.

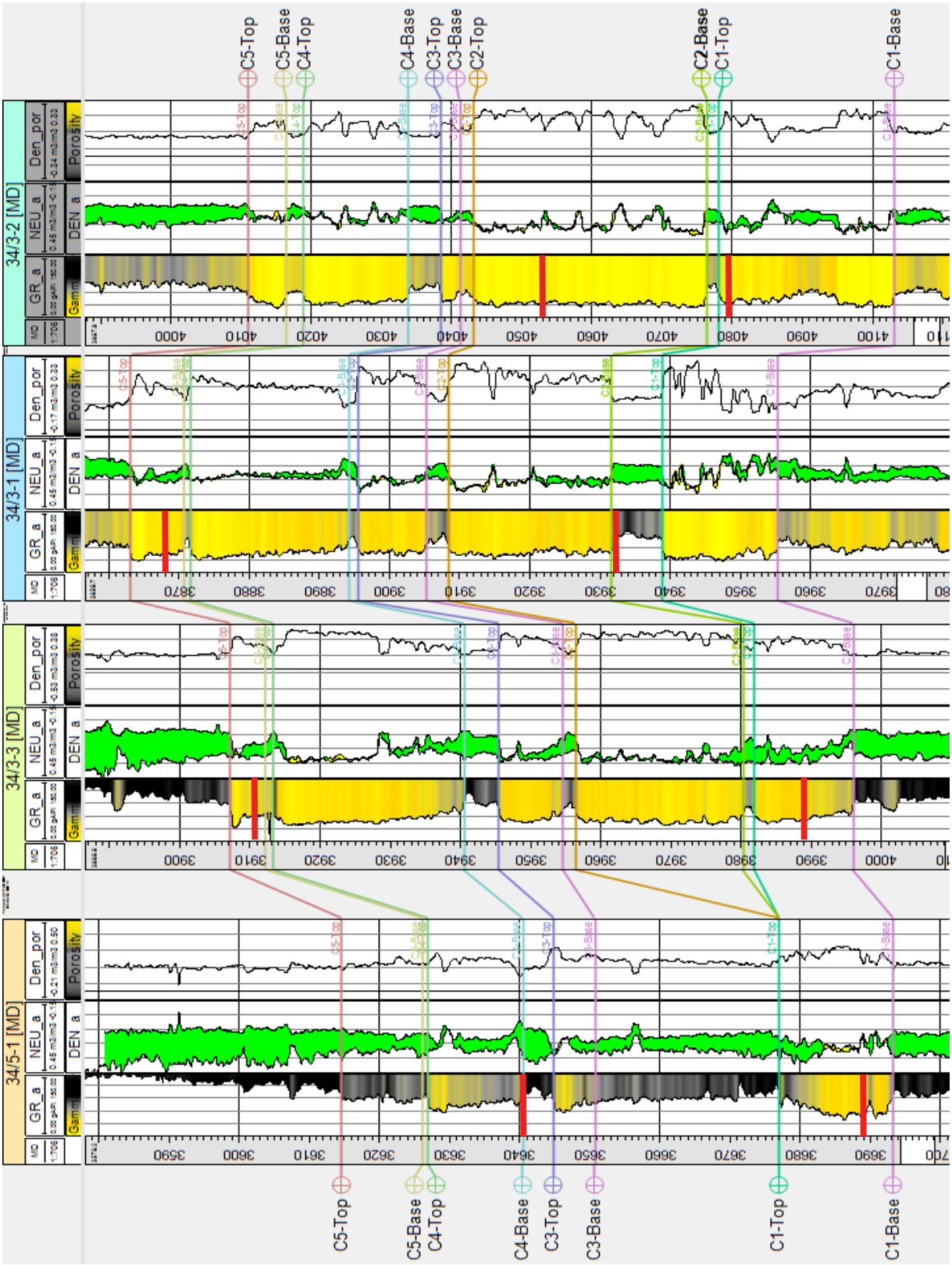


*Figure 5.4.10.1. Well correlation of the wells in MD. The red lines represent the cored intervals.*

# *Chapter 6 – Mineralogical and petrographic analysis*

## 6.1 Introduction

The four wells studied have been mineralogical and petrographic analyzed using point counting, grain size analysis and SEM. Due to limited time in SEM, 16 thin sections were selected, which is presented below in table 6.2.2. The selection is based on the lateral and vertical distribution of the different sandstones. Point counting, grain size analysis and SEM were performed on all of the 45 selected thin sections.

The goal is to observe and compare the mineralogical and petrographic differences and similarities in the different Cook sandstones.

The XRD results from well 34/3-2 S, 34/3-1 S and 34/3-3 S are presented in section 6.2.4.

## 6.2 Results

All of the thin sections and stubs were received named in Measured Depth (MD). A recalculation was conducted to *True Vertical Depth* (SSTVD), due to the curvatures of the wells. The water depths were removed to obtain the *true vertical depth,* from the sea floor down to the actual depth.

In order to only obtain the *true burial depth*, from the seafloor down to the actual depth, the water depth is also removed. Table 6.2.1 show the *true burial depth*.

Unless specified by mMD, all samples are referred to as SSTVD minus water depth, in the notation of meter.

| Sample depth - SSTVD minus water Depth | | | | Sands |
|---|---|---|---|---|
| 34-5-1 S | 34-3-3 S | 34-3-1 S | 34-3-2 S | C5 |
| 3067,10 | 3455,25 | 3322,80 | 3610,30 | C4 |
| 3069,05 | 3459,15 | 3322,90 | 3611,05 | C3 |
| 3074,65 | 3463,10 | 3324,20 | 3615,05 | C2 |
| 3075,35 | 3467,00 | 3326,90 | 3616,80 | C1 |
| 3078,00 | 3479,65 | 3327,70 | 3619,05 | |
| 3079,00 | 3482,60 | 3333,50 | 3626,50 | |
| 3105,60 | 3485,55 | 3338,20 | 3628,25 | |
| 3106,30 | 3508,05 | 3338,70 | 3630,50 | |
| 3107,05 | 3516,90 | 3339,70 | 3636,80 | |
| 3112,50 | | 3351,31 | 3643,30 | |
| 3114,90 | | 3351,33 | | |
| 3116,00 | | 3352,35 | | |
| | | 3365,65 | | |
| | | 3376,85 | | |

*Table 6.2.1. All the samples in adjusted depths: SSTVD minus water depth.*

| Sample Depth - MD | | | | Sample Depth - SSTVD minus Water depth | | | |
|---|---|---|---|---|---|---|---|
| 34-5-1 S | 34-3-3 S | 34-3-1 S | 34-3-2 S | 34-5-1 S | 34-3-3 S | 34-3-1 S | 34-3-2 S |
| | 3925,12 | 3885,70 | | | 3459,20 | 3338,20 | |
| 3645,75 | 3949,06 | 3901,13 | | 3074,60 | 3482,70 | 3352,50 | |
| | 3975,06 | 3915,60 | 4057,75 | 3105,60 | 3508,10 | 3365,70 | 3615,10 |
| | | 3927,81 | 4061,75 | | | 3376,90 | 3619,10 |
| | | | 4073,25 | | | | 3630,60 |
| 3677,73 | 3984,06 | | 4079,50 | 3114,90 | 3517,00 | | 3636,85 |
| 3686,32 | | | | 3116,00 | | | |
| 3688,50 | | | | | | | |

| Sands |
|---|
| C5 |
| C4 |
| C3 |
| C2 |
| C1 |

*Table 6.2.2: Selected samples to SEM in both MD and SSTVD minus water depth.*

### 6.2.1 Chlorite coating

Atomic percentage (Table 6.2.1.1) of the chlorite coating (see Figure 6.2.1.2 for example) was analyzed in SEM by removing a part of the coating from the surface of a detrital grain. The Fe/ Fe+Mg ratio is higher than 0,5 (see figure 6.2.1.1), indicating that all the chlorite coating samples corresponds as chamosites (Foster, 1962). All of the Fe has been calculated as $Fe^{2+}$. The complete table of atomic percentage is presented in appendix I.

| Sample | Mg | Al_tet | Al_okt | Si | Fe | No analyzed |
|---|---|---|---|---|---|---|
| **1** | 0,774 | 0,779 | 1,949 | 3,221 | 2,693 | 4 |
| **2** | 0,932 | 0,602 | 2,047 | 3,398 | 2,300 | 3 |
| **3** | 0,920 | 0,983 | 1,693 | 3,017 | 3,032 | 6 |
| **4** | 0,833 | 1,008 | 1,820 | 2,992 | 2,940 | 3 |
| **5** | 0,861 | 1,141 | 1,488 | 2,859 | 3,476 | 6 |
| **6** | 0,733 | 1,119 | 1,405 | 2,881 | 3,719 | 1 |
| **7** | 0,826 | 1,100 | 1,503 | 2,900 | 3,469 | 6 |

*Table 6.2.1.1. Measured average atomic percentage of the chlorite coating from SEM analysis. Sample 1-4 is from 34/3-3 S, 3949,06 mMD. Sample 5-7 is from 34/3-2 S, 4061,75 mMD.*

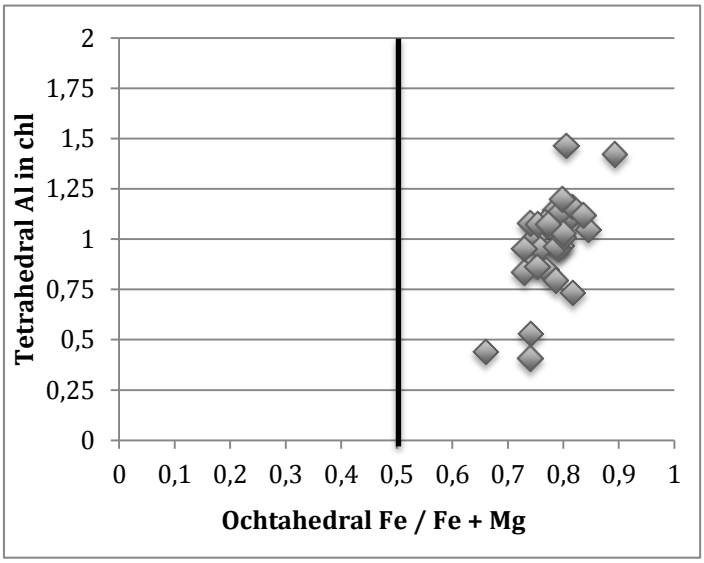


*Figure 6.2.1.1. Chlorite analysis plotted as in Bailey and Brown (1962) and all the samples are classified as chamosites, due to higher values than 0,5 in the Fe/Fe+Mg ratio (Foster, 1962).*

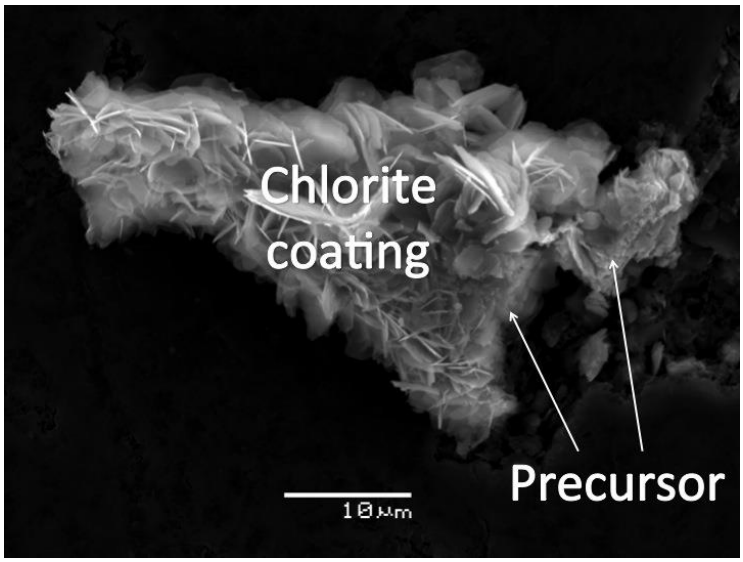


*Figure 6.2.1.2. The coating was removed from the surface of a detrital grain and analyzed to observe the atomic percentage of the chlorite coating. The precursor was also observed and classifies as a berthierine. 34/3-2 S – 4061,25 mMD.*

Chlorite coating has been observed in all the SEM samples. Chlorite coating was not observed in well 34/3-1 S using the point counting method.

The qualities of the chlorite coating observed in the samples are listed in Table 6.2.1.2, which gives a range from 1-4 in effectiveness, and illustrated in Figure 6.2.1.4.

The effectiveness of the coating from the different Cook sandstones is presented in Table 6.2.1.3 and illustrated in Figure 6.2.1.3. No coating was found in 34/3-1 S, and therefore it is no plot for the core.

| Effectiveness | Description | Distribution | Porosity preserving |
|---|---|---|---|
| **4** | Thick (> 5µm) coats that covers the whole grain | Abundant | Very good |
| **3** | Medium to thick (3-5 µm) coats that covers most of the grain | Extensive, but patchy distributed | Good |
| **2** | Medium (2-3µm) coats that covers about 50% of the grain | Moderate | Moderate |
| **1** | Thin or absent (< 2µm) coats that occur some places | Shows here and there | Minor |

*Table 6.2.1.2. Scale from 1-4 of the effectiveness of chlorite coating observed in the different samples.*

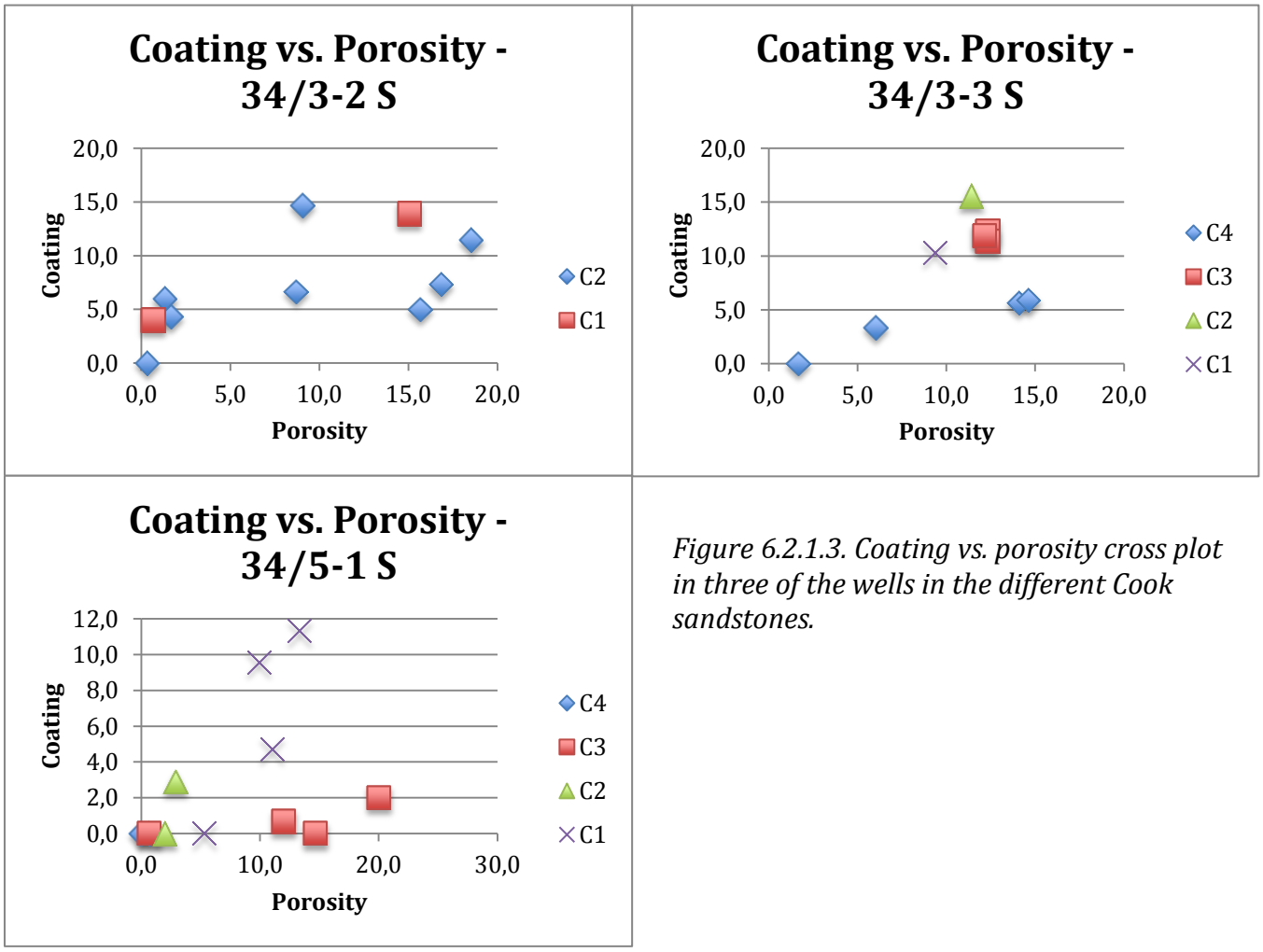


*Figure 6.2.1.3. Coating vs. porosity cross plot in three of the wells in the different Cook sandstones.*

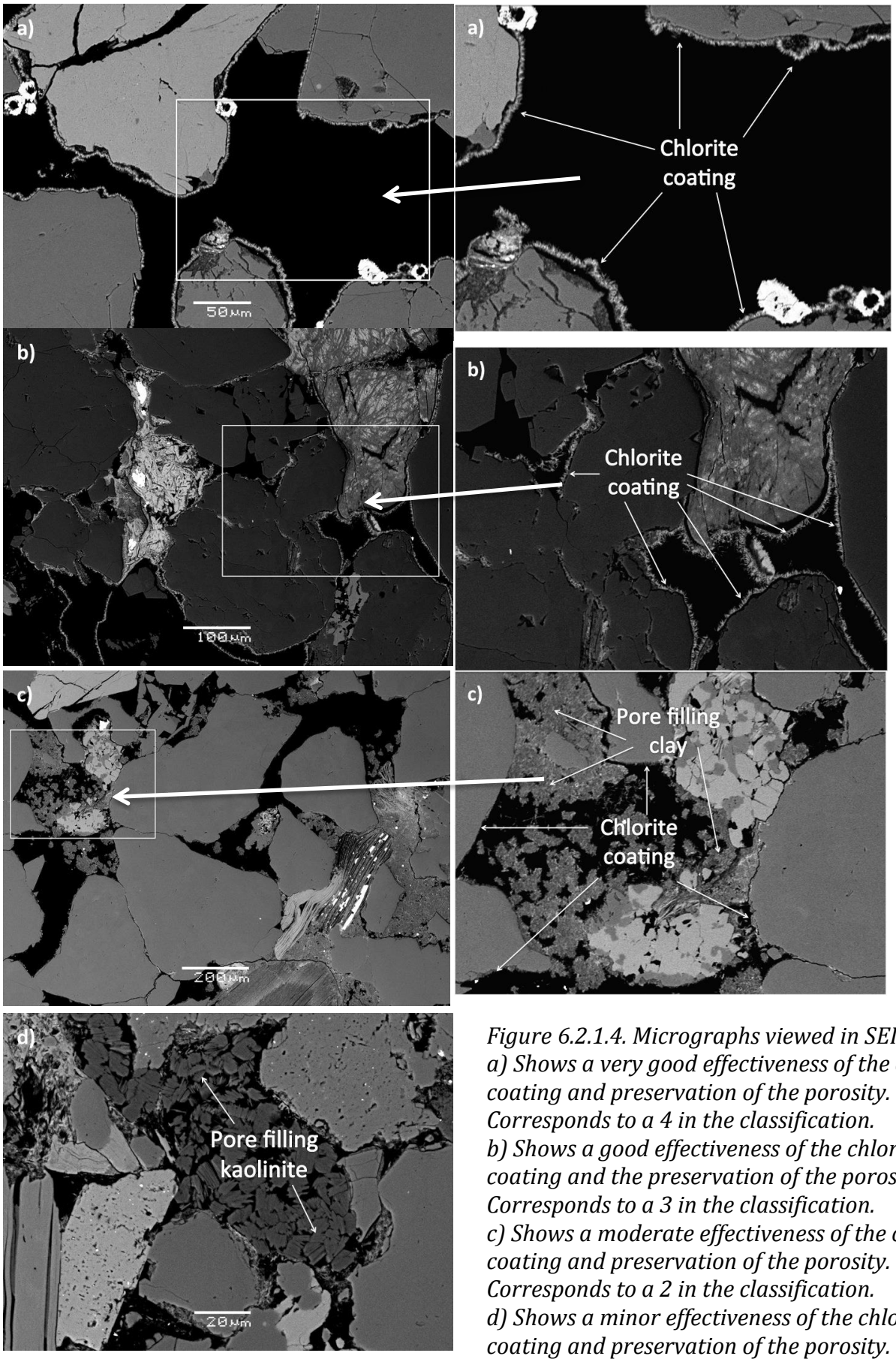


*Figure 6.2.1.4. Micrographs viewed in SEI mode. a) Shows a very good effectiveness of the chlorite coating and preservation of the porosity. Corresponds to a 4 in the classification. b) Shows a good effectiveness of the chlorite coating and the preservation of the porosity. Corresponds to a 3 in the classification. c) Shows a moderate effectiveness of the chlorite coating and preservation of the porosity. Corresponds to a 2 in the classification. d) Shows a minor effectiveness of the chlorite coating and preservation of the porosity. Corresponds to a 2 in the classification*

| Well | Cook sand | Effectiveness | Comments |
|---|---|---|---|
| **34/3-2 S** | C1 | 4 | The coating is good, but high amount of pore filling clay |
| | C2 | 3 | Generally good coating, but some samples are filled with carbonate cement and clay |
| **34/3-3 S** | C1 | 4 | Good coating, despite high amount of clay |
| | C2 | 2 | Moderate coating, despite low amount of pore filling clay and carbonate cement |
| | C3 | 2-3 | Moderate coating, with moderate amounts of clay, low or no carbonate cement |
| | C4 | 4 | Very good coating, despite high amount of clay and carbonate cement |
| **34/5-1 S** | C1 | 3 | Good coating, but high amounts of pore filling kaolinite and clay destroys some of the porosity |
| | C3 | 3-4 | Thin, but extremely good coating. The point counting did not get all the coating, but the SEM pictures show a thin, but good coating |
| | C4 | 1 | No coating |

*Table 6.2.1.3. Effectiveness of the chlorite coatings in the different Cook sandstones*

### 6.2.2 Quartz cement

Not much quartz cement was found in the samples (see Figure 6.2.3.2,4,6,8). However, as illustrated in Figure 6.2.2.5-6, when the quartz cement grows, it occupies the pore space efficiently.

a) b)

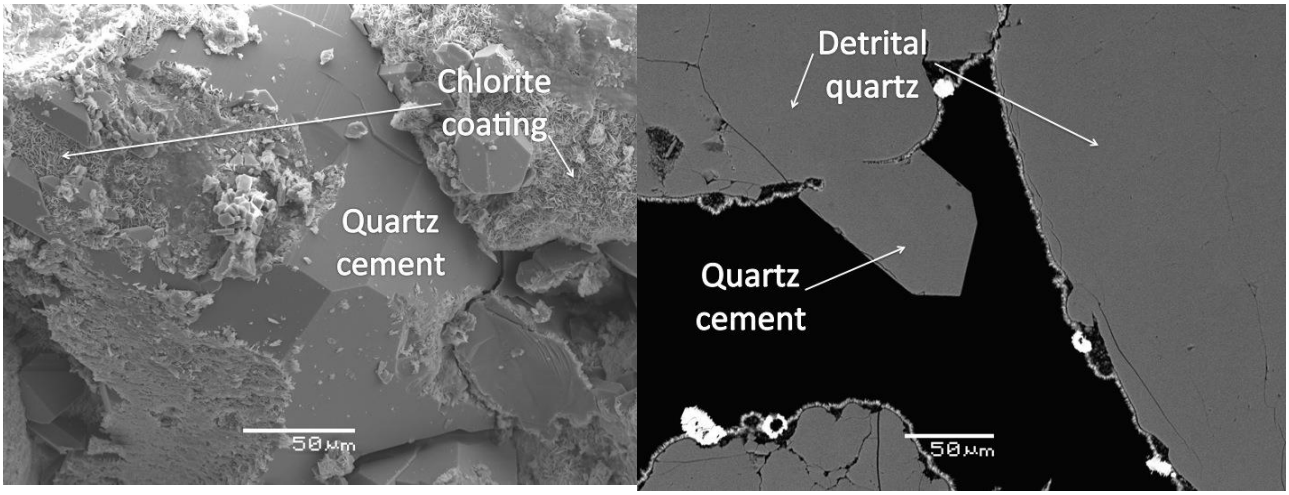


*Figure 6.2.1.5.*
*a) Quartz overgrowth occupying pore space. Well 34/5-1, depth: 3688.50 mMD.*
*b) Quartz cement growing into the pore space destroying the porosity. Well 34/3-3, depth: 3949,06 mMD.*

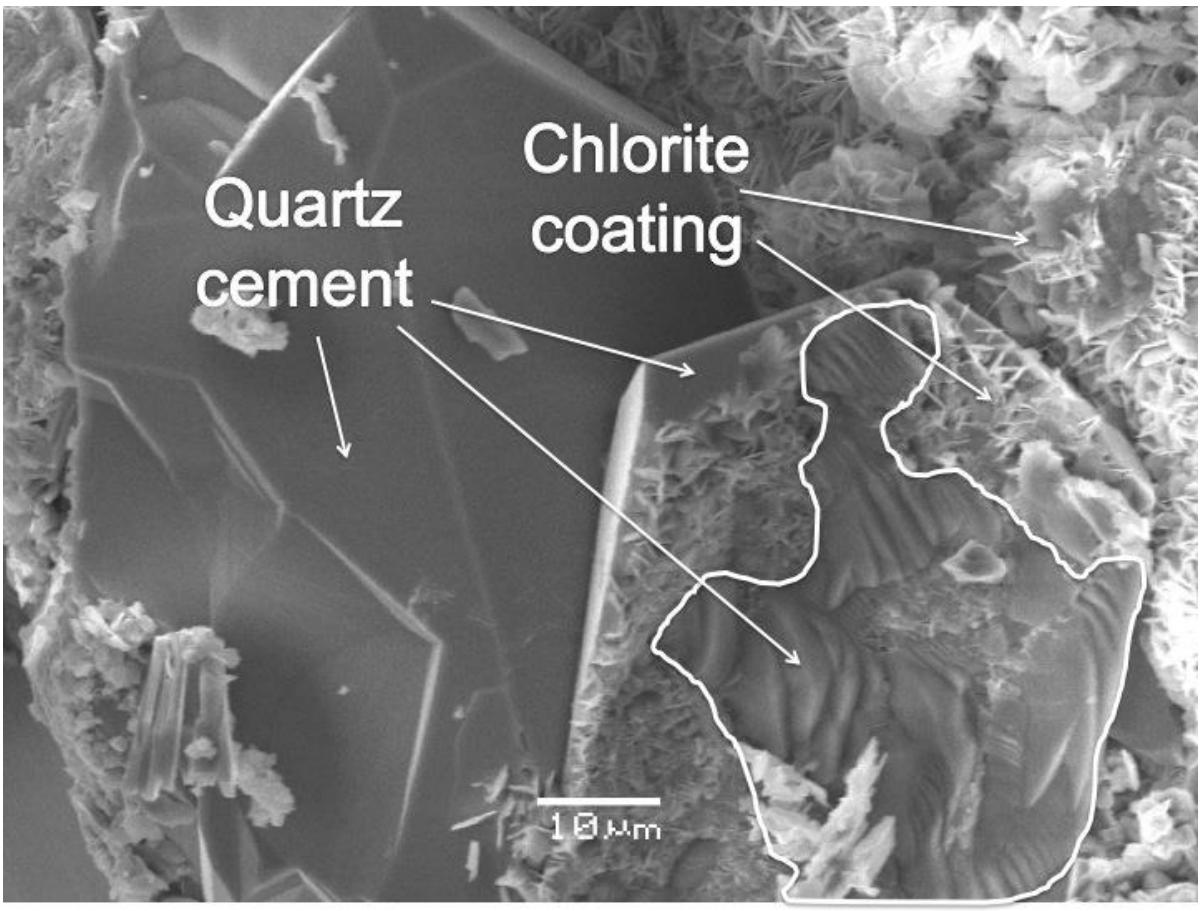


*Figure 6.2.1.6. Quartz cement is growing around the initial grain. Well 34/5-1, depth: 3688.50 mMD. The chlorite coating, which used to cover the grain (that now is gone), has been observed in the quartz cement. The red line represents the connection between the old grain and the cement.*

### 6.2.3 Mineralogy assemblage and Point counting

*Point counting* is an efficient method to estimate the mineralogical composition of a sample. The *point counting observation* can give an indication of the mineralogical assemblage, porosity, matrix-content < 30µm, IGV, and percentage of coatings. The obtained data can be of great importance to increase the understanding of, in particular for this thesis, the reservoir quality and depositional environment. The observations of the mineralogical composition in the different wells are presented in four figures (Figure 6.2.3.2,4,6,8). The calculated percentages from point counting are presented in appendix VI. What is described as "clay mix" (fine-grained constituents) in Figures 6.2.3.2,4,6,8 is different proportions of muscovite, illite, smectite and chlorite (Figure 6.2.3.1). The fine-grained constituents of the different sandstone units merely consist of detrital mud drapes and authigenic clay minerals. The precursor in Figure 6.2.1.2 consists of the same minerals as the fine-grained constituents found in Figure 6.2.3.1, spectrum 1, 5 and 9.

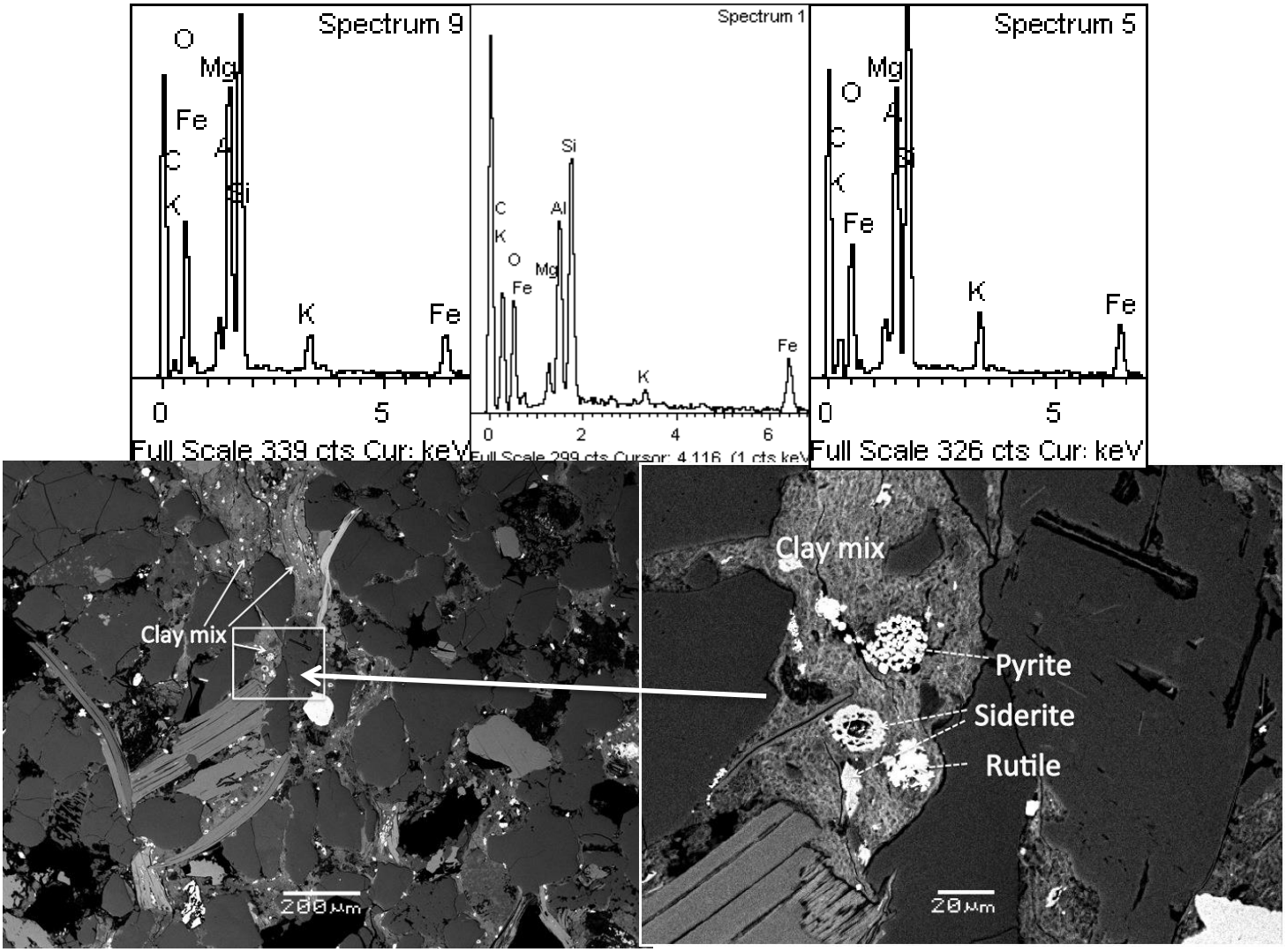


*Figure 6.2.3.1. The chemical compositions of the measured clay mix in three spectrums and how it looks like in SEM micrographs. Spectrums from left – 34/3-1 S – 3901,13 mMD, 34/3-3 S – 3984,06mMD, 34/3-3 S – 3959,06 mMD, Pictures -*

The results from Well 34/3-2 S are presented in Figure 6.2.3.2: Quartz is dominating in all of the samples. There are variations between the amounts of fine-grained constituents, which can reflect the individual thin sections due to the observed mud drapes and mud lamina in the sediments (see Figure 6.2.3.3 c). The colored squares represent different Cook sandstones.

- There are two samples from the C1 sandstone. The lower sample contains high amounts of pore filling clay minerals and low amounts of chlorite coating (see Figure 6.2.3.3 c). The upper sample contains high amounts of chlorite coating and low amounts of pore filling clay minerals (see Figure 6.2.3.3 a). The amount of feldspar is almost the same in both samples.
- The C2 sandstone samples vary in the mineral assemblage. There are high amounts of carbonate cement in particularly 3610,30 m and 3626,50 m (Figure 6.2.3.3 e). In the rest of the samples there is no or very little carbonate cement (Figure 6.2.3.3 a, b) except 3615,05 m.

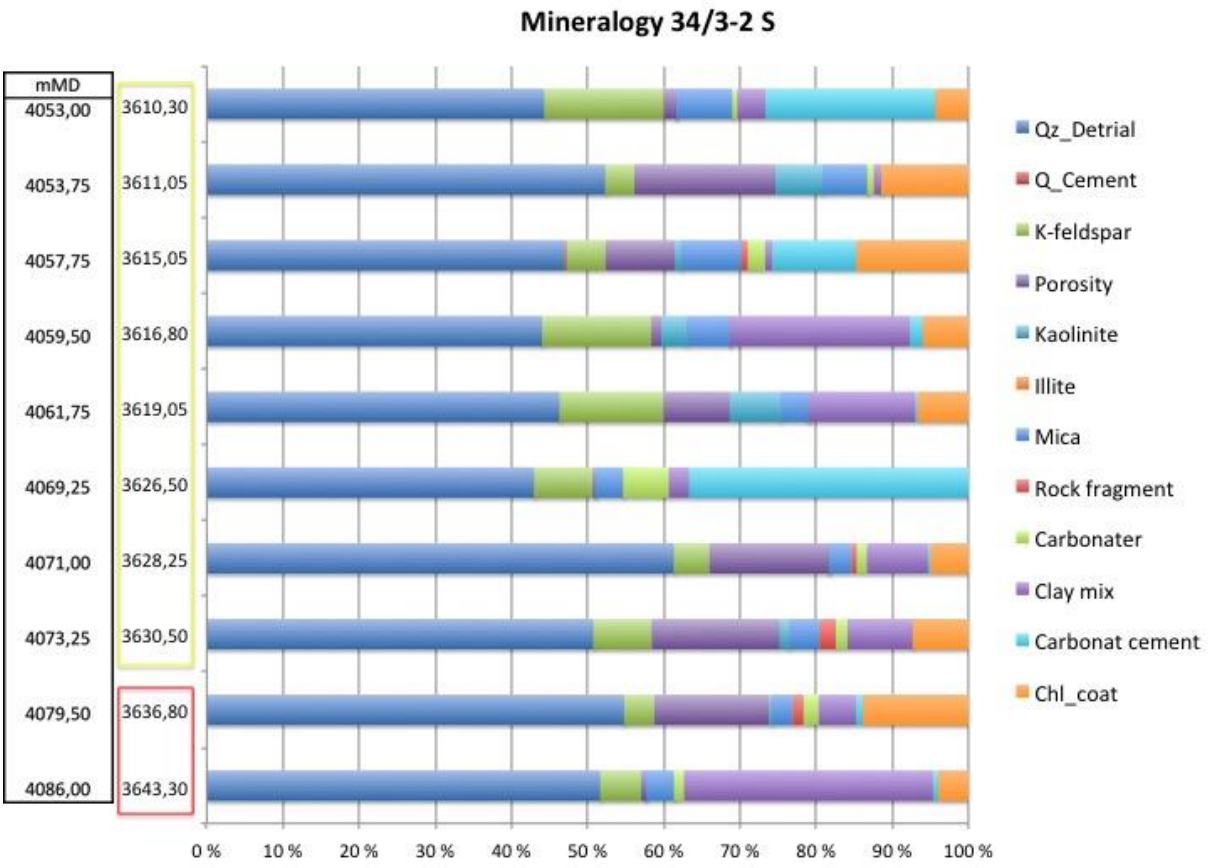


*Figure 6.2.3.2. Observed Mineralogical assemblage in well 34/3-2 S from point counting. The square represents the different Cook sandstones; red: C1 sandstone, yellow: C2 sandstone.*

Chlorite coating cover the grains, even if the samples are filled with carbonate cement (see Figure 6.2.3.3 e). The feldspar content is generally higher in the C2 sandstone than the C1, but differs between the samples. Figure 6.2.3.3 d shows a partly dissolved feldspar grain.

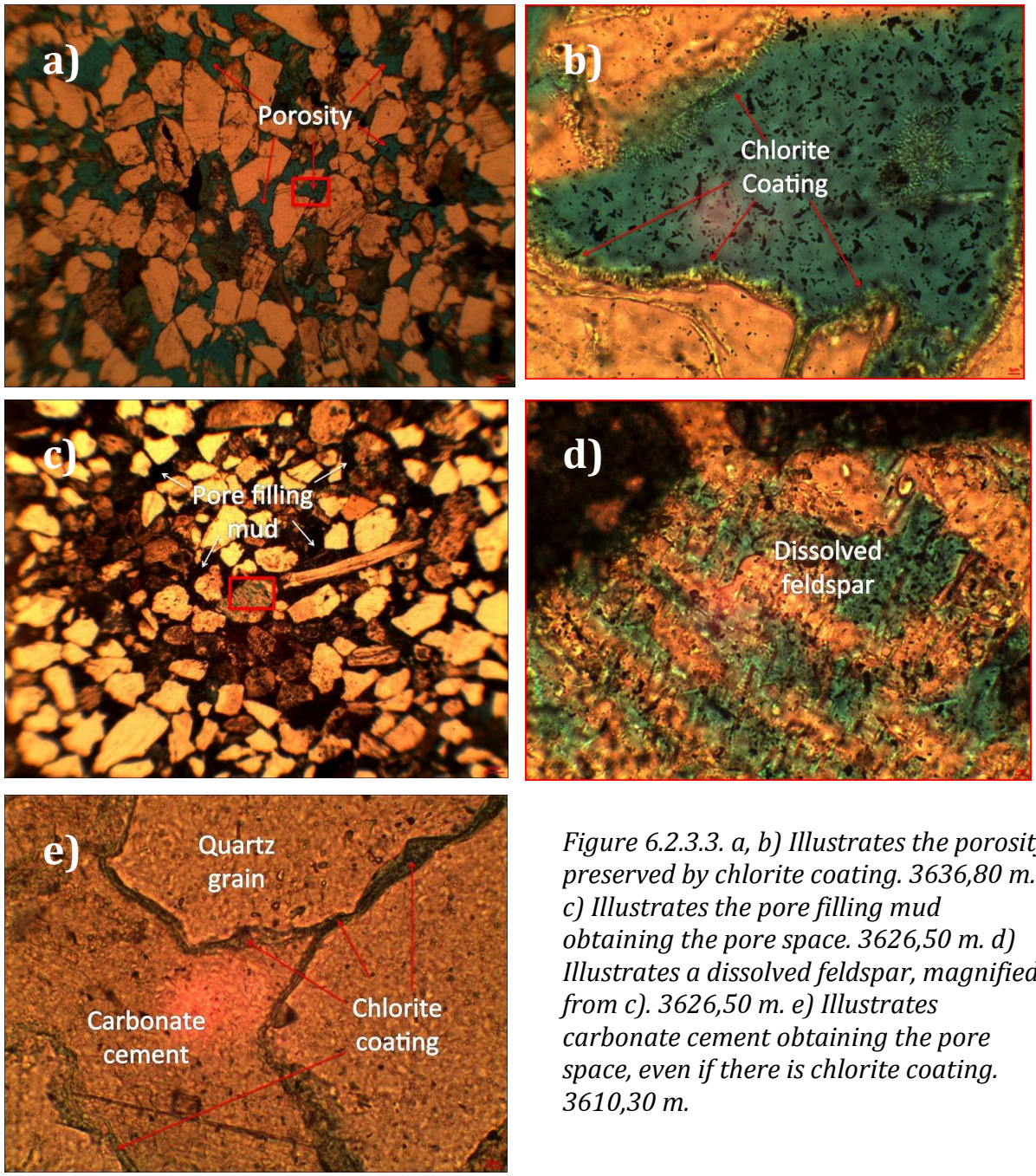


*Figure 6.2.3.3. a, b) Illustrates the porosity preserved by chlorite coating. 3636,80 m. c) Illustrates the pore filling mud obtaining the pore space. 3626,50 m. d) Illustrates a dissolved feldspar, magnified from c). 3626,50 m. e) Illustrates carbonate cement obtaining the pore space, even if there is chlorite coating. 3610,30 m.*

Well 34/3-1 S, as illustrated in Figure 6.2.3.4, is dominated by quartz in all the samples except 3324,20 m and 3338,70 m. However, there are some differences between the sandstone samples with respect to porosity (Figure 6.2.3.5 a, b), carbonate cement (Figure 6.2.3.5 c, d, g) and pore filling fine-grained constituents (Figure 6.2.3.5 e, f):

- There are two samples from the C2 sandstone. The lower samples have higher porosity due to less carbonate cement. The upper sample contains about 33% carbonate cement and almost no porosity.
- The C3 sandstone samples have similar mineral assemblage, except the deepest sample, which contain illite and much less feldspar than the other samples.
- The C4 sandstone samples differ much in the content of carbonate cement and quartz. Sample 3338,70 m contains about 45% carbonate cement (Figure 6.2.3.5 g), 38% detrital quartz and very little porosity. Sample 3338,20 contains about 5% carbonate cement, 59% detrital quartz and about 18% porosity (Figure 6.2.3.5 a, b).
- There are three samples from the C5 sandstone. The lower sample has the highest percentage of carbonate cement (~50%)(Figure 6.2.3.5 g) and the lowest percentage of detrital quartz (~34%) in all the samples from this well.
- The two upper samples contain high amounts of detrital carbonates (15,9% and 20,3%) and authigenic kaolinite (Figure 6.2.3.5 f).

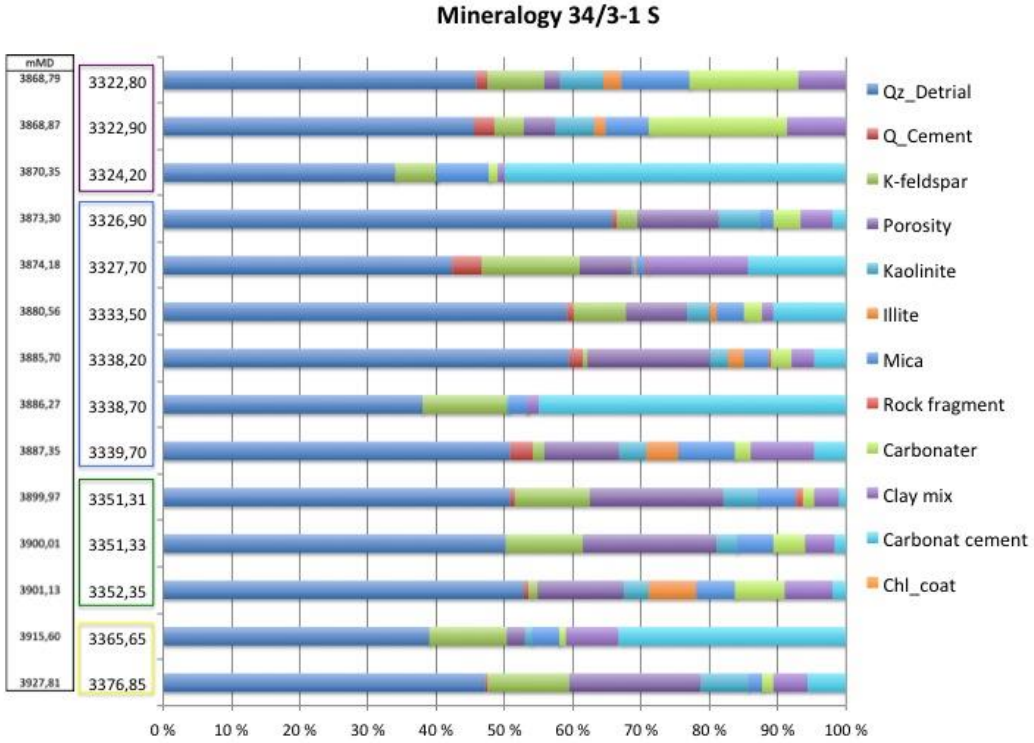


*Figure 6.2.3.4. Observed Mineralogical assemblage in well 34/3-1 S from point counting. The square represents the different Cook sandstones; yellow: C2 sandstone, green: C3 sandstone, blue: C4 sandstone, purple: C5 sandstone.*

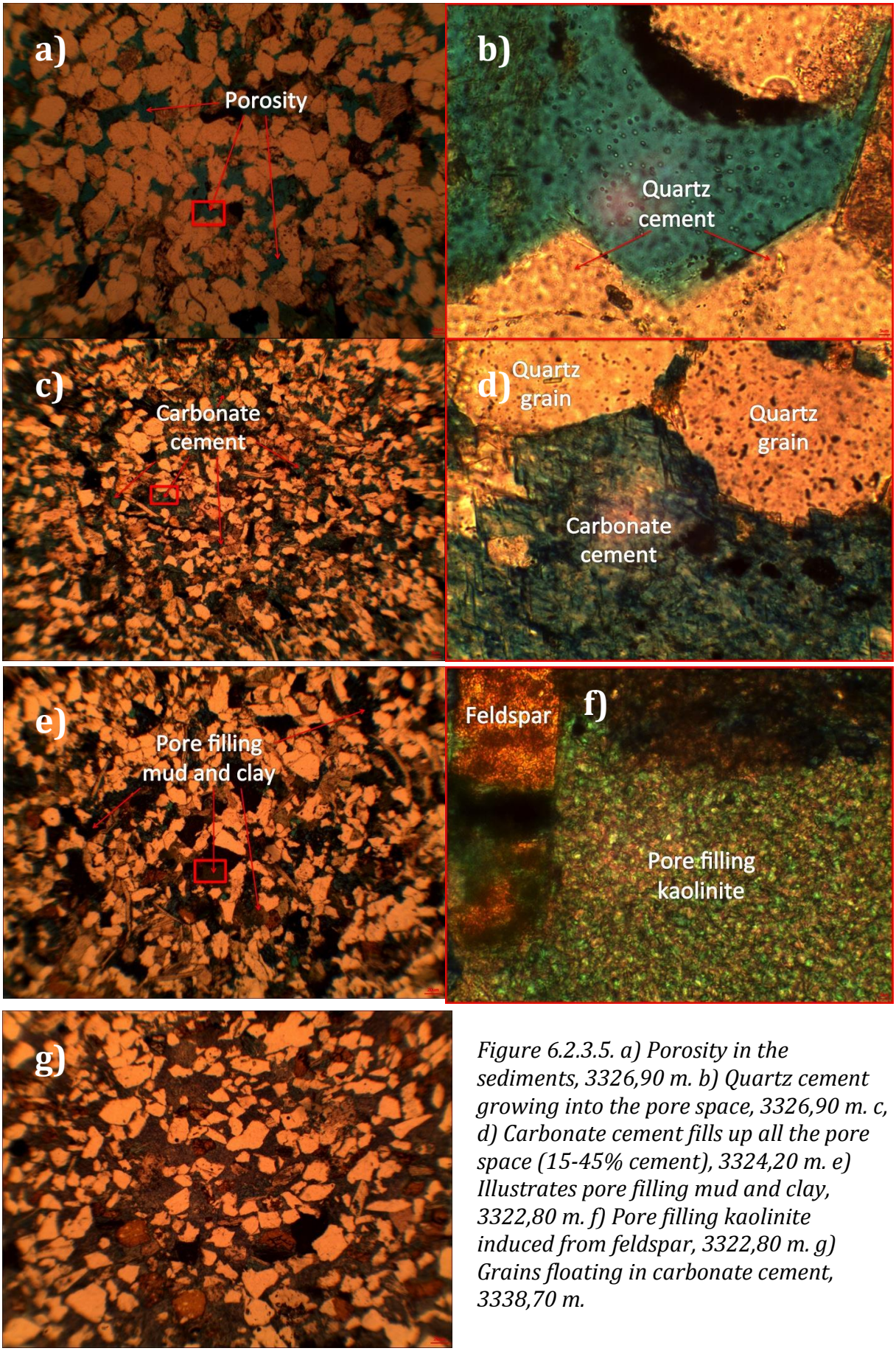


*Figure 6.2.3.5. a) Porosity in the sediments, 3326,90 m. b) Quartz cement growing into the pore space, 3326,90 m. c, d) Carbonate cement fills up all the pore space (15-45% cement), 3324,20 m. e) Illustrates pore filling mud and clay, 3322,80 m. f) Pore filling kaolinite induced from feldspar, 3322,80 m. g) Grains floating in carbonate cement, 3338,70 m.*

Well 34/3-3 S, as illustrated in Figure 6.2.3.6 (below), is dominated by quartz in all the samples. Only sample 3463,10 m distinguish itself from the other samples, with respect to carbonate cement, low porosity, and no chlorite coating (see Figure 6.2.3.7 c, d).

- The C1 sandstone sample contains a high amount of both chlorite coating and pore filling clay minerals (Figure 6.2.3.7 c). The porosity in the sample is not so high.
- The C2 sandstone has less pore filling clay minerals, more chlorite coting and porosity than the C1 sandstone sample (see Figure 6.2.3.7 a, b).
- The C3 sandstone samples have similar mineralogy and differs little between the samples.
- The C4 sandstone samples as mention above has one carbonate cemented sample, 3463,10 m (Figure 6.2.3.7 c, d). Sample 3467 m have little porosity and moderate amounts of pore filling clay minerals (Figure 6.2.3.7 c). The two upper samples have similar mineralogy.

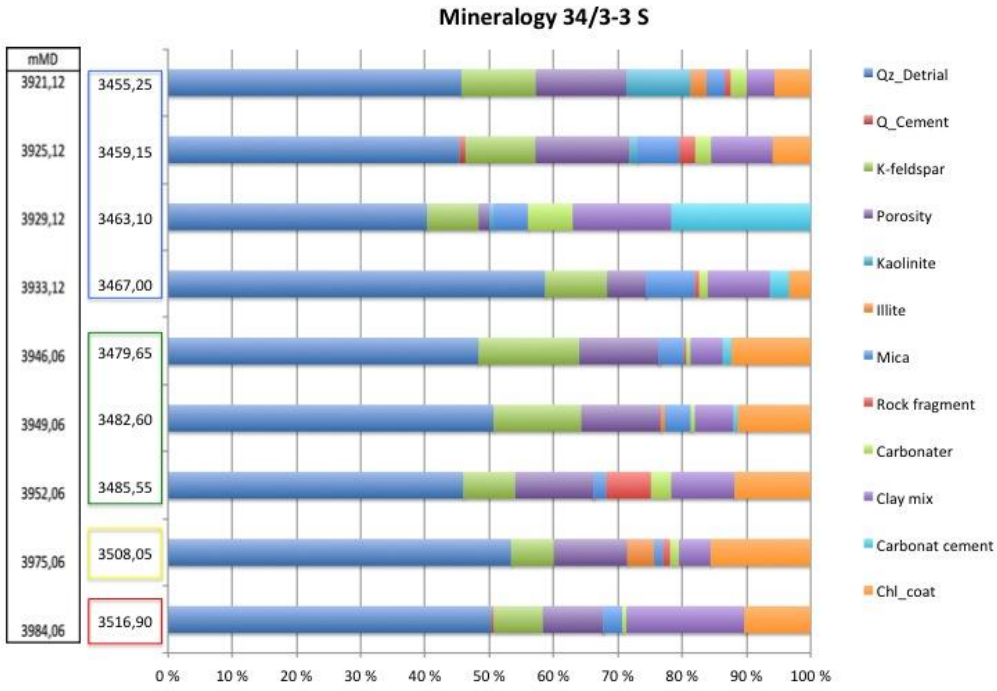


*Figure 6.2.3.6. Observed Mineralogical assemblage in well 34/3-1 S from point counting. The square represents the different Cook sandstones; red: C1 sandstone, yellow: C2 sandstone, green: C3 sandstone, blue: C4 sandstone, purple: C5 sandstone.*

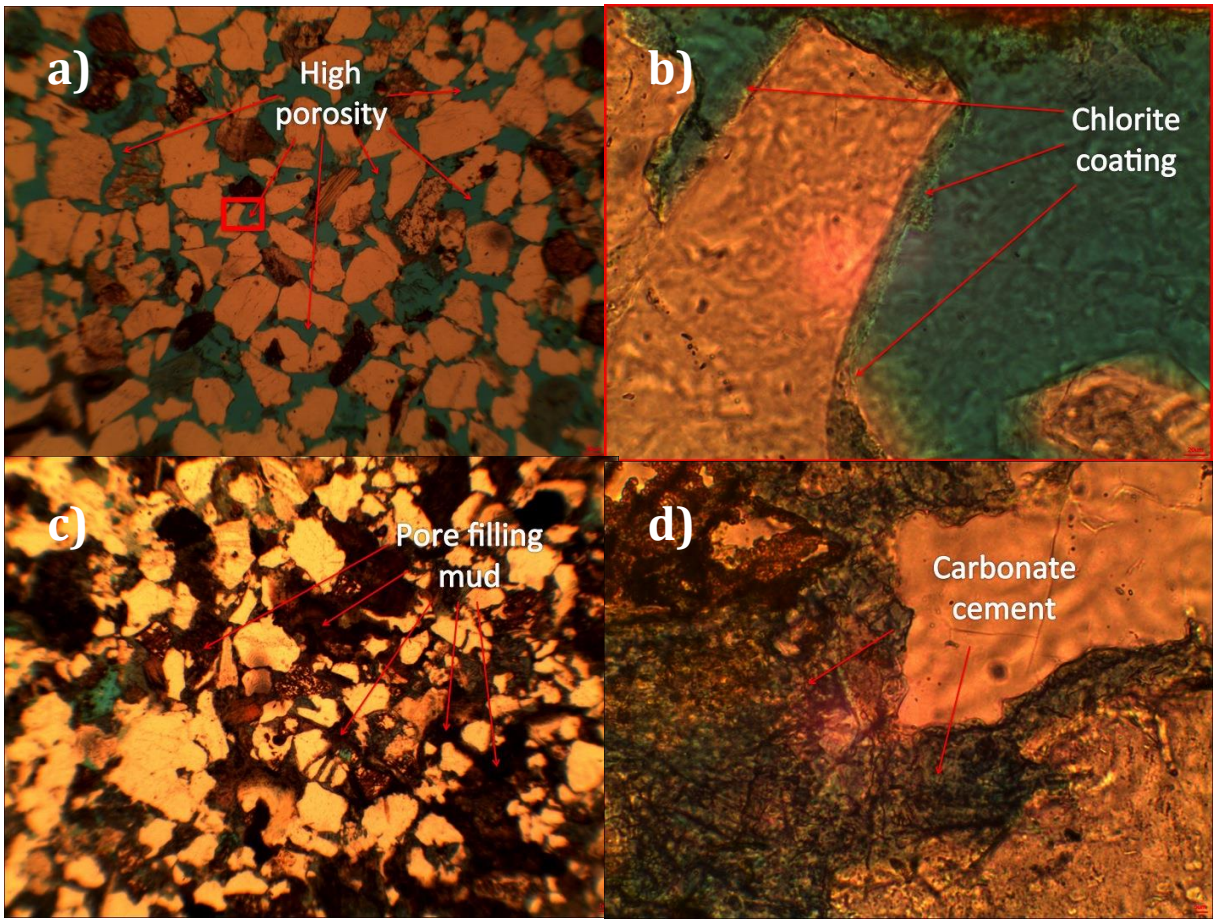


*Figure 6.2.3.7. a) High porosity preserved in the sediments, 3508,05 m. b) High preserving due to chlorite coating, 3508,05 m. c) Pore filling mud obtaining the pore space, 3463,10 m. d) Carbonate cement occupying the pore space, 3463,10 m.*

Well 34/5-1 S, as illustrated in Figure 6.2.3.8 (below), is dominated by quartz in all the samples except 3106,30 m.

- The mineralogical composition differs much in the C1 sandstone samples. The three deepest samples contain moderate to high amounts of chlorite coating. 3107,05 m is the sample that contain the lowest amount of detrital quartz (~30%) in all the samples from all the wells. The same sample has a very high percentage of pore filling kaolinite (~18%). 3106,30 m is dominated by detrital pore filling fine-grained constituents (see Figure 6.2.3.9 a). The upper sample (3105,60 m) contains little chlorite coating, high amounts of detrital mica (~16%) and has almost no porosity.
- The C3 sandstone samples have similar mineralogy in all the samples except 3075,35 m. The three similar samples have moderate to high porosity (see Figure 6.2.3.9 b)

and detrital pore filling mud. The last sample distinguishes from the others, due to high (~21%) content of carbonate cement.

- The C4 sandstone samples have similar mineralogy, high amounts of detrital pore filling mud and mica. Both samples contain no porosity or chlorite coating.

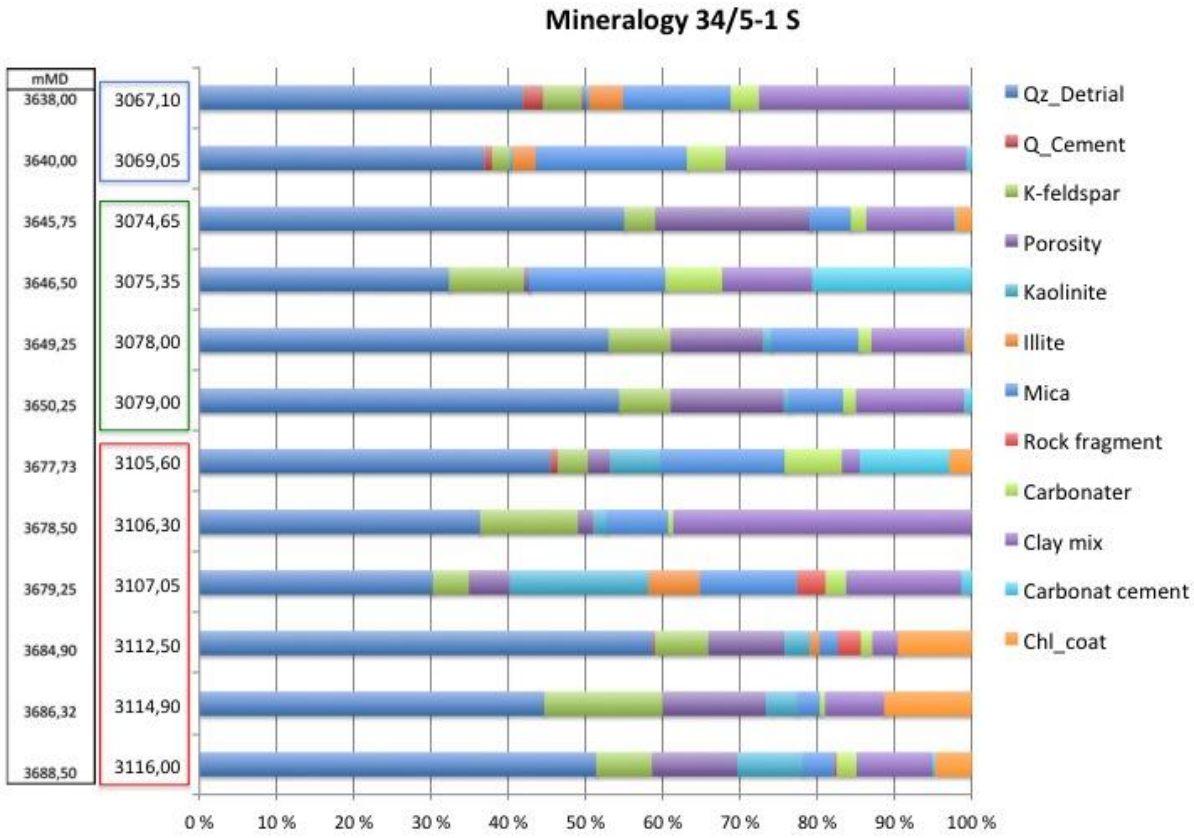


*Figure 6.2.3.8 Observed Mineralogical assemblage in well 34/3-1 S from point counting. The square represents the different Cook sandstones; red: C1 sandstone, green: C3 sandstone, blue: C4 sandstone.*

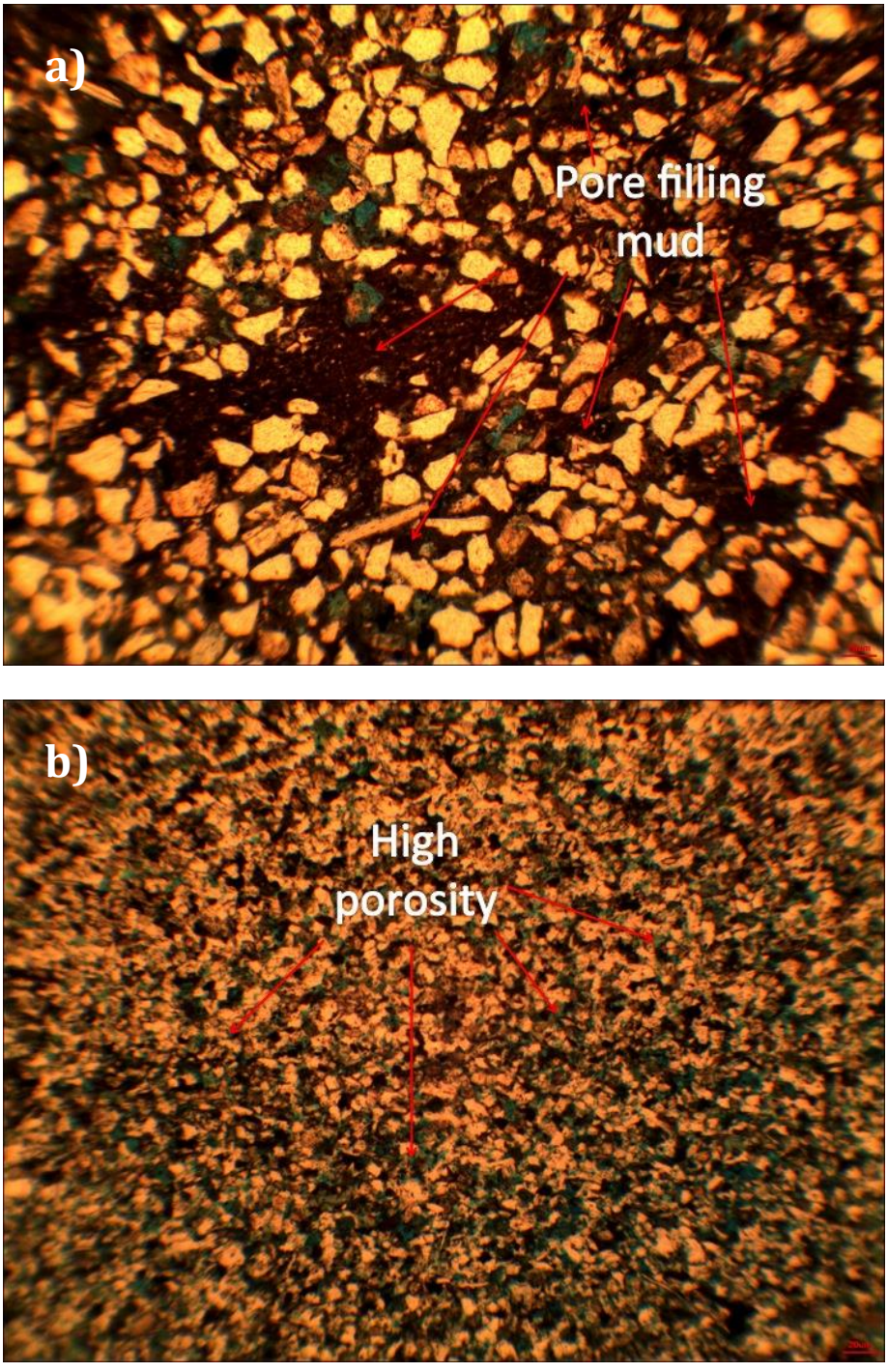


*Figure 6.2.3.9. a) Pore filling mud, destroying porosity, 3069,05 m. b) Preserving of high porosity, even if the grain size is very small (5-10μm), 3079 m.*

The *quartz–feldspar ratio* has been plotted in Figure 6.2.3.10 (below). There are differences in the samples, but quartz dominates throughout the samples. This *ratio* can be used to identify the maturity of the sediments. Especially since the source rock most likely was granitic in the composition (Ziegler, 1982, Underhill, 1998). See Figure 6.2.3.11 for the composition of granite.

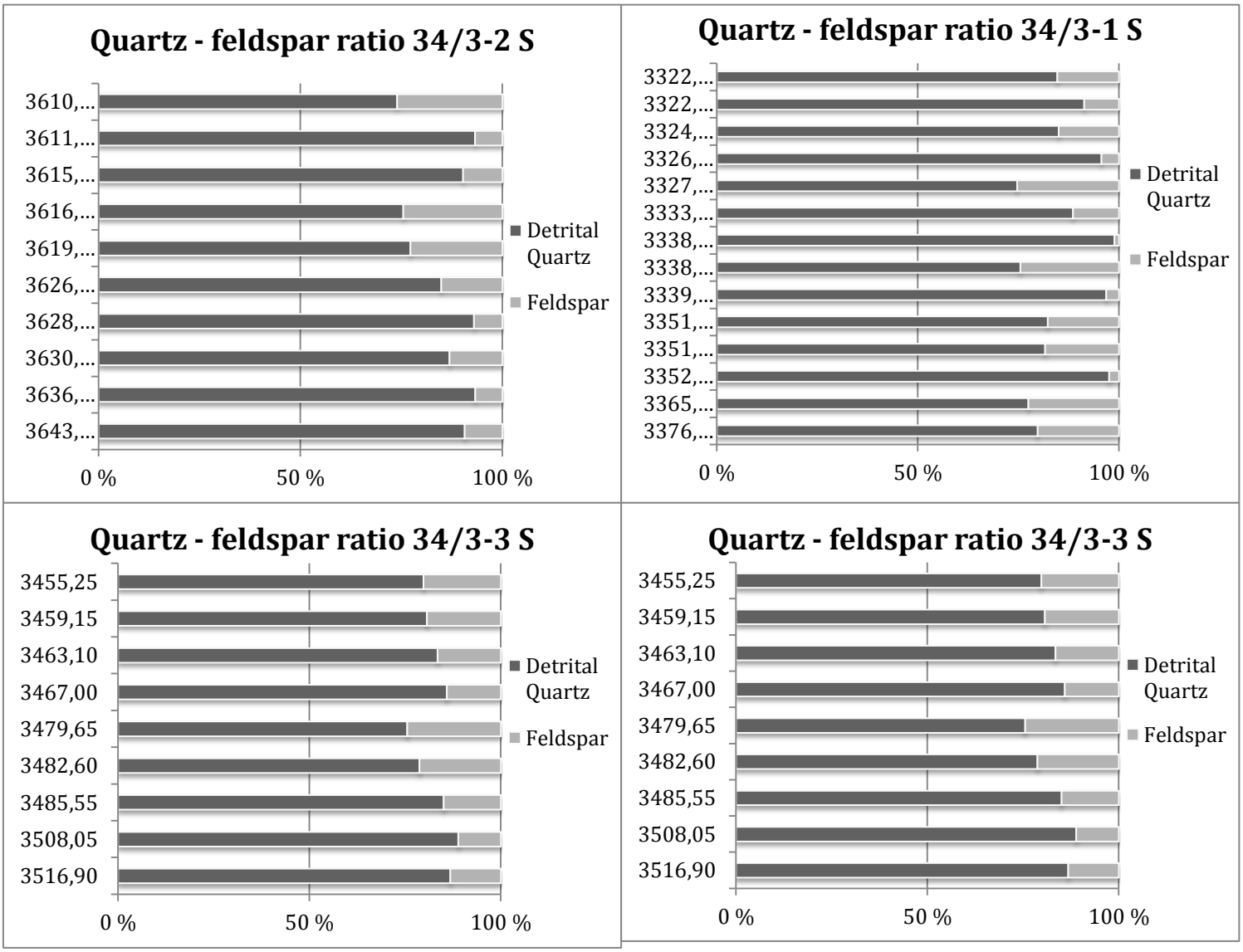


*Figure 6.2.3.10. Quartz – Feldspar ratio from point counting in the different wells. Depth is measured in SSTVD.*

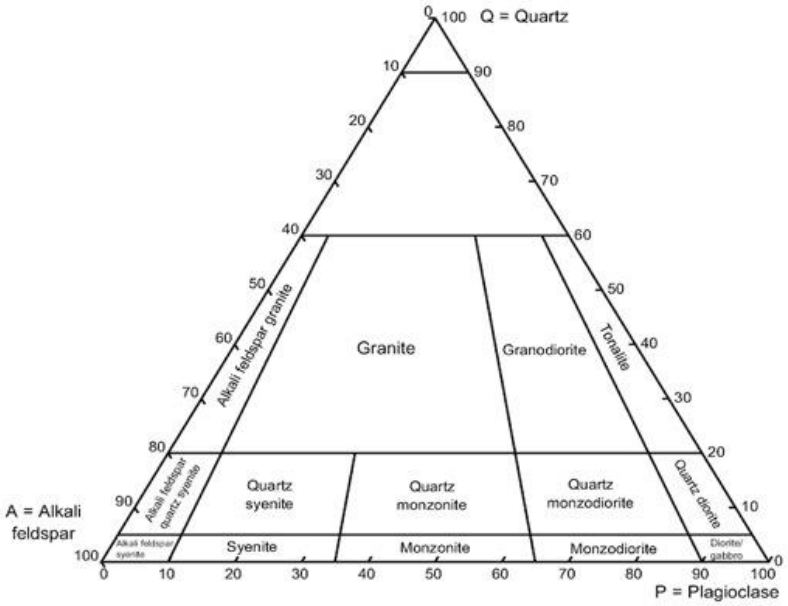


*Figure 6.2.3.11. The Streckeisen diagram shows the composition of a granite, after Streckeisen (1976).*

Figure 6.2.3.12 (below) illustrates the sandstone classification from all the wells:

- The content of matrix < 30µm is generally below 15%, which puts the sediments into the arenite classification. However, there are some samples with a higher percentage representing wacke classification.
- The reason for the occasionally high percentage of matrix < 30µm is due to mud drapes that goes through all of the sandstones.
- The *point counting* focused on the sand and not the mud drapes.

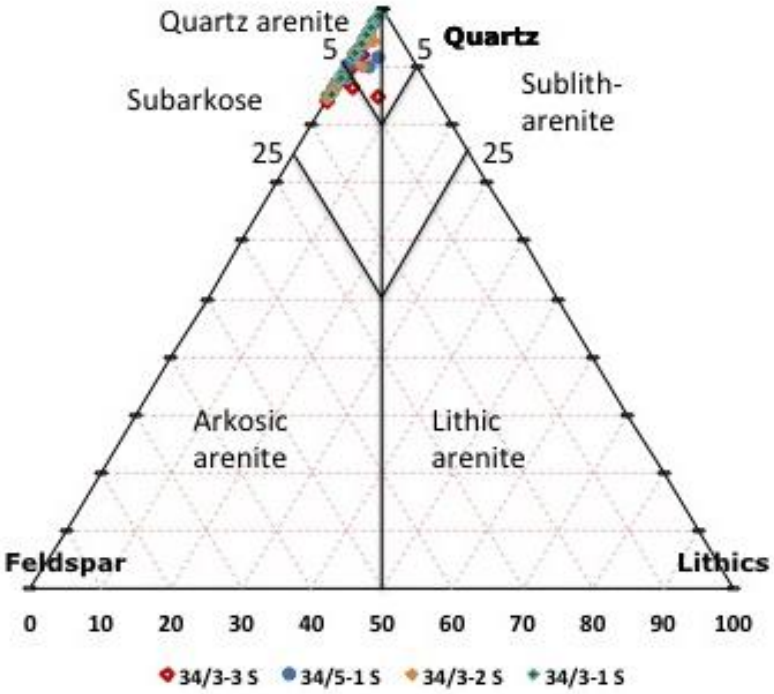


*Figure 6.2.3.12. Sandstone classification after Dott (1964). The samples plot in the quartz arenite and subarkose field.*

IGV values have been calculated from the *point counting* and ranges between 19,9% - 51% in well 34/3-1 S. There are some of the IGV data that is abnormal high and low. The high values are most likely in response to dissolution of carbonate grains replaced by carbonate cement. The low values are most likely in response to high proportion of mud drapes.

Figure 6.2.3.13 (below) show the IGV from all the samples. The average calculated IGV values ranges from 33,4% - 35,4% in the four cores.

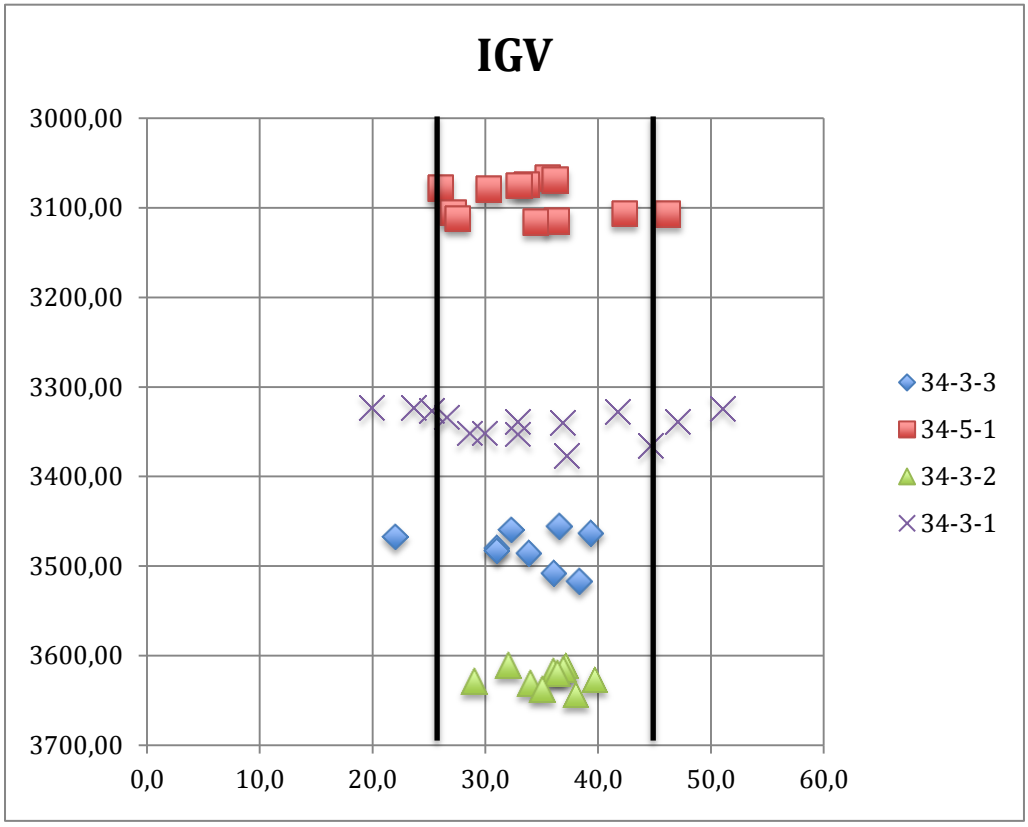


*Figure 6.2.3.13. IGV values from all the sample depths calculated from point counting. The black lines represent the lowest and highest IGV expected in a normal quartz rich arenite.*

Albitization has been observed and Figure 6.2.3.14 illustrates this process where albite is seen to replace K-feldspar (see Eq. 3.1.6.1). Albitization has no direct influence on porosity.

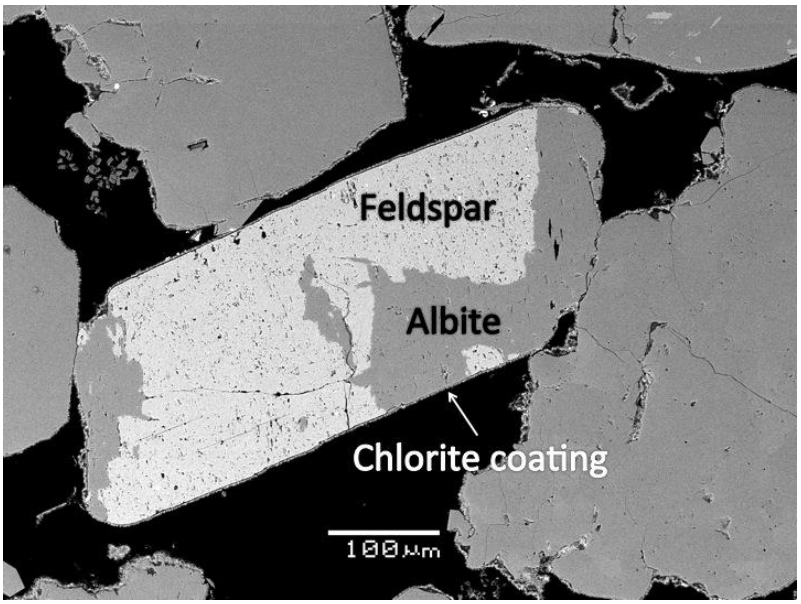


*Figure 6.2.3.14. Albitization of a K-feldspar grain, 34/5-1 S – 3686,32 mMD*

Sample 34/5-1 S - 3688,50 m (Figure 6.2.3.15) show how kaolinite forms from K-feldspar and replaces the grain. The kaolinite starts to build out from a grain, but can also enter the pore space and fill it up and destroy some of the porosity and permeability. Pore filling kaolinite is observed in all the samples, but in various amounts. Small or no amounts of illite formed from kaolinite and K-feldspar are observed.

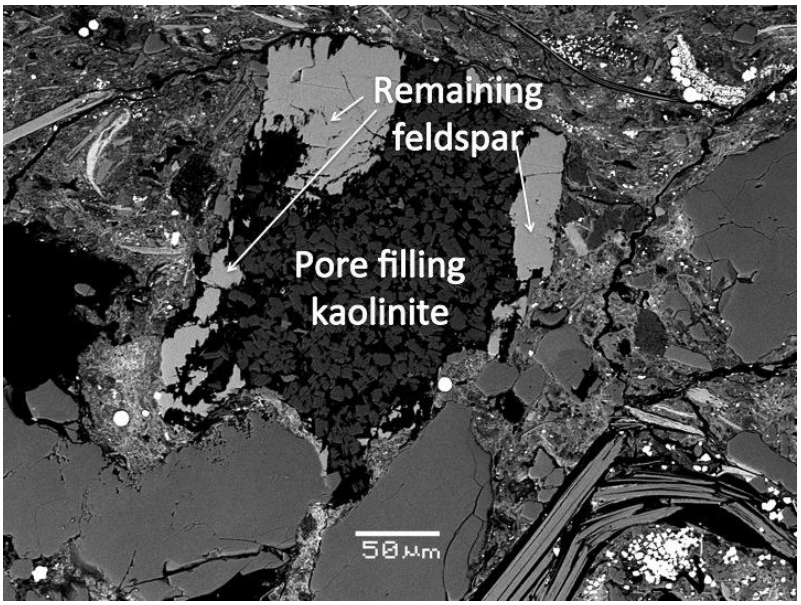


*Figure 6.2.3.15. Pore filling kaolinite in a dissolved K-feldspar grain. 34/5-1 S – 3688,50 mMD*

In various amounts, pyrite and siderite have been observed in all the samples analyzed in SEM (Figure 6.2.3.16). Generally the Fe-rich minerals are often associated with either pore filling detrital clay matrix or mica. This is particularly true for siderite and pyrite cement, due to reducing conditions in the clay matrix.

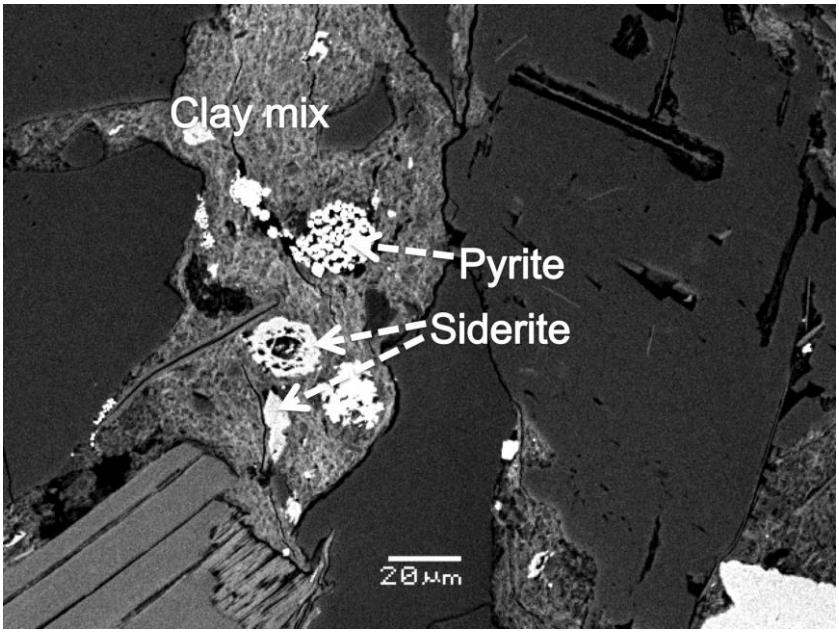


*Figure 6.2.3.16. Formation of Fe- rich minerals inside the clay matrix, due to reducing conditions, 34/3-1 S – 3901,13 mMD.*

Ooids are found in some of the samples (see Figure 6.2.3.17). The presence of ooids is an indication of the water depth, or rather the agitation in the water from waves and tides (Davies et al., 1978). Mixtures of clay in thin layers, some times around a quartz grain, build up these ooids. Inside the detrital clay matrix siderite and pyrite are observed.

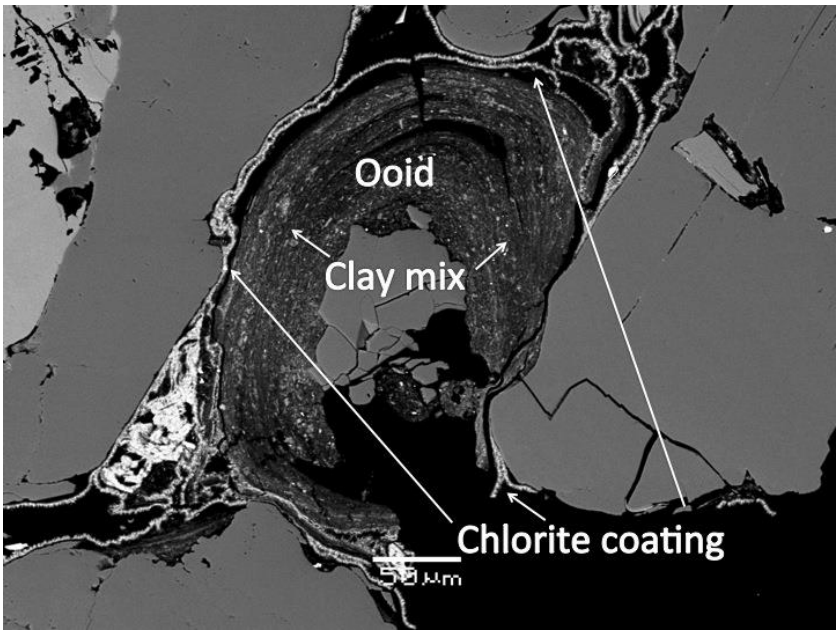


*Figure 6.2.3.17. Ooid pellet, consisting of sheet-like clay minerals around a quartz grain. Chlorite coating covers the ooid, 34/3-3 S – 3984,06 mMD.*

### 6.2.4 Grain size distribution

The different depositional environments are often revealed by their differences in grain size distribution (Klovan, 1966, Visher, 1969). The average grain size and sorting of all the sandstone samples from each well have been plotted in table 6.2.4.1. The total grain size analysis is illustrated in appendix II.

| Well | Sands | Depth – SSTVD | Average grain size | Sorting |
|---|---|---|---|---|
| **34-3-2 S** | C2 | 3610,3 | 298,86 | Well |
| **34-3-2 S** | C2 | 3611,05 | 266,26 | Moderately well |
| **34-3-2 S** | C2 | 3615,05 | 258,74 | Well |
| **34-3-2 S** | C2 | 3616,8 | 270,6 | Well |
| **34-3-2 S** | C2 | 3619,05 | 298,72 | Well |
| **34-3-2 S** | C2 | 3626,5 | 285,22 | Well |
| **34-3-2 S** | C2 | 3628,25 | 538,76 | Well |
| **34-3-2 S** | C2 | 3630,5 | 422,92 | Well |
| **34-3-2 S** | C1 | 3636,8 | 332,38 | Moderately well |
| **34-3-2 S** | C1 | 3643,3 | 309,834 | Moderately well |
| | | | | |
| **34-3-1 S** | C5 | 3322,8 | 242,34 | - |
| **34-3-1 S** | C5 | 3322,9 | 210,28 | - |
| **34-3-1 S** | C5 | 3324,2 | 184,7 | Moderately well |
| **34-3-1 S** | C4 | 3326,9 | 353,06 | Well |
| **34-3-1 S** | C4 | 3327,7 | 379,74 | Well |
| **34-3-1 S** | C4 | 3333,5 | 342,5 | Well |
| **34-3-1 S** | C4 | 3338,2 | 271,28 | Well |
| **34-3-1 S** | C4 | 3338,7 | 316,48 | Well |
| **34-3-1 S** | C4 | 3339,7 | 283,02 | Moderately well |
| **34-3-1 S** | C3 | 3351,31 | 278,06 | Well |
| **34-3-1 S** | C3 | 3351,33 | 298,12 | Well |
| **34-3-1 S** | C3 | 3352,35 | 252,78 | Moderately well |
| **34-3-1 S** | C2 | 3365,65 | 306,42 | Well |
| **34-3-1 S** | C2 | 3376,85 | 256,34 | Well |
| | | | | |
| **34-3-3 S** | C4 | 3455,25 | 374,84 | Well |
| **34-3-3 S** | C4 | 3459,15 | 350,2 | Well |
| **34-3-3 S** | C4 | 3463,1 | 331,62 | Moderately well |
| **34-3-3 S** | C4 | 3467 | 343,06 | Well |
| **34-3-3 S** | C3 | 3479,65 | 319,46 | Well |
| **34-3-3 S** | C3 | 3482,6 | 492,54 | Moderately well |
| **34-3-3 S** | C3 | 3485,55 | 619,86 | Moderately well |

| | | | | |
|---|---|---|---|---|
| **34-3-3 S** | C2 | 3508,05 | 450,82 | Well |
| **34-3-3 S** | C1 | 3516,9 | 622,3 | Moderately well |
| | | | | |
| **34-5-1 S** | C4 | 3067,1 | 79,8 | Well |
| **34-5-1 S** | C4 | 3069,05 | 70,9 | Moderately well |
| **34-5-1 S** | C3 | 3074,65 | 76,6 | Well |
| **34-5-1 S** | C3 | 3075,35 | 74,44 | Well |
| **34-5-1 S** | C3 | 3078 | 61,58 | Moderately |
| **34-5-1 S** | C3 | 3079 | 58,14 | Poorly |
| **34-5-1 S** | C1 | 3105,6 | 200,92 | Well |
| **34-5-1 S** | C1 | 3106,3 | 224,4 | Moderately well |
| **34-5-1 S** | C1 | 3107,05 | 284,6 | Well |
| **34-5-1 S** | C1 | 3112,5 | 553,6 | Well |
| **34-5-1 S** | C1 | 3114,9 | 414,48 | Moderately |
| **34-5-1 S** | C1 | 3116 | 342,28 | Moderately |

*Table 6.2.4.1. Average grain size distribution and sorting of all the sandstone samples in the four wells.*

### 6.2.5 X-Ray Diffraction (XRD)

Bulk and clay fraction XRD was provided by BG. All the samples that were given are presented in Table 6.2.5.1&2 (below).

| Depth | 34/3-2 S Quartz | Feldspar | Kaolinite | Illite | Mica | Carbonate | Chlorite | Pyrite |
|---|---|---|---|---|---|---|---|---|
| **4053.00** | 39,9 | 9,0 | 1,7 | 0.3 | 8,8 | 35,7 | 4,7 | 0,0 |
| **4058.50** | 38,0 | 7,0 | 1,8 | 0.2 | 14,3 | 34,4 | 4,4 | 0,0 |
| **4065.70** | 56,9 | 16,7 | 2,7 | 0.1 | 14,4 | 1,0 | 8,2 | 0,0 |
| **4071.00** | 67,9 | 9,4 | 2,1 | 0.3 | 13,5 | 2,1 | 4,9 | 0,0 |
| **4076.00** | 72,5 | 12,2 | 2,7 | 0.2 | 6,5 | 1,0 | 4,9 | 0,0 |
| **4079.50** | 71,2 | 9,1 | 1,8 | TR | 8,7 | 0,8 | 8,4 | 0,0 |
| | **34/3-1 S** | | | | | | | |
| **3868.69** | 39,6 | 11,4 | 21,9 | 0,3 | 12,1 | 11,8 | 2,9 | 0,0 |
| **3868.74** | 40,2 | 8,5 | 20,2 | 0,3 | 12,5 | 13,9 | 3,1 | 1,2 |
| **3868.79** | 37,2 | 9,5 | 23,0 | 0,4 | 11,4 | 14,8 | 3,9 | 0,0 |
| **3868.84** | 40,5 | 6,5 | 23,3 | TR | 12,3 | 14,4 | 3,0 | 0,0 |
| **3868.87** | 39,3 | 7,5 | 21,8 | 0,2 | 11,8 | 16,8 | 2,6 | 0,0 |
| **3874.18** | 55,4 | 8,3 | 10,1 | 0,0 | 12,8 | 11,7 | 1,7 | 0,0 |
| **3877.54** | 64,3 | 10,2 | 11,7 | 0,0 | 4,4 | 7,0 | 2,4 | 0,0 |
| **3880,56** | 59,5 | 9,4 | 9,9 | 0,3 | 8,1 | 10,8 | 2,0 | 0,0 |
| **3880.65** | 51,5 | 11,3 | 10,8 | 0,7 | 8,6 | 13,9 | 2,5 | 0,7 |

| | | | | | | | | |
|---|---|---|---|---|---|---|---|---|
| **3883,17** | 58,1 | 13,0 | 11,0 | TR | 5,6 | 9,9 | 2,3 | 0,0 |
| **3883,22** | 59,2 | 11,1 | 9,4 | 0,2 | 4,8 | 13,5 | 1,3 | 0,7 |
| **3883,27** | 58,4 | 9,5 | 10,0 | 0,0 | 7,4 | 12,5 | 2,0 | TR |
| **3886,27** | 34,3 | 6,9 | 4,7 | 0,3 | 4,0 | 48,1 | 1,6 | 0,0 |
| **3896,44** | 55,3 | 16,9 | 5,3 | 0,0 | 14,1 | 4,5 | 3,7 | 0,0 |
| **3896,47** | 52,4 | 13,8 | 8,3 | 0,0 | 14,5 | 4,3 | 6,7 | 0,0 |
| **3899,97** | 61,4 | 17,9 | 5,7 | 0,0 | 6,3 | 3,9 | 4,8 | 0,0 |
| **3900,01** | 61,5 | 12,9 | 8,4 | 0,0 | 7,1 | 3,6 | 6,5 | 0,0 |
| **3911,76** | 62,4 | 11,9 | 6,5 | 0,0 | 10,8 | 3,0 | 5,4 | 0,0 |
| **3918,44** | 66,9 | 15,5 | 4,5 | 0,0 | 6,6 | 2,3 | 4,2 | 0,0 |
| **3924,47** | 61,4 | 12,1 | 5,5 | 0,0 | 8,6 | 2,6 | 9,8 | 0,0 |
| **3927,76** | 57,9 | 23,0 | 6,0 | 0,0 | 3,9 | 3,1 | 6,1 | 0,0 |
| **3927,81** | 67,0 | 13,7 | 6,3 | 0,0 | 3,4 | 2,3 | 7,3 | 0,0 |
| | **34/3-3 S** | | | | | | | |
| **3915,80** | 63,2 | 11,7 | 5,7 | 0,0 | 9,6 | 4,9 | 4,9 | 0,0 |
| **3917,80** | 48,4 | 9,5 | 7,4 | 0,0 | 20,7 | 5,1 | 8,9 | 0,0 |
| **3921,12** | 69,4 | 9,8 | 5,9 | 0,0 | 8,6 | 0,6 | 5,7 | 0,0 |
| **3924,12** | 55,3 | 22,2 | 5,0 | 0,0 | 9,3 | 1,9 | 6,3 | 0,0 |
| **3925,12** | 60,2 | 10,8 | 7,3 | 0,0 | 12,9 | 3,4 | 5,4 | 0,0 |
| **3929,12** | 28,7 | 11,0 | 7,8 | 0,0 | 30,3 | 8,9 | 12,4 | 0,9 |
| **3933,12** | 60,0 | 13,1 | 4,8 | 0,0 | 10,0 | 3,2 | 8,9 | 0,0 |
| **3947,06** | 61,0 | 15,5 | 2,6 | 0,0 | 8,7 | 5,5 | 6,7 | 0,0 |
| **3949,06** | 70,9 | 10,3 | 1,6 | 0,0 | 7,8 | 3,5 | 5,9 | 0,0 |
| **3952,06** | 73,4 | 9,7 | 0,4 | 0,0 | 7,9 | 3,9 | 4,7 | 0,0 |
| **3959,06** | 70,0 | 15,5 | 1,3 | 0,0 | 8,5 | 0,4 | 4,3 | 0,0 |
| **3965,06** | 71,3 | 14,6 | 2,7 | 0,0 | 6,6 | 0,3 | 4,5 | 0,0 |
| **3984,06** | 76,2 | 8,7 | 0,5 | 0,0 | 8,1 | 0,4 | 6,1 | 0,0 |

*Table 6.2.5.1. Bulk XRD results from three of the four wells, in mMD. TR = Traces*

| | **34/3-2 S** | | | | | |
|---|---|---|---|---|---|---|
| **Depth** | **Illite/smectite** | **Illite** | **Kaolinite** | **Chlorite** | **Quartz** | **Carbonate** |
| **4053.00** | 6,6 | 7,3 | 14,2 | 70,4 | 1,5 | 0,0 |
| **4058.50** | 3,8 | 13,1 | 7,4 | 68,9 | 0,9 | 5,9 |
| **4065.70** | 1,8 | 8,9 | 11,5 | 76,2 | 1,6 | 0,0 |
| **4071.00** | 4,9 | 8,1 | 10,1 | 73,8 | 3,0 | 0,0 |
| **4076.00** | 3,0 | 7,1 | 11,9 | 75,8 | 2,2 | 0,0 |
| **4079.50** | Tr | 9,8 | 9,7 | 76,8 | 3,7 | 0,0 |
| | **34/3-1 S** | | | | | |
| **3868.69** | 6,5 | 14,7 | 67,4 | 9,1 | 2,3 | 0,0 |
| **3868.74** | 6,1 | 11,1 | 68,9 | 6,2 | 2,7 | 4,8 |
| **3868.79** | 5,5 | 13,8 | 68,5 | 10,0 | 2,3 | 0,0 |

| | | | | | | |
|---|---|---|---|---|---|---|
| **3868.84** | Tr | 14,2 | 73,9 | 9,6 | 2,3 | 0,0 |
| **3868.87** | 4,1 | 14,5 | 70,9 | 8,1 | 2,4 | 0,0 |
| **3874.18** | 0,0 | 22,3 | 64,7 | 10,0 | 3,0 | 0,0 |
| **3877.54** | 0,0 | 13,1 | 75,5 | 8,1 | 3,3 | 0,0 |
| **3880,56** | 6,7 | 16,4 | 65,7 | 8,0 | 3,2 | 0,0 |
| **3880.65** | 10,7 | 15,6 | 62,7 | 7,3 | 3,6 | 0,0 |
| **3883,17** | Tr | 18,9 | 67,8 | 8,9 | 4,4 | 0,0 |
| **3883,22** | 6,0 | 13,4 | 63,3 | 7,2 | 4,6 | 5,4 |
| **3883,27** | 0,0 | 19,7 | 61,8 | 7,6 | 5,0 | 6,0 |
| **3886,27** | 7,6 | 17,4 | 40,5 | 8,2 | 3,9 | 22,5 |
| **3896,44** | 0,0 | 9,4 | 52,1 | 37,3 | 1,2 | 0,0 |
| **3896,47** | 0,0 | 16,1 | 46,4 | 35,5 | 1,9 | 0,0 |
| **3899,97** | 0,0 | 14,8 | 49,9 | 30,4 | 5,0 | 0,0 |
| **3900,01** | 0,0 | 11,3 | 51,2 | 35,7 | 1,7 | 0,0 |
| **3911,76** | 0,0 | 15,8 | 47,6 | 32,7 | 3,9 | 0,0 |
| **3918,44** | 0,0 | 15,1 | 46,1 | 36,5 | 2,2 | 0,0 |
| **3924,47** | 0,0 | 11,1 | 36,3 | 51,1 | 1,6 | 0,0 |
| **3927,76** | 0,0 | 9,9 | 54,2 | 33,9 | 2,0 | 0,0 |
| **3927,81** | 0,0 | Tr | 58,2 | 39,6 | 2,2 | 0,0 |
| | **34/3-3 S** | | | | | |
| **3915,80** | 0,0 | 10,0 | 66,0 | 22,0 | 2,0 | 0,0 |
| **3917,80** | 0,0 | 16,0 | 59,0 | 22,0 | 3,0 | 0,0 |
| **3921,12** | 0,0 | 8,0 | 70,0 | 19,0 | 3,0 | 0,0 |
| **3924,12** | 0,0 | 9,0 | 70,0 | 18,0 | 3,0 | 0,0 |
| **3925,12** | 0,0 | 6,0 | 80,0 | 12,0 | 3,0 | 0,0 |
| **3929,12** | 0,0 | 33,0 | 32,0 | 27,0 | 4,0 | 3,5 |
| **3933,12** | 0,0 | 11,0 | 53,0 | 33,0 | 3,0 | 0,0 |
| **3947,06** | 0,0 | 15,0 | 23,0 | 59,0 | 2,0 | 0,0 |
| **3949,06** | 0,0 | 14,0 | 19,0 | 65,0 | 2,0 | 0,0 |
| **3952,06** | 0,0 | 12,0 | 16,0 | 68,0 | 3,0 | 0,0 |
| **3959,06** | 0,0 | 15,0 | 35,0 | 45,0 | 5,0 | 0,0 |
| **3965,06** | 3,0 | 11,0 | 44,0 | 41,0 | 2,0 | 0,0 |
| **3984,06** | 0,0 | 7,0 | 13,0 | 79,0 | 1,0 | 0,0 |

*Table 6.2.5.2. XRD clay fraction results from three of the four wells, in mMD. Tr = Traces*

# *Chapter 7 – Discussion*

## 7.1 Introduction

This chapter will bring chapter 5 and 6 together and put different angles on the main purpose. Chlorite coating are observed (Figure 6.2.3.2,4,6,8 represent the four wells) in three of the four wells through the method of *point counting* (not observed in 34/3-1 S). Bulk XRD results (Table 6.2.5.1) show a high content of kaolinite in the C5 sandstone samples of 34/3-1 S. Clay fraction XRD results (Table 6.2.5.2) show very high amounts of kaolinite in 34/3-1 S and 34/3-3 S. In 34/3-2 S there is low amounts of kaolinite, but very high amounts of chlorite.

The mineralogy differs between the samples both vertically in the cores and lateral between the cores. However the *quartz – feldspar* ratio (Figure 6.2.3.10) show a general trend of maturity, due to high content of quartz. There is not observed any terrestrial organic material in the cores, e.g. coal, which could imply the distance to shore and the reworking processes of the sediments.

The connection between the depositional environment and the porosity preserving chlorite coating will no be discussed.

## 7.2 Depositional environment

All of the sandstones represented in the different cores could represent the same depositional environment with several sub environments. Mud drapes and sand dunes repeat it self vertically throughout all the cores. The Cook Formation consists of wide lateral sandstone packages (Vollset and Doré, 1984, Marjanac and Steel, 1997, Folkestad et al., 2012). As mentioned in chapter 2, the climate changed in the Early Jurassic from semi-arid to more humid. This led to an increase of erosion and deep weathering of the Caledonian orogeny. The eroded and weathered sediments were transported out into the continental shelf through the fluvial systems. Granitic rocks contain high amounts of feldspar (see Figure 6.2.3.11) (Streckeisen, 1976). The Cook Formation sandstones have a general trend of high *quartz – feldspar* ratio (see Figure 6.2.3.10). In the weathering of the granitic source rock, much of the feldspar must have been dissolved and transported out as clay minerals instead of grains.

The iron-rich chlorite coating indicates that the depositional environment had to be relatively close to a fluvial system, due to the need of iron in the formation of the precursor. The amount of iron decreases in more distal deposits due to the density of iron rich minerals (Ehrenberg, 1993).

The Cook Formation could have been deposited from one big sediment system like e.g. the Sognefjord, and reworked by the tidal system. Vollset and Doré (1984) shows that the Cook Formation is extensive and found in the northern Horda platform and throughout the East Shetland Basin. This indicates that there could have been several systems supplying the sediments, due to the extensive lateral distribution of the Cook Formation.

There has not been observed any root-traces e.g. mangrove plants or terrestrial organic material like coal in the cores and samples. This could indicate that the depositional environment was further out from the shore and that the sediments have been reworked. Livbjerg and Mjøs (1989) concludes the Cook sandstones in the Oseberg area to be offshore sand ridges. This corresponds to the interpreted distance to shore of the depositional environment. The slightly upwards-coarsening sandstone units, which contain kaolinite and chlorite, indicate that the distance from the shore is not far away. Diagenetic kaolinite forms when percolating groundwater flows through the sediments (Bjørlykke, 1994) (see chapter 3).

### 7.2.1 Grain size and deposition

The results from the grain size analysis (Table 6.2.4.1) show a general trend of medium to coarse sand grains in all the cores, except 34/5-1 S, which constitutes very fine sand and silt in some of the samples. Table 6.2.4.1 show both upwards coarsening and upwards fining units inside the different sandstones.

- The sandstones in the cored interval in well 34/3-2 S, are interpreted to have been deposited in a nearshore delta slope environment. The C1 sandstone looks upwards coarsening and the C2 sandstone look aggradational in grain size (Table 6.2.4.1) and gamma log (Figure 5.4.10.1). However there are some challenges related to this interpretation. The grain size is analyzed in *thin sections* and meters separate these *thin sections,* which can give wrong data of the development of the grain size

distribution. However, the gamma log (Figure 5.4.10.1) and the digitalized cored interval (Figure 5.4.1.1) matches the observed grain size results. It is important to mention that there were only two samples analyzed from the C1 sandstone, but the samples are in conformity with the cored interval (Figure 5.4.1.1).

- The sandstones in the cored interval in well 34/3-1 S, are interpreted to have been deposited in a pro delta-nearshore delta slope setting as compound dunes and tidal bars. Each sandstone shows an upward coarsening grain size trend (Table 6.2.4.1). The digitalized cored interval (Figure 5.4.2.1) and the gamma log (Figure 5.4.10.1) show the same trend. The sandstones could represent stages of regression, and the mudstone flooding surfaces. All the sandstones have a sharp transition to the underlying and overlying mudstone (see Figure 5.4.10.1), which could be interpreted as tidal channels (Reineck and Singh, 1975). However the sandstones are not upwards fining, but rather upwards coarsening, that again leads to the interpretation of migrating tidal bars and prograding compound dunes. Yoshida et al. (1999) concludes that the offshore, upwards coarsening sandstones of the Tilje Formation, Mid-Norway are tidal sandbars deposited as part of a macrotidal estuary.

- The sandstones in the cored interval of 34/3-3 S, are interpreted to have been deposited in a pro delta-delta front setting as tidal bars and compound dunes. The grain size analysis (Table 6.2.4.1) shows that the sand-grains in the lower part of the cored interval are larger than the grains in the upper part. This could indicate a rise in the relative sea level from the lower part to the upper part of the cored interval. There is important to note that the mudstone separating the C3 and C4 sandstones is thicker than the mudstone separating the C3 and C4 sandstones in 34/3-1 S and 34/3-2 S. This could imply that the deposition of the mudstone between the C3 and C4 sandstone in well 34/3-3 S was more distal from shore then the two eastwards. The average grain size in the sandstones is larger in well 34/3-3 S compared to the other wells, indicating higher energy and potentially more proximal location of deposition. All of the sandstones in well 34/3-3 S are upwards coarsening. The transitions between all the underlying mudstones to the sandstones are generally smooth. This insinuates an alternating deposition of regression and transgression,

which could be due to fluctuation of the relative sea level. This interpretation are also found in Charnock et al. (2001) of the Cook Formation in northern North Sea.

- The sandstones in the cored interval of 34/5-1 S, are interpreted to have been deposited in a nearshore delta slope setting as both upward coarsening and fining units. The grain size in the C1 sandstone (Table 6.2.4.1) shows a distinct difference with the C3 sandstone. The C1 sandstone consists of medium and coarse sand, while the C3 sandstone consists of silt and very fine sand. This could imply that there was an increase in the relative sea level between the depositions of the two sandstones. Based on the gamma log (Figure 5.4.10.1) and digitalized core interval (Figure 5.4.4.1); the C1 sandstone could be an upwards fining tidal bar due to increasing of the relative sea level, and the C3 sandstone a upwards coarsening prograding tidal bar in a more distal setting.

### 7.2.2 Lateral trends

The lateral distribution of the Cook sandstones C1-C5 is described in section 5.4.5-9. The description of the lateral distribution lists the facies associations (FA), which constitutes the different sandstones in the cores. The interpretation of the different facies associations, which builds up the sandstones, are related and occur often in the same environment. In each bullet point beneath, representing the different Cook sandstones, the overlying mud and siltstones are also included. The reason for this is that the overlying mud and silt indicates something about the change in the deposition from the sandstones.

- The C1 sandstone consists of FA1.1, FA1.2 and FA3. All of these FA reflect a shallow marine environment in a tidally dominated deltaic setting. FA1.1 and FA3 are quite similar and contain several of the same facies, but FA3 builds up more specific as a tidal bar. FA1.1 on the other hand, could represent several cycles of FA3 mixed with FA2.1. FA1.2 could represent sediments deposited during a transgression, due to the silt and mud content. The C1 sandstone, which is observed in three of the four wells, has a similarity in the vertically stacking of the FA. Hence the most reasonable to

interpret is a stable depositional system with continually supply of sediments in the deposition of the C1 sandstone.

- The C2 sandstone consists of FA1.1, FA1.2, FA2.3 and FA3. All of these FA reflect a shallow marine environment in a tidally dominated deltaic setting. FA1.1 and FA3 are quite similar and contain several of the same facies, but FA3 builds up more specific as a tidal bar. FA3 represents a part of a system, while FA1.1 could contain FA3 in a bigger system, without becoming a bigger sequence of several FA. FA1.2 and FA2.3 could represent sediments deposited during a transgression. But again FA1.2 represents a bigger system that could contain mixtures of FA2.3 and other muddy and silty FA, while FA2.3 represents a more specific marine flooding in a tidal compound dune.

- The C3 sandstone consists of FA1.1, FA2.1, FA2.2, FA2.3, FA4.1 and FA4.2. All of these FA reflect a shallow marine environment in a tidally dominated deltaic setting. FA1.1, FA2.1 and FA2.2 are quite similar and contain several of the same facies, but FA2.1 and FA2.2 is a part of an up building compound dune in a more proximal setting, while FA1.1 is more general and could combine FA2.1, FA2.2 and FA3 in a bigger system. Hence FA1.1 could also deposit in a larger area. FA2.3 and FA4.1 could represent sediments deposited during a transgression, due to high content of silt and mud. FA4.2 is interpreted to represents a shallow offshore mudstone, due to high content of mud, and minor content of silt. FA4.2 are interpreted to be the most distal FA.

- The C4 sandstone consists of FA1.2, FA2.1 and FA2.2. All of these FA reflect a shallow marine environment in a tidally dominated deltaic setting. FA2.1 and FA2.2 represent the up building of a compound dune. FA1.2 reflects a bigger system, which also is more distal than FA2.1 and FA2.2, due to more silt and mud.

- The C5 sandstone consists of FA1.1, which reflects a shallow marine environment in a tidally dominated deltaic setting. FA1.1 could be a migrating tidal bar in a delta front environment.

To state that the overall depositional environment was tidally influenced is not unlikely by now. As proposed in chapter 5 and above, the interpretation of the gamma log (Figure 5.4.10.1) gives an impression of an upwards coarsening and aggradational system, where the sediment supply is in balance with the accommodation space. The Early Jurassic was tectonically inactive (see chapter 2). This can imply that the fluctuation of the relative sea level was the biggest cause of regression and transgression.

As discussed above, the sandstones show similarities in the lateral trends in all the cores. A stable depositional system with continually supply of sediments is needed to obtain similar lateral trends in the different cores. Figure 7.2.2.1 illustrates how the interpretation of the sandstones could have been deposited in the connection with a delta. Other studies on the Cook Formation are presented in Table 7.2.2.1. The overall interpretation could be a migrating system with prograding compound dunes and tidal bars. Percentages of the different observed facies in the cores are illustrated in appendix IV.

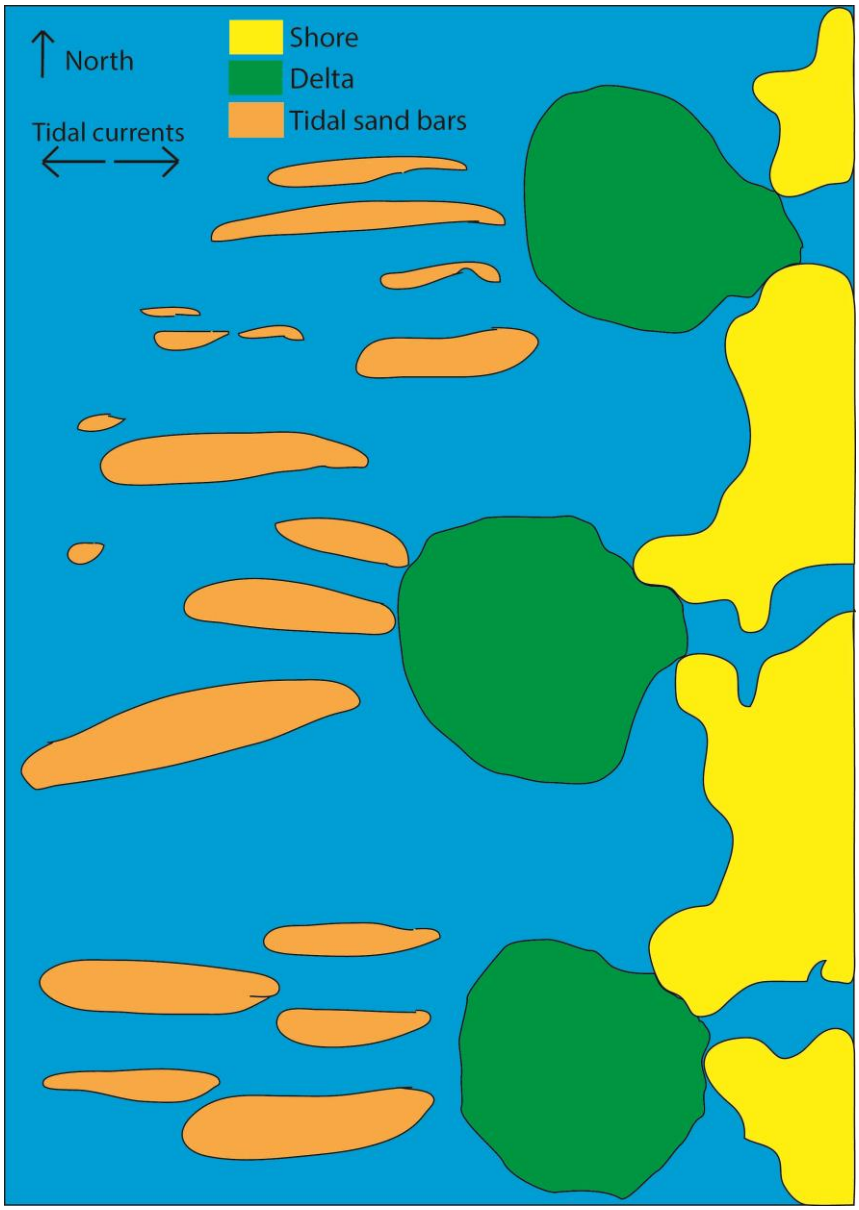


*Figure 7.2.2.1. Illustration of how the interpreted depositional environment looked like. The detrital sediments are interpreted to have been transported by fluvial rivers and deposited out into a tidally influenced deltaic environment. The scale is not included because the sediment supplying systems could vary greatly in size.*

| Study | Deposition | Area |
|---|---|---|
| (Martinius and Berg, 2011) | Offshore and lower shoreface setting at the base. Upwards in the Formation units the interpretation is highstand upper delta plain deposits, as well as transgressive tidally dominated estuarine fill | Northern North Sea |
| (Folkestad et al., 2012) | "… ***a mixed-energy tidal-fluvial delta capped by a wave-dominated estuary***" | Kvitebjørn/Valemon area |
| (Marjanac and Steel, 1997) | Four tongues consisting of a heterolithic unit and a sandstone unit. The heterolithic units have been interpreted to be shoreface deposits, due to fall in the sea level, while the sandstone units have been interpreted to be largely estuarine deposits | Northern North Sea |
| (Charnock et al., 2001) | Five sandstone sequences deposited in transgressive and prograding shoreface and estuarine deposits | Northern North Sea |
| (Livbjerg and Mjøs, 1989) | Subtidal sand body and offshore sand ridge | Oseberg area |
| This study | Prograding compound dunes and migrating tidal bars | Knarr area |

*Table 7.2.2.1. Depositional environment and location of this and other studies done on the Cook Formation.*

Compared to the other studies done on the Cook Formation there is the interpretation of Livbjerg and Mjøs (1989), which is the most comparable depositional environment to the Knarr area.

## 7.3 Clays

The clay minerals found in the Cook sandstones are dominated by kaolinite, chlorite and illite (See Figure 7.3.1, from Table 6.2.5.2, 34/5-1 S is not included, due to no XRD data). The amount differs between the cores.

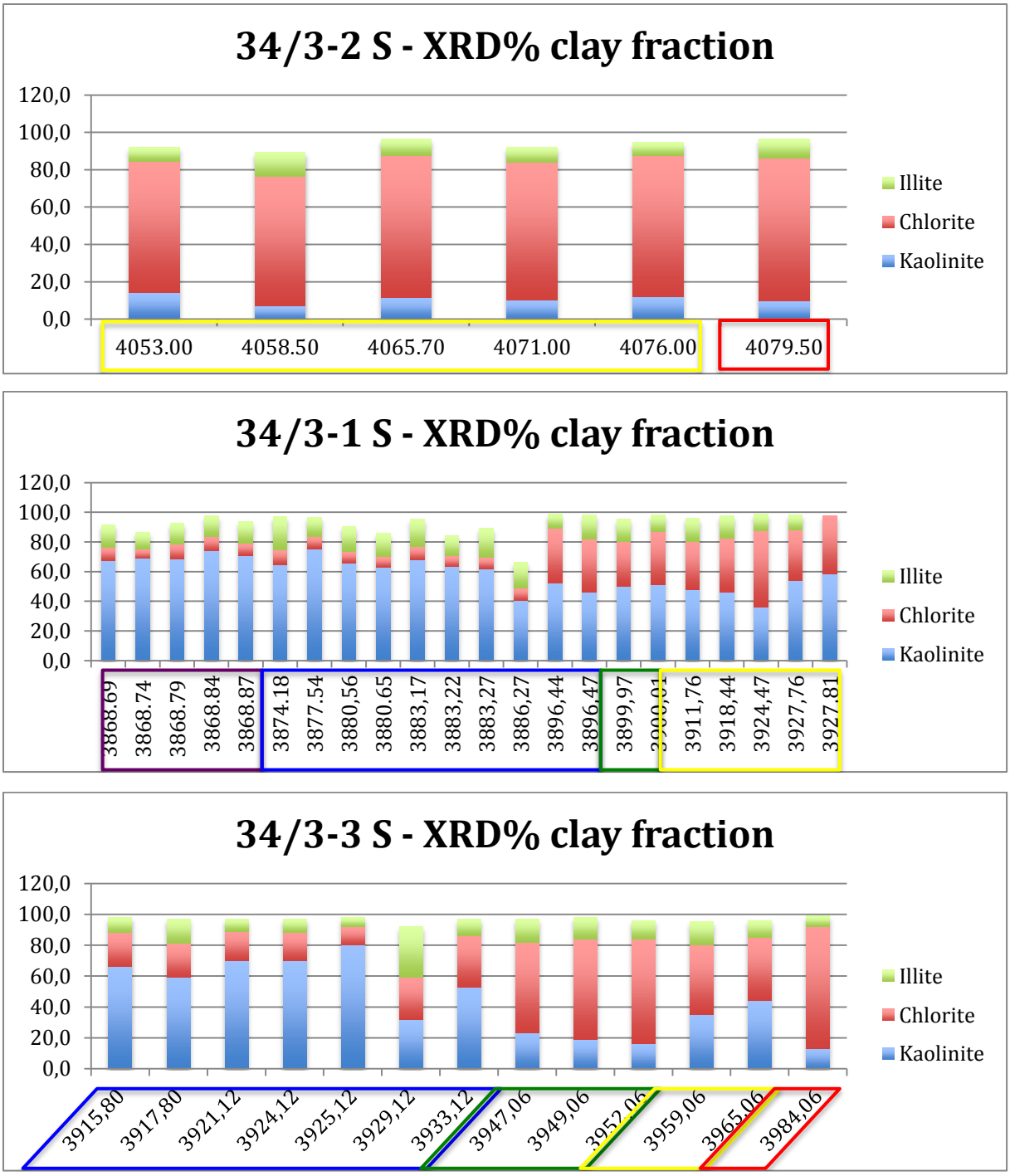


*Figure 7.3.1 show the XRD, clay fraction percentage of the three dominant components in the samples. The results are from three of the four cores. The colored squares represent the different Cook sandstones: Red – C1, Yellow – C2, Green – C3, Blue – C4 and Purple – C5.*

### 7.3.1 Kaolinite

Kaolinite can both occur as detrital and authigenic clay. In the samples from the three different wells, there is different amount of kaolinite. Figure 7.3.1 illustrate the percentage of the three dominant clay components. In the C5 and C4 sandstone in 34/3-

1 S, and the C4 sandstone in 34/3-3 S the kaolinite percentage is exceptionally high in several samples. But in 34/3-2 S the percentage is stable and much lower. This indicates that the sediments found in the different wells have experienced different modifications after deposition. If the sediments were exposed to percolating meteoric water over a long period of time, it is also expected that the percentage of kaolinite would be high. However if the sediments were reworked, much of the pore filling kaolinite (see Figure 6.2.3.10) would be lost. The average amount of detrital feldspar, in well 34/3-2 S, 34/3-1 S and 34/3-3 S, ranges from 10,6% to 12,5% (Table 6.2.5.1). The upper five samples (C5 sandstone) in well 34/3-1 S contain lower amounts of feldspar (Table 6.2.5.1), which could indicate that the high percentage of authigenic kaolinite derived from the detrital K-feldspar (Eq. 3.1.5.1).

### 7.3.2 Chlorite

The chlorite observed in the clay fraction XRD results (Table 6.2.5.2) can both be detrital and authigenic by origin. Figure 7.3.1 show that where the kaolinite percentage is high, the chlorite percentage is lower and vice versa. As established in section 7.3.1, it looks like the amount of kaolinite and reworking of the sediments have a connection. In the same way, it could be that the reworking of the sediments also gave a higher percentage of chlorite, due to redistribution of the sediments and lack of kaolinite. The chlorite is observed as different constituents; random pore filling clay (Figure 6.2.3.11), orientated sheet-like structure in ooids (Figure 6.2.3.12) and as coatings (Figure 6.2.1.4).

#### 7.3.2.1 Chlorite coating

A chlorite coating can recrystallize from an iron-rich clay rim situated around a detrital grain between 90-120°C. Without the precursor there is not possible for the chlorite to grow as a coating on detrital grains. The precursor is referred to as “clay mix” in Figure 6.2.3.1. The precursor lies flat on the grains, while the chlorite coating stands like a house of cards (Figure 6.2.1.2).

The formation of the chlorite coating is not the focus in this thesis, but rather the precursor of the chlorite coating. The reason for this is that the formation of the precursor is the link between the chlorite coating and depositional environment. There are several ways to get a precursor to stick to a grain. The depositional environment is

interpreted to be in a tidal dominated system, hence there are also expected to be much mud and clay minerals in the sediments. The sandstones show an overall aggradational vertical trend. The stabile aggradational system could have caused the sand bars and compound dunes to build up and be subaerial exposed in the low tides. A subaerial exposure of the sand bars and dunes would created a vadose zone were the detrital clay could stick to the grains and create a precursor for the chlorite coating. Figure 7.3.2.1.1 a, illustrates how a tidal sand bar could be subaerial exposed. However there is also likely that storms would stir up the water column with fine-grained constituents in suspension. Subaquatic infiltration of tidal currents could transport the suspended fine-grained constituents in to the sand bars and compound dunes, without any subaerial exposure (Figure 7.3.2.1.1 b).

There is observed different categories of bioturbation the sandstones. An organic rim around each grain could also work as glue for the mud to stick to the grains and create a clay rim (Needham et al., 2005). Worms or other sediment eating species could create that organic rim. This is more unlikely, due to reworking and erosion of the sediments in a tidally dominated system.

The mud drapes in the sandstones can say something about a failed subaquatic infiltration. The pore filling clay minerals in Figure 6.2.3.1 have a random orientation. The random orientation could be due to the process of infiltration. Whenever seen an orientation of the mud drapes the preservation witness about the failure of the infiltration. A combination between the subaerial exposure and subaquatic infiltration could be very likely.

As mentioned in chapter 3, chlorite (i.g. chamosite) needs Fe-rich minerals to form. Combined with the depositional system interpreted in chapter 5 and discussed in section 7.2, there is likely that the iron rich sediments came from fluvial rivers and was transported out into the Cook system (Ehrenberg, 1993). Even if the depositional environment was supplied with sediments from rivers and delta fronts, there are no traces of organic terrestrial material as mention in section 7.2. This gives an indication that the depositional environment was not proximal to the shore, but still not too distal.

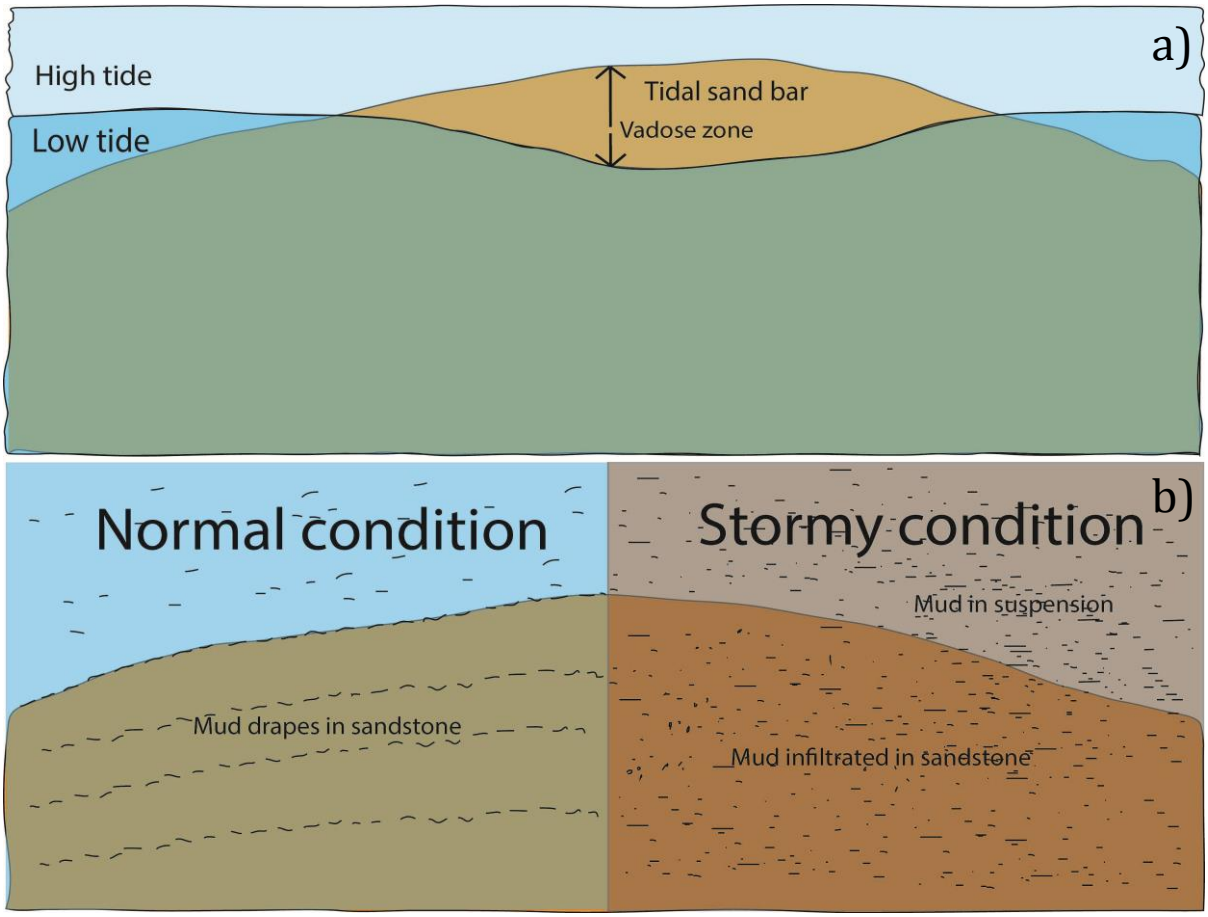


*Figure 7.3.2.1.1. a) Illustrates how a tidal sand bar could be subaerial exposed in low tides. b) Left: illustrates normal condition in the weather and water, which gives alternating mud drapes and sandstone. Right: illustrates how the weather condition could affect the fine-grained constituents in the water column and cause subaquatic infiltration of the fine-grained constituents in to the sediments.*

Since there is observed chlorite coating in all samples in SEM, but to a less degree in 34/3-1 S, the reworking of the sediments must have happened before the precursor was attached to the grains. There is not found any direct evidence for subaerial exposure in the sediments, but there is interpreted that…

- The sediments have in different degrees been percolated with meteoric water, due to pore filling kaolinite.
- The amount of kaolinite and chlorite in the samples can indicate if the sediments have been reworked or not.
- Due to minor tectonic activity, the interpreted sand compound dunes and tidal bars had the possibility to migrate in a stable environment to create a wide and long sandstone carpet.

By stating these points, the two first points indicates the distance to shore. The third point tells something about the distribution and the stableness of the depositional system. Hillier (1994) suggest that the formation of the precursor to the chlorite coating occur at surface level or close to the surface level, in the early history of diagenesis. This strengthens the interpretation of a subaerial exposure and subaquatic infiltration, due to the need of a precursor to form the coating. Aagaard et al. (2000) concludes that Fe-rich chlorite coatings (i.e. chamosite) require a Fe-rich precursor e.g. berthierine, and a temperature corresponding to about 100°C to start to form. Both articles (Hillier, 1994, Aagaard et al., 2000) agree on the early diagenesis of a precursor, but Aagaard et al. (2000) indicate that the precursor can occur as a porosity preserver until the chlorite starts to recrystallize at intermediate depth (90-120°C). And the completeness of the precursor is also of importance for the preservation of the porosity. Worden and Morad (2003) are also stating that chloritization of coatings originates from berthierine or other precursors as odinite or smectite. The same conditions, temperature and precursor, as mention above have been reached in the Knarr area.

The different Cook sandstones have been characterized with respect to grain coating effect (Table 6.2.1.3). If there is a dune or tidal bar, which is subaerial exposed twice a day, and there is for a period of time created a stable vadose zone. It is possible to imagine that clay is attached to the detrital grains and creates a clay rim. The stability of the dunes could also affect the completeness of the clay rim around each detrital grain. The effectiveness of the chlorite coatings (Table 6.2.1.3) in the different Cook sandstones is proposed (except 34/3-1 S, due to no observed coating in point counting). The reason for this is to see the completeness of the coating and the function of porosity preservation. Most of the coatings are of high effectiveness, and surrounds mostly every grain. The precursor could however also been attached to the grains in a later stage in the burial process. Iijima and Matsumoto (1982) state that the reaction between kaolinite and siderite formed berthierine at low to medium temperatures (65-130°C). There is however not likely to obtain the same reservoir quality that exist in the Cook Formation, Knarr area, by introducing the precursor at that late stages in the burial process. Quartz cement starts to precipitate around 70-80°C (see chapter 3) and from Table 6.2.4.2, there is minor quartz cement. The precursor, which also have worked as a coating must have been attached to the grains at a much earlier stage.

Further study on the relation between the pore filling clogs in the sandstones and the chlorite coating could be of interest. This could be of importance because the precursor of the chlorite coating could originate from the pore filling clogs.

### 7.3.3 Illite

From both Bulk and clay fraction XRD (Table 6.2.5.1&2), the percentage of illite is quite stable. As mention in chapter 3, the temperature for forming illite from K-feldspar and kaolinite is about 140°C. Illite can also form from smectite at much lower temperatures (~70°C), but as seen in the XRD results (Table 6.2.5.1&2), there is minor smectite in the system. There is expected to have minor smectite in the system, due to the temperature in the Cook sandstones. The occurrence of on going albitization indicates the temperature range of the sandstone (~65-105°C) (Saigal et al., 1988). The wells have a temperature ranging from 135-148°C at the well bottom (NPD, 2014b). Hence the amount of illite in the sediments is most likely derived from smectite.

Albitization of K-feldspar is observed in all the samples. From Eq. 3.1.7.1, it is needed K-feldspar together with kaolinite to form illite. Since there is much albitization in the samples, there is less K-feldspar left for the formation of illite.

## 7.4 Petrography

The petrographic results in this thesis have been used to interpret the depositional environment and the connection between the grain coating and the depositional environment.

### 7.4.1 Carbonates and porosity

Figure 6.2.2.2-5 illustrates and gives an overview of the mineralogical composition in the four-cored wells. The porosity in the sediments is not possible to obtain from the XRD results, but in point counting the porosity is included.

Carbonate cement is closely related to porosity loss in the observed *thin sections*. Figure 7.4.1.1 show the relation between the porosity and the carbonate cement.

As mentioned in chapter 3, carbonate cement have the ability to precipitate early in the burial. From the illustrations below (Figure 7.4.1.1) it suggests that when carbonate cement is precipitated, it dominates and destroys the porosity partly or completely. Carbonate cement is found in all the cores, but not all the sandstones.

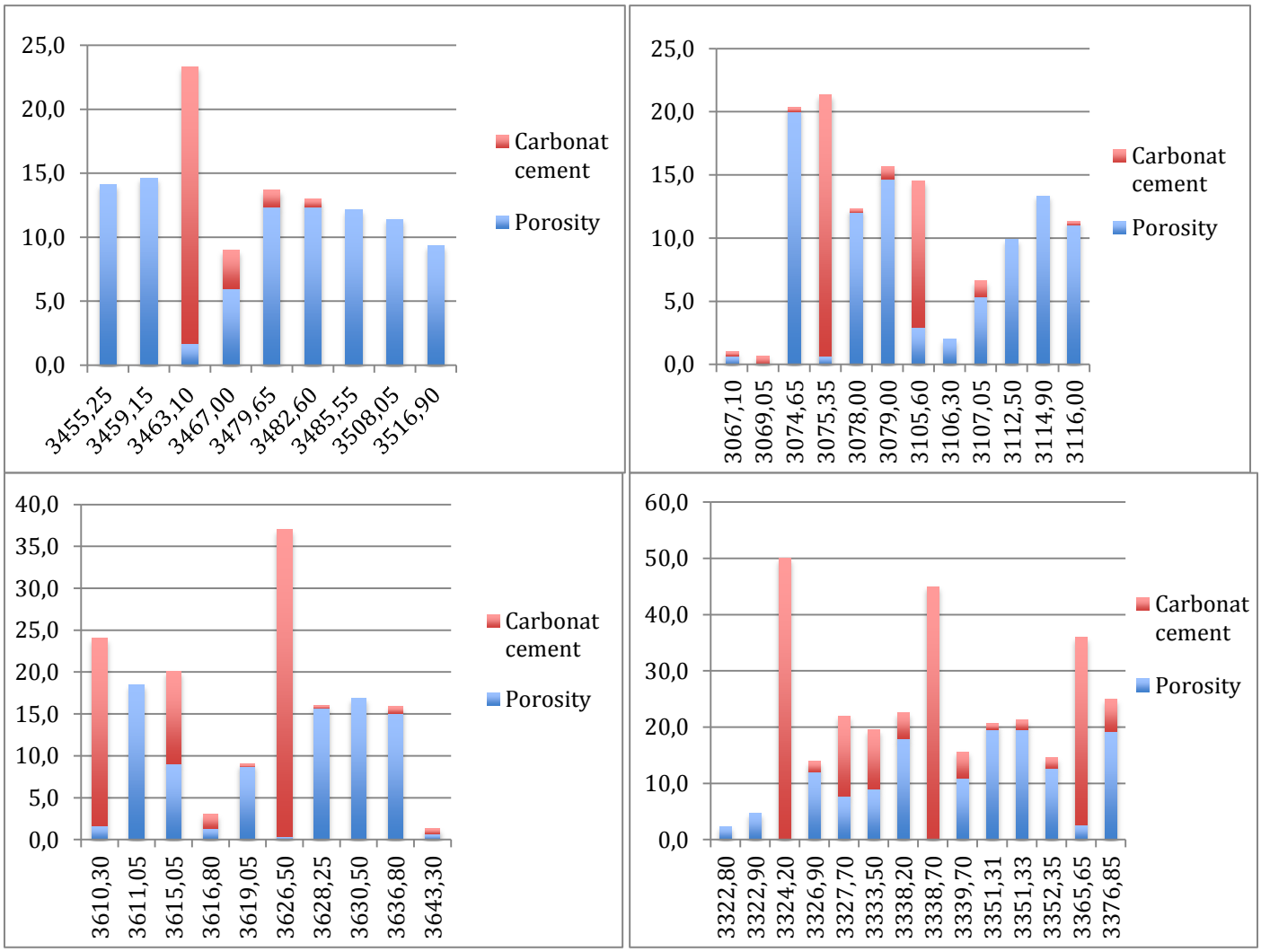


*Figure 7.4.1.1. Illustration of the relation between porosity and carbonate cement, obtained from point counting. Top left – 34/3-3 S. Top right – 34/5-1 S. Low left – 34/3-2 S. Low right 34/3-1 S.*

The IGV is strongly influenced by carbonate cement. As mentioned in chapter 6, the abnormal high IGV values are in connection with carbonate cementation. Values higher than 45% (see Figure 6.2.2.8) represent a liquid state of the grains since sands are deposited with an IGV of about 40-42% (grain supported). In the *thin sections* the grains

are in many places not touching each other and floats in a carbonate cement (see Figure 6.2.2.3 e). This could be due to dissolution of grain supporting carbonates, which has been replaced by the dissolved cement. The values observed and calculated lower than 26% (see Figure 6.2.2.8) are not in connection with carbonate cement, but rather matrix supported. This can be due to detrital mud drapes in the *thin sections*, leaving less room for porosity and authigenic clays to precipitate and grow.

### 7.4.2 Mineral assemblage

The mineral assemblage observed in point counting (Figure 6.2.3.2,4,6,8) is in accordance with the XRD results (Table 6.2.5.1&2.). As described in section 6.2.2, there are big and small differences in the cores, but there are some signatures in the sediments that reflects the depositional system and particularly with respect to reworking of the sediments. This is also discussed above in section 7.3.
The samples that contain high percentages (> 20%) of kaolinite in the Bulk XRD have also a low porosity percentage from the point counting.

#### 7.4.2.1 – 34/3-2 S

The two samples from the C1 sandstone is separated by 6,5 meter. The cored interval of the C1 sandstone is only about two meter. Both samples in the C1 sandstone have minor amounts of kaolinite, which could indicate reworking of the sediments. The porosity is preserved in the upper sample of the C1 sandstone due to a high percentage of chlorite coating and lack of mud drapes.

The samples in the C2 sandstone that contain high amounts of carbonate cement have no relation and are not related to a specific FA.
There are generally minor amounts of pore filling kaolinite, which could indicate reworking of the sediments. The variable porosity in the samples from the C2 sandstone is strongly in relation with the pore filling fine-grained constituents and carbonate cement.

#### 7.4.2.2 – 34/3-1 S

There is not observed any chlorite coating in this well using the method of point counting. The reason for that could be due to thin coatings, which is difficult to see. Still there is observed good porosity in many of the samples.

The two samples from the C2 sandstone are fairly immature with respect to a high amount of feldspar and moderate amounts of detrital quartz grains. Sample 3376,85 m contains about 20% porosity even if there is not observed any coating.
The carbonate cement seems to be the greatest porosity destroyer in this well. As discussed above, sample 3322,80 m, 3322,90 m and 3326,90 m contains moderate amounts of pore filling kaolinite. This could indicate that the sediments around these samples have had minor reworking after deposition. The rest of the samples contain minor amounts of pore filling kaolinite.

#### 7.4.2.3 – 34/3-3 S

The moderate amount of pore filling kaolinite (~10%) in sample 3455,25 m could indicate minor reworking of the sediments in the middle of the C4 sandstone. Rest of the samples contains minor amounts of pore filling kaolinite, which could imply more reworking of the sediments. There is generally a high percentage of chlorite coating in all the samples, except the C4 sandstone. The high amounts of chlorite coating could indicate that the precursor was attached to the detrital grains in a stable system.

#### 7.4.2.4 – 34/5-1 S

The change of the proximity in the depositional environment could be interpreted with respect to the mineralogical composition in the samples. The chlorite coating observed in the three lower samples from the C1 sandstone, could reflect a proximal depositional environment. The samples in the upper C1 sandstone, C3 sandstone and C4 sandstone could reflect a more distal depositional environment.

### 7.4.3 Quartz cement

Quartz cement is the most important porosity-destroying constituent (Walderhaug, 1994b). There is however observed minor amounts of quartz cement in point counting

(Figure 6.2.3.2,4,6,8) and XRD (Table 6.2.5.1&2). Figure 6.2.3.5&6 illustrates how the quartz cement efficiently destroys the porosity. A corresponding sandstone at similar depth in the north sea would be expected to have a much higher bulk percentage of quartz cement, (c.f. Bjørlykke and Egeberg, 1993, Walderhaug, 1996) This indicates that the chlorite coatings have retarded the quartz cementation very well.

# *Chapter 8 - Conclusion*

- There is reasonable to indicate that the sediments originate from eroded and weathered basement rock in the Caledonian orogeny in the east. Fluvial systems transported the sediments out into the ocean and deposited them in a tidally influenced deltaic system. The depositional environment is interpreted to be an aggradational system with balance in the incoming sediments and the subsidence of the sedimentary basin.

- The Fe-rich chlorite coating, (i.g. chamosite) recrystallized from an iron rich precursor e.g. berthierine, which could have been attached to the grains in an interpreted vadose zone or through subaquatic infiltration of muddy water. The vadose zone has been interpreted to be a result of subaerial exposure of tidal sand bars and compound dunes during low tides. There is however not any sufficient evidence of a subaerial exposure to state it as a conclusion and needs further investigation.

- The completeness of the chlorite coating indicates a stable system, which allowed the precursor to stick to the grains and create a good clay rim. The clay rim worked as a porosity preserving coating until the recrystallization of the chlorite.

- There is not observed much quartz cement in the samples, which indicates that the chlorite coating have worked as a very good porosity preserving mechanism.

- The biggest porosity destroyer in the system seems to be the authigenic carbonate cement and detrital mud drapes. The carbonate cement varies in the timing of precipitation, due to some samples with fully developed chamosite coatings and carbonate cement in the pore space. Others with no coating and pore filling carbonate surrounding the grains. The detrital mud drapes occur as a result of a tidally influenced depositional system.

- Reworking of the sediments seems to be recognized in the sediments with respect to the amount of kaolinite and chlorite.

# *References*

BADLEY, M. E., PRICE, J. D., RAMBECH DAHL, C. & AGDESTEIN, T. 1988. The structural evolution of the northern Viking Graben and its bearing upon extensional modes of basin formation. *Journal of the Geological Society,* 145**,** 455-472.

BAILEY, S. W. & BROWN, B. E. 1962. CHLORITE POLYTYPISM. 1. REGULAR AND SEMI-RANDOM 1-LAYER STRUCTURES. *American Mineralogist,* 47**,** 819-&.

BJØRKUM, P. A. 1996. How important is pressure in causing dissolution of quartz in sandstones? *Journal of Sedimentary Research,* 66.

BJØRLYKKE, K. 1994. Fluid-flow processes and diagenesis in sedimentary basins. *Geological Society, London, Special Publications,* 78**,** 127-140.

BJØRLYKKE, K. 1998. Clay mineral diagenesis in sedimentary basins - a key to the prediction of rock properties. Examples from the North Sea Basin. *Clay Minerals,* 33**,** 15-34.

BJØRLYKKE, K. 2014. Relationships between depositional environments, burial history and rock properties. Some principal aspects of diagenetic process in sedimentary basins. *Sedimentary Geology,* 301**,** 1-14.

BJØRLYKKE, K. & EGEBERG, P. 1993. Quartz cementation in sedimentary basins. *AAPG bulletin,* 77**,** 1538-1548.

BJØRLYKKE, K., NEDKVITNE, T., RAMM, M. & SAIGAL, G. C. 1992. Diagenetic processes in the Brent Group (Middle Jurassic) reservoirs of the North Sea: an overview. *Geological Society, London, Special Publications,* 61**,** 263-287.

BLOCH, S., LANDER, R. H. & BONNELL, L. 2002. Anomalously high porosity and permeability in deeply buried sandstone reservoirs: Origin and predictability. *AAPG bulletin,* 86**,** 301-328.

BLOTT, S. J. & PYE, K. 2001. GRADISTAT: a grain size distribution and statistics package for the analysis of unconsolidated sediments. *Earth surface processes and Landforms,* 26**,** 1237-1248.

CHARNOCK, M. A., KRISTIANSEN, I. L., RYSETH, A. & FENTON, J. P. G. 2001. Sequence Stratigraphy of the Lower Jurassic Dunlin Group, Northern North Sea. *In:* OLE, J. M. & TOM, D. (eds.) *Norwegian Petroleum Society Special Publications.* Elsevier.

CHUHAN, F. A., KJELDSTAD, A., BJØRLYKKE, K. & HØEG, K. 2002. Porosity loss in sand by grain crushing—Experimental evidence and relevance to reservoir quality. *Marine and Petroleum Geology,* 19**,** 39-53.

DAVIES, P. J., BUBELA, B. & FERGUSON, J. 1978. The formation of ooids. *Sedimentology,* 25**,** 703-730.

DOTT, R. H. 1964. Wacke, Graywacke and Matrix--What Approach to Immature Sandstone Classification? *Journal of Sedimentary Research,* 34.

EHRENBERG, S. 1993. Preservation of anomalously high porosity in deeply buried sandstones by grain-coating chlorite: examples from the Norwegian continental shelf. *AAPG Bulletin,* 77**,** 1260-1286.

FAWAD, M., MONDOL, N. H., JAHREN, J. & BJØRLYKKE, K. 2011. Mechanical compaction and ultrasonic velocity of sands with different texture and mineralogical composition. *Geophysical Prospecting,* 59**,** 697-720.

FOLK, R. L. & WARD, W. C. 1957. Brazos River bar: a study in the significance of grain size parameters. *Journal of Sedimentary Research,* 27.

FOLKESTAD, A., VESELOVSKY, Z. & ROBERTS, P. 2012. Utilising borehole image logs to interpret delta to estuarine system: A case study of the subsurface Lower Jurassic Cook Formation in the Norwegian northern North Sea. *Marine and Petroleum Geology,* 29**,** 255-275.

FOSTER, M. D. 1962. Interpretation of the composition and a classification of the chlorites: US Geol. *Survey Prof. Paper,* 414.
GABRIELSEN, R. H., FÆRSETH, R. B., STEEL, R. J., IDIL, S. & KLØVJAN, O. S. 1990. Architectural styles of basin fill in the northern Viking Graben. *Publication International Lithosphere Program,* 181**,** 158-179.
GLENNIE, K. W. & UNDERHILL, J. R. 1998. Origin, Development and Evolution of Structural Styles. *In:* GLENNIE, K. W. (ed.) *Petroleum Geology of the North Sea.* Blackwell Science Ltd.
GRADSTEIN, F. 2013. Northern Vikig Graben
Tampen - Horda Platform. Norlex.
HAY, J. T. C. 1978. Structural development in the northern North Sea. *Journal of Petroleum Geology,* 1**,** 65-77.
HEALD, M. & LARESE, R. 1974. Influence of coatings on quartz cementation. *Journal of Sedimentary Research,* 44.
HILLIER, S. 1994. Pore-lining chlorites in siliciclastic reservoir sandstones: electron microprobe, SEM and XRD data, and implications for their origin. *Clay Minerals,* 29**,** 665-680.
HITCHON, B. 1984. Geothermal gradients, hydrodynamics, and hydrocarbon occurrences, Alberta, Canada. *AAPG Bulletin,* 68**,** 713-743.
IIJIMA, A. & MATSUMOTO, R. 1982. Berthierine and chamosite in coal measures of Japan. *Clays and Clay Minerals,* 30**,** 264-274.
JAHREN, J. & AAGAARD, P. 1992. Diagenetic illite-chlorite assemblages in arenites. I. Chemical evolution. *Clays and Clay Minerals,* 40**,** 540-540.
KLOVAN, J. 1966. The use of factor analysis in determining depositional environments from grain-size distributions. *Journal of Sedimentary Research,* 36**,** 115-125.
KYRKJEBØ, R., GABRIELSEN, R. H. & FALEIDE, J. I. 2004. Unconformities related to the Jurassic–Cretaceous synrift–post-rift transition of the northern North Sea. *Journal of the Geological Society,* 161**,** 1-17.
LIVBJERG, F. & MJØS, R. 1989. The Cook Formation, an offshore sand ridge in the Oseberg area, northern North Sea. *In:* COLLINSON, J. D. (ed.) *Correlation in Hydrocarbon Exploration.* Springer Netherlands.
MANHEIM, F. & PAULL, C. 1981. Patterns of groundwater salinity changes in a deep continental-oceanic transect off the southeastern Atlantic coast of the USA. *Journal of Hydrology,* 54**,** 95-105.
MARCHAND, A. M., SMALLEY, P. C., HASZELDINE, R. S. & FALLICK, A. E. 2002. Note on the importance of hydrocarbon fill for reservoir quality prediction in sandstones. *AAPG bulletin,* 86**,** 1561-1572.
MARCHAND, A. M. E., HASZELDINE, R. S., SMALLEY, P. C., MACAULAY, C. I. & FALLICK, A. E. 2001. Evidence for reduced quartz-cementation rates in oil-filled sandstones. *Geology,* 29**,** 915-918.
MARJANAC, T. & STEEL, R. J. 1997. Dunlin Group sequence stratigraphy in the northern North Sea; a model for Cook Sandstone deposition. *AAPG bulletin,* 81**,** 276-292.
MARTINIUS, A. W. & BERG, J. H. 2011. *Atlas of Sedimentary Structures in Estuarine and Tidally-influenced River Deposits of the Rhine-Meuse-Scheldt System: Their Application to the Interpretation of Analogous Outcrop and Subsurface Depositional Systems*, EAGE publications.
MORAD, S. 2009. Carbonate Cementation in Sandstones: Distribution Patterns and Geochemical Evolution (Special Publication 26 of the IAS). *The International association of sedimentologists,* 72**,** 1-24.

MUTO, T. & STEEL, R. J. 1997. The Middle jurassic Oseberg delta, northern North Sea: A sedimentological and sequence stratigraphic interpretation. *AAPG bulletin,* 81**,** 1070-1086.

NEEDHAM, S. J., WORDEN, R. H. & MCILROY, D. 2005. Experimental production of clay rims by macrobiotic sediment ingestion and excretion processes. *Journal of Sedimentary Research,* 75**,** 1028-1037.

NPD. 2012. *Recoverable resources* [Online]. Available: http://www.npd.no/Global/Engelsk/3-Publications/Facts/Facts2013/Figures/Chapter-04/Table-4-1.pdf [Accessed 09.04. 2014].

NPD. 2013a. *Faktakart* [Online]. Available: http://npdmap1.npd.no/website/NPDGIS/viewer.htm [Accessed 18.11. 2013].

NPD. 2013b. *Knarr* [Online]. Available: http://www.npd.no/publikasjoner/faktahefter/fakta-2013/kap-11/knarr/ [Accessed 15.11. 2013].

NPD. 2014a. *Fields with Cook fm. as reservoir* [Online]. Available: http://www.npd.no/no/tema/geologi/letemodeller/nordsjoen/ovre-trias-til-midtre-jura/ [Accessed 18.02.14 2014].

NPD. 2014b. *NPD - Fact pages* [Online]. Available: http://factpages.npd.no/factpages/Default.aspx?culture=no [Accessed 19.05.14.

NØTTVEDT, A. & JOHANNESSEN, E. P. 2007a. Grunnlaget for Norges oljerikdom. Sein jura, et øyhav vokser fram. *In:* RAMBERG, I. B., BRYHNI, I. & NØTTVEDT, A. (eds.) *Et land blir til: Norges geologi.*

NØTTVEDT, A. & JOHANNESSEN, E. P. 2007b. Norge omkranses av kystsletter og deltaer; Tidlig- og midtjura; 206-160 Ma. *In:* RAMBERG, I. B., BRYHNI, I. & NØTTVEDT, A. (eds.) *Et land blir til: Norges geologi.*

OELKERS, E. H., BJØRKUM, P. A., WALDERHAUG, O., NADEAU, P. H. & MURPHY, W. M. 2000. Making diagenesis obey thermodynamics and kinetics: the case of quartz cementation in sandstones from offshore mid-Norway. *Applied Geochemistry,* 15**,** 295-309.

PAXTON, S., SZABO, J., AJDUKIEWICZ, J. & KLIMENTIDIS, R. 2002. Construction of an intergranular volume compaction curve for evaluating and predicting compaction and porosity loss in rigid-grain sandstone reservoirs. *AAPG bulletin,* 86**,** 2047-2067.

PITTMAN, E. D., LARESE, R. E. & HEALD, M. T. 1992. Clay coats: Occurrence and relevance to preservation of porosity in sandstones.

REINECK, H. E. & SINGH, I. B. 1975. Depositional Sedimentary Environments. Springer-Verlag, New York.

SAIGAL, G. C. & BJØRLYKKE, K. 1987. Carbonate cements in clastic reservoir rocks from offshore Norway—relationships between isotopic composition, textural development and burial depth. *Geological Society, London, Special Publications,* 36**,** 313-324.

SAIGAL, G. C., BJØRLYKKE, K. & LARTER, S. 1992. The Effects of Oil Emplacement on Diagenetic Processes: Examples from the Fulmar Reservoir Sandstones, Central North Sea: Geologic Note (1). *AAPG Bulletin,* 76**,** 1024-1033.

SAIGAL, G. C., MORAD, S., BJORLYKKE, K., EGEBERG, P. K. & AAGAARD, P. 1988. Diagenetic albitization of detrital K-feldspar in Jurassic, Lower Cretaceous, and Tertiary clastic reservoir rocks from offshore Norway, I. Textures and origin. *Journal of Sedimentary Research,* 58.

SHINN, E. A. & ROBBIN, D. M. 1983. Mechanical and chemical compaction in fine-grained shallow-water limestones. *Journal of Sedimentary Research,* 53.
SLATT, R. M. 2006. Geologic controls on reservoir quality. *Stratigraphic reservoir characterization for petroleum geologists, geophysicists, and engineers* 1. ed. Elsevier.
SPENCER, A. M. & LARSEN, V. B. 1990. Fault traps in the Northern North Sea. *Geological Society, London, Special Publications,* 55**,** 281-298.
STEEL, R. Triassic–Jurassic megasequence stratigraphy in the Northern North Sea: rift to post-rift evolution. Geological Society, London, Petroleum Geology Conference series, 1993. Geological Society of London, 299-315.
STRECKEISEN, A. 1976. To each plutonic rock its proper name. *Earth-science reviews,* 12**,** 1-33.
TORSÆTER, J. in press. Reservoir quality of the Lower Jurassic Cook Formation located in the Knarr area, northern North Sea.
UNDERHILL, J. R. 1998. Jurassic. *In:* GLENNIE, K. W. (ed.) *Petroleum Geology of the North Sea.* Blackwell Science Ltd.
VISHER, G. S. 1969. Grain size distributions and depositional processes. *Journal of Sedimentary Research,* 39.
VOLLSET, J. & DORÉ, A. G. 1984. *A revised Triassic and Jurassic lithostratigraphic nomenclature for the Norwegian North Sea*, Oljedirektoratet.
WALDERHAUG, O. 1994a. Precipitation rates for quartz cement in sandstones determined by fluid-inclusion microthermometry and temperature-history modeling. *Journal of Sedimentary Research,* 64.
WALDERHAUG, O. 1994b. Temperatures of quartz cementation in Jurassic sandstones from the Norwegian continental shelf--evidence from fluid inclusions. *Journal of Sedimentary Research,* 64.
WALDERHAUG, O. 1996. Kinetic modeling of quartz cementation and porosity loss in deeply buried sandstone reservoirs. *AAPG bulletin,* 80**,** 731-745.
WARREN, E. A. & SMALLEY, P. C. 1994. Part 1: Compendium of North Sea Oil and gas fields. *Geological Society, London, Memoirs,* 15**,** 3-77.
WORDEN, R. & MORAD, S. 2003. Clay minerals in sandstones: controls on formation, distribution and evolution. *International association of sedimentologists,* 34**,** 3-41.
YOSHIDA, S., JOHNSON, H. D., GUPTA, R. & MARTINIUS, A. W. 1999. Outcrop Studies of Lower Cretaceous Tidal Sandstone Bodies for Reservoir Characterization of the Tilje Formation (Lower Jurassic), Offshore Mid-Norway.
ZIEGLER, P. A. 1982. *Geological atlas of western and central Europe*.
AAGAARD, P., JAHREN, J., HARSTAD, A., NILSEN, O. & RAMM, M. 2000. Formation of grain-coating chlorite in sandstones. Laboratory synthesized vs. natural occurrences. *Clay Minerals,* 35**,** 261-269.
AASE, N. E., BJORKUM, P. A. & NADEAU, P. H. 1996. The effect of grain-coating microquartz on preservation of reservoir porosity. *AAPG bulletin,* 80**,** 1654-1673.
AASE, N. E. & WALDERHAUG, O. 2005. The effect of hydrocarbons on quartz cementation: diagenesis in the Upper Jurassic sandstones of the Miller Field, North Sea, revisited. *Petroleum Geoscience,* 11**,** 215-223.

References

# *Appendix*

# *Appendix I*

**Excel table – Atomic quantification of the chlorite coating**

| Sample | Mg | Al_tet | Al_okt | Si | Fe |
|---|---|---|---|---|---|
| **1** | 0,952113861 | 1,008203043 | 1,820654841 | 2,991796957 | 2,821005399 |
| | 0,826416375 | 0,96664028 | 1,613931924 | 3,03335972 | 3,23600588 |
| | 0,605226029 | 0,733675715 | 2,045939387 | 3,266324285 | 2,692702748 |
| | 0,710835913 | 0,407292742 | 2,314688682 | 3,592707258 | 2,020777434 |
| **2** | 0,921096149 | 0,836522561 | 2,011103236 | 3,163477439 | 2,480510276 |
| | 1,021542738 | 0,439193885 | 2,144822794 | 3,560806115 | 1,980820014 |
| | 0,852657819 | 0,530889982 | 1,983696018 | 3,469110018 | 2,437243145 |
| **3** | 0,922332506 | 0,951612903 | 1,782382134 | 3,048387097 | 2,879900744 |
| | 1,025661481 | 0,95279883 | 1,790985241 | 3,04720117 | 2,764260072 |
| | 0,84046589 | 0,848718802 | 1,862762063 | 3,151281198 | 2,789750416 |
| | 0,897996254 | 0,954759607 | 1,459499347 | 3,045240393 | 3,390134529 |
| | 0,780672667 | 1,108479394 | 1,606821412 | 2,891520606 | 3,363334912 |
| | 1,054347826 | 1,079710145 | 1,655797101 | 2,920289855 | 3,001811594 |
| **4** | 0,882039856 | 1,142468127 | 1,650946899 | 2,857531873 | 3,212773858 |
| | 0,863268223 | 1,086231539 | 1,89614102 | 2,913768461 | 2,835636017 |
| | 0,755171976 | 0,794517071 | 1,913440792 | 3,205482929 | 2,771925371 |
| **5** | 0,910608415 | 1,464801704 | 1,379842284 | 2,535198296 | 3,752029011 |
| | 0,915544967 | 1,133293627 | 1,414889815 | 2,866706373 | 3,528767123 |
| | 0,719343025 | 1,04805238 | 1,266896016 | 2,95194762 | 3,904339141 |
| | 0,961589757 | 1,074153107 | 1,756468392 | 2,925846893 | 2,940784209 |
| | 0,811427228 | 0,961674112 | 1,786973901 | 3,038325888 | 2,988948977 |
| | 0,847941296 | 1,161027313 | 1,325723604 | 2,838972687 | 3,743986955 |
| **6** | 0,733280143 | 1,119444314 | 1,404984277 | 2,880555686 | 3,718965598 |
| **7** | 0,926666667 | 1,01 | 1,243333333 | 2,99 | 3,713333333 |
| | 0,837650493 | 1,197616442 | 1,632007783 | 2,802383558 | 3,313146054 |
| | 0,891525424 | 1,030508475 | 1,372881356 | 2,969491525 | 3,56440678 |
| | 0,881889764 | 1,074953417 | 1,781090341 | 2,925046583 | 2,983951434 |
| | 0,859788184 | 0,862985413 | 1,966295877 | 3,137014587 | 2,622260707 |
| | 0,556636368 | 1,42369638 | 1,024610642 | 2,57630362 | 4,618295859 |

*Measured atomic percentage of the chlorite coating from SEM analysis. Sample 1-4 is from 34/3-3 S, 3949,06 MD. Sample 5-7 is from 34/3-2 S, 4061,75 MD.*

# *Appendix II*

## Excel table – Grain size analysis

| 4053,00 | 34/3-2 S 4053,75 | 4057,75 | 4059,50 | 4061,75 | 4069,25 | 4071,00 | 4073,25 | 4079,50 | 4086,00 |
|---|---|---|---|---|---|---|---|---|---|
| **89,0** | 119,0 | 88,0 | 83,0 | 97,0 | 98,0 | 96,0 | 64,0 | 78,0 | 49,0 |
| **108,0** | 152,0 | 106,0 | 107,0 | 129,0 | 116,0 | 187,0 | 77,0 | 105,0 | 55,0 |
| **113,0** | 154,0 | 119,0 | 114,0 | 157,0 | 152,0 | 209,0 | 86,0 | 105,0 | 69,0 |
| **117,0** | 160,0 | 124,0 | 126,0 | 161,0 | 153,0 | 220,0 | 99,0 | 136,0 | 72,0 |
| **142,0** | 161,0 | 129,0 | 154,0 | 171,0 | 156,0 | 232,0 | 116,0 | 140,0 | 77,0 |
| **164,0** | 167,0 | 135,0 | 157,0 | 175,0 | 178,0 | 249,0 | 152,0 | 146,0 | 100,0 |
| **168,0** | 171,0 | 142,0 | 158,0 | 184,0 | 187,0 | 300,0 | 156,0 | 147,0 | 134,0 |
| **179,0** | 178,0 | 165,0 | 180,0 | 224,0 | 192,0 | 337,0 | 166,0 | 154,0 | 138,0 |
| **188,0** | 184,0 | 167,0 | 199,0 | 224,0 | 193,0 | 378,0 | 171,0 | 170,0 | 139,0 |
| **208,0** | 187,0 | 177,0 | 204,0 | 230,0 | 195,0 | 386,0 | 179,0 | 189,0 | 139,0 |
| **210,0** | 190,0 | 178,0 | 205,0 | 236,0 | 204,0 | 400,0 | 193,0 | 194,0 | 159,0 |
| **212,0** | 191,0 | 182,0 | 209,0 | 248,0 | 212,0 | 411,0 | 209,0 | 204,0 | 160,0 |
| **212,0** | 201,0 | 186,0 | 214,0 | 249,0 | 222,0 | 439,0 | 265,0 | 204,0 | 161,0 |
| **234,0** | 203,0 | 188,0 | 220,0 | 249,0 | 228,0 | 464,0 | 282,0 | 211,0 | 182,0 |
| **243,0** | 204,0 | 191,0 | 224,0 | 253,0 | 229,0 | 470,0 | 305,0 | 217,0 | 187,0 |
| **244,0** | 206,0 | 203,0 | 225,0 | 254,0 | 235,0 | 481,0 | 306,0 | 219,0 | 202,0 |
| **247,0** | 211,0 | 209,0 | 230,0 | 256,0 | 235,0 | 487,0 | 312,0 | 238,0 | 209,0 |
| **262,0** | 211,0 | 221,0 | 232,0 | 256,0 | 249,0 | 504,0 | 325,0 | 242,0 | 214,0 |
| **267,0** | 217,0 | 222,0 | 234,0 | 257,0 | 270,0 | 505,0 | 334,0 | 257,0 | 221,0 |
| **267,0** | 240,0 | 223,0 | 237,0 | 259,0 | 270,0 | 510,0 | 388,0 | 259,0 | 223,0 |
| **271,0** | 244,0 | 225,0 | 240,0 | 259,0 | 271,0 | 513,0 | 399,0 | 262,0 | 229,0 |
| **278,0** | 245,0 | 231,0 | 244,0 | 263,0 | 273,0 | 526,0 | 401,0 | 265,0 | 238,0 |
| **284,0** | 247,0 | 239,0 | 253,0 | 265,0 | 278,0 | 541,0 | 419,0 | 269,0 | 248,0 |
| **288,0** | 247,0 | 247,0 | 254,0 | 278,0 | 297,0 | 549,0 | 426,0 | 301,0 | 259,0 |
| **294,0** | 248,0 | 258,0 | 257,0 | 279,0 | 302,0 | 557,0 | 430,0 | 303,0 | 266,0 |
| **304,0** | 252,0 | 259,0 | 264,0 | 280,0 | 307,0 | 559,0 | 441,0 | 305,0 | 271,0 |
| **305,0** | 262,0 | 260,0 | 269,0 | 284,0 | 308,0 | 559,0 | 455,0 | 309,0 | 271,0 |
| **308,0** | 274,0 | 260,0 | 280,0 | 310,0 | 309,0 | 563,0 | 471,0 | 328,0 | 279,0 |
| **311,0** | 275,0 | 260,0 | 283,0 | 311,0 | 320,0 | 582,0 | 472,0 | 334,0 | 280,0 |
| **316,0** | 278,0 | 272,0 | 287,0 | 312,0 | 327,0 | 587,0 | 492,0 | 350,0 | 284,0 |
| **330,0** | 290,0 | 274,0 | 288,0 | 317,0 | 328,0 | 601,0 | 495,0 | 353,0 | 288,0 |
| **336,0** | 303,0 | 275,0 | 288,0 | 326,0 | 330,0 | 607,0 | 519,0 | 355,0 | 334,0 |
| **339,0** | 313,0 | 277,0 | 303,0 | 331,0 | 333,0 | 607,0 | 546,0 | 355,0 | 345,0 |
| **341,0** | 313,0 | 280,0 | 304,0 | 334,0 | 337,0 | 616,0 | 549,0 | 355,0 | 365,0 |
| **358,0** | 314,0 | 294,0 | 304,0 | 342,0 | 341,0 | 624,0 | 571,0 | 356,0 | 375,0 |
| **367,0** | 320,0 | 296,0 | 309,0 | 347,0 | 343,0 | 631,0 | 573,0 | 373,0 | 382,0 |
| **378,0** | 320,0 | 304,0 | 315,0 | 350,0 | 347,0 | 642,0 | 576,0 | 392,0 | 391,0 |
| **385,0** | 326,0 | 339,0 | 318,0 | 353,0 | 347,0 | 652,0 | 607,0 | 410,0 | 397,0 |

| | | | | | | | | | |
|---|---|---|---|---|---|---|---|---|---|
| **388,0** | 335,0 | 339,0 | 325,0 | 354,0 | 349,0 | 652,0 | 617,0 | 435,0 | 407,0 |
| **396,0** | 337,0 | 340,0 | 331,0 | 354,0 | 352,0 | 661,0 | 623,0 | 464,0 | 432,0 |
| **421,0** | 341,0 | 354,0 | 340,0 | 366,0 | 355,0 | 668,0 | 626,0 | 495,0 | 440,0 |
| **422,0** | 348,0 | 369,0 | 351,0 | 372,0 | 361,0 | 733,0 | 636,0 | 497,0 | 480,0 |
| **425,0** | 349,0 | 370,0 | 362,0 | 386,0 | 364,0 | 750,0 | 652,0 | 506,0 | 485,0 |
| **429,0** | 353,0 | 371,0 | 390,0 | 391,0 | 370,0 | 752,0 | 662,0 | 513,0 | 567,0 |
| **430,0** | 355,0 | 385,0 | 408,0 | 425,0 | 380,0 | 758,0 | 672,0 | 583,0 | 606,0 |
| **435,0** | 369,0 | 395,0 | 415,0 | 429,0 | 381,0 | 786,0 | 674,0 | 599,0 | 630,2 |
| **449,0** | 382,0 | 425,0 | 432,0 | 431,0 | 384,0 | 824,0 | 695,0 | 610,0 | 638,0 |
| **483,0** | 411,0 | 440,0 | 442,0 | 444,0 | 386,0 | 830,0 | 697,0 | 654,0 | 658,0 |
| **493,0** | 413,0 | 445,0 | 447,0 | 489,0 | 392,0 | 835,0 | 700,0 | 828,0 | 821,0 |
| **505,0** | 542,0 | 499,0 | 515,0 | 685,0 | 515,0 | 908,0 | 865,0 | 845,0 | 935,5 |
| | | | | | | | | | |
| **298,9** | 266,3 | 258,7 | 270,6 | 298,7 | 285,2 | 538,8 | 422,9 | 332,4 | 309,8 |

| | **34/5-1 S** | | | | | | | | | | |
|---|---|---|---|---|---|---|---|---|---|---|---|
| **3638,00** | **3640,00** | **3645,75** | **3646,50** | **3649,25** | **3650,25** | **3677,73** | **3678,50** | **3679,25** | **3684,90** | **3686,32** | **3688,50** |
| **28** | 34 | 26 | 34 | 31 | 28 | 95 | 108 | 101 | 156 | 84 | 161 |
| **39** | 36 | 45 | 36 | 32 | 30 | 97 | 124 | 134 | 196 | 136 | 163 |
| **47** | 36 | 48 | 40 | 34 | 33 | 104 | 132 | 136 | 217 | 143 | 168 |
| **48** | 38 | 49 | 42 | 36 | 34 | 113 | 137 | 142 | 253 | 145 | 175 |
| **50** | 39 | 52 | 43 | 39 | 36 | 126 | 137 | 149 | 255 | 148 | 176 |
| **51** | 40 | 53 | 46 | 39 | 38 | 129 | 139 | 175 | 286 | 152 | 181 |
| **59** | 45 | 54 | 49 | 39 | 38 | 133 | 146 | 177 | 306 | 178 | 185 |
| **59** | 45 | 58 | 55 | 40 | 40 | 144 | 149 | 178 | 310 | 199 | 199 |
| **60** | 46 | 60 | 58 | 41 | 40 | 147 | 154 | 180 | 324 | 202 | 210 |
| **61** | 47 | 60 | 58 | 41 | 41 | 158 | 163 | 188 | 349 | 208 | 210 |
| **63** | 48 | 61 | 58 | 44 | 42 | 161 | 165 | 193 | 361 | 221 | 211 |
| **64** | 50 | 62 | 59 | 45 | 42 | 162 | 166 | 209 | 366 | 239 | 217 |
| **64** | 51 | 62 | 59 | 48 | 46 | 162 | 173 | 210 | 406 | 247 | 226 |
| **64** | 52 | 62 | 60 | 49 | 46 | 168 | 181 | 214 | 413 | 269 | 228 |
| **65** | 52 | 64 | 62 | 49 | 47 | 176 | 185 | 216 | 438 | 275 | 228 |
| **68** | 53 | 64 | 62 | 50 | 47 | 179 | 189 | 219 | 447 | 283 | 232 |
| **69** | 55 | 64 | 63 | 51 | 50 | 182 | 192 | 233 | 448 | 288 | 233 |
| **69** | 58 | 66 | 63 | 53 | 50 | 182 | 194 | 235 | 454 | 291 | 238 |
| **69** | 59 | 67 | 64 | 53 | 50 | 184 | 195 | 240 | 473 | 293 | 245 |
| **69** | 61 | 69 | 65 | 54 | 51 | 185 | 199 | 247 | 510 | 327 | 247 |
| **69** | 64 | 69 | 66 | 55 | 51 | 186 | 201 | 252 | 517 | 337 | 254 |
| **71** | 65 | 70 | 67 | 55 | 52 | 187 | 204 | 253 | 537 | 342 | 256 |
| **73** | 66 | 72 | 67 | 56 | 52 | 189 | 209 | 260 | 541 | 346 | 266 |
| **73** | 66 | 73 | 69 | 60 | 53 | 192 | 210 | 268 | 541 | 360 | 284 |
| **73** | 66 | 74 | 72 | 61 | 53 | 194 | 215 | 279 | 549 | 363 | 290 |
| **74** | 67 | 76 | 73 | 61 | 55 | 199 | 217 | 294 | 552 | 364 | 295 |
| **74** | 73 | 76 | 75 | 62 | 56 | 202 | 221 | 299 | 552 | 373 | 295 |

| | | | | | | | | | | | |
|---|---|---|---|---|---|---|---|---|---|---|---|
| **75** | 75 | 76 | 76 | 63 | 56 | 202 | 222 | 301 | 554 | 378 | 299 |
| **77** | 75 | 77 | 76 | 63 | 59 | 202 | 223 | 312 | 557 | 410 | 299 |
| **79** | 77 | 77 | 77 | 66 | 59 | 204 | 229 | 322 | 570 | 435 | 310 |
| **80** | 78 | 78 | 77 | 68 | 62 | 209 | 235 | 323 | 593 | 441 | 323 |
| **82** | 80 | 82 | 78 | 69 | 62 | 214 | 237 | 330 | 594 | 453 | 327 |
| **82** | 80 | 85 | 82 | 69 | 63 | 215 | 237 | 333 | 612 | 460 | 334 |
| **83** | 81 | 86 | 85 | 70 | 66 | 222 | 239 | 333 | 622 | 483 | 337 |
| **84** | 84 | 86 | 86 | 70 | 67 | 227 | 243 | 340 | 627 | 485 | 345 |
| **85** | 86 | 86 | 87 | 70 | 68 | 228 | 251 | 344 | 646 | 497 | 349 |
| **86** | 87 | 87 | 87 | 73 | 68 | 228 | 254 | 350 | 675 | 507 | 352 |
| **87** | 88 | 87 | 88 | 74 | 69 | 235 | 256 | 356 | 696 | 507 | 360 |
| **87** | 89 | 92 | 88 | 74 | 70 | 238 | 266 | 358 | 730 | 527 | 360 |
| **92** | 94 | 92 | 90 | 75 | 74 | 239 | 272 | 366 | 744 | 567 | 465 |
| **96** | 94 | 94 | 90 | 76 | 75 | 242 | 273 | 372 | 780 | 576 | 487 |
| **98** | 95 | 95 | 97 | 81 | 78 | 245 | 275 | 379 | 782 | 594 | 489 |
| **103** | 97 | 96 | 98 | 82 | 80 | 259 | 276 | 395 | 795 | 611 | 496 |
| **109** | 99 | 96 | 98 | 82 | 83 | 260 | 293 | 399 | 821 | 620 | 502 |
| **122** | 99 | 98 | 98 | 85 | 83 | 273 | 300 | 410 | 859 | 651 | 558 |
| **130** | 102 | 100 | 115 | 88 | 84 | 286 | 317 | 415 | 874 | 732 | 577 |
| **130** | 106 | 101 | 116 | 91 | 84 | 295 | 344 | 416 | 878 | 734 | 613 |
| **132** | 115 | 113 | 118 | 92 | 97 | 297 | 347 | 423 | 913 | 1019 | 617 |
| **141** | 122 | 120 | 119 | 97 | 97 | 325 | 350 | 442 | 975 | 1071 | 1078 |
| **177** | 130 | 170 | 131 | 123 | 102 | 365 | 576 | 530 | 1026 | 1153 | 1164 |
| | | | | | | | | | | | |
| **79,8** | 70,9 | 76,6 | 74,44 | 61,58 | 58,14 | 200,92 | 224,4 | 284,6 | 553,6 | 414,48 | 342,28 |

| **3921,12** | **34/3-3 S 3925,12** | **3929,12** | **3933,12** | **3946,06** | **3949,06** | **3952,06** | **3975,06** | **3984,06** |
|---|---|---|---|---|---|---|---|---|
| **86** | 155 | 145 | 77 | 128 | 136 | 138 | 180 | 193 |
| **116** | 235 | 178 | 162 | 144 | 148 | 184 | 206 | 231 |
| **138** | 238 | 189 | 178 | 145 | 155 | 198 | 228 | 252 |
| **148** | 244 | 192 | 190 | 146 | 187 | 199 | 290 | 254 |
| **172** | 250 | 205 | 194 | 152 | 193 | 217 | 295 | 271 |
| **178** | 260 | 211 | 197 | 159 | 197 | 236 | 303 | 275 |
| **211** | 269 | 220 | 200 | 165 | 212 | 292 | 309 | 280 |
| **217** | 274 | 225 | 223 | 171 | 218 | 352 | 318 | 282 |
| **238** | 282 | 226 | 230 | 175 | 229 | 386 | 324 | 293 |
| **244** | 284 | 234 | 238 | 199 | 270 | 401 | 349 | 337 |
| **249** | 284 | 241 | 245 | 212 | 293 | 406 | 369 | 345 |
| **253** | 290 | 248 | 246 | 217 | 307 | 407 | 389 | 399 |
| **260** | 290 | 261 | 256 | 239 | 309 | 420 | 390 | 403 |
| **266** | 292 | 264 | 258 | 253 | 358 | 451 | 407 | 405 |
| **267** | 294 | 266 | 262 | 258 | 359 | 464 | 411 | 409 |
| **270** | 297 | 268 | 267 | 260 | 370 | 487 | 425 | 438 |

| | | | | | | | | |
|---|---|---|---|---|---|---|---|---|
| **274** | 303 | 269 | 272 | 269 | 375 | 491 | 430 | 471 |
| **295** | 305 | 270 | 278 | 279 | 376 | 492 | 432 | 479 |
| **303** | 311 | 281 | 290 | 291 | 379 | 492 | 437 | 485 |
| **303** | 313 | 281 | 292 | 297 | 391 | 496 | 441 | 486 |
| **308** | 319 | 295 | 293 | 302 | 391 | 520 | 449 | 488 |
| **325** | 328 | 301 | 294 | 306 | 395 | 520 | 453 | 508 |
| **327** | 330 | 303 | 314 | 308 | 398 | 523 | 453 | 510 |
| **359** | 333 | 306 | 322 | 312 | 410 | 536 | 461 | 519 |
| **362** | 334 | 315 | 331 | 315 | 420 | 537 | 463 | 551 |
| **369** | 338 | 322 | 335 | 323 | 427 | 542 | 464 | 557 |
| **372** | 339 | 337 | 337 | 335 | 442 | 575 | 475 | 557 |
| **383** | 340 | 337 | 349 | 339 | 461 | 577 | 481 | 557 |
| **384** | 347 | 341 | 356 | 341 | 470 | 591 | 481 | 604 |
| **404** | 354 | 343 | 366 | 344 | 488 | 608 | 482 | 615 |
| **412** | 369 | 344 | 376 | 346 | 495 | 615 | 491 | 615 |
| **424** | 373 | 353 | 382 | 352 | 509 | 626 | 493 | 621 |
| **427** | 373 | 359 | 394 | 362 | 547 | 628 | 495 | 654 |
| **441** | 380 | 360 | 395 | 369 | 556 | 648 | 495 | 673 |
| **452** | 381 | 372 | 396 | 372 | 558 | 672 | 504 | 693 |
| **480** | 383 | 376 | 418 | 389 | 564 | 678 | 504 | 749 |
| **483** | 386 | 376 | 429 | 391 | 604 | 694 | 510 | 762 |
| **502** | 388 | 383 | 438 | 407 | 604 | 696 | 514 | 763 |
| **507** | 392 | 400 | 448 | 418 | 645 | 723 | 515 | 800 |
| **533** | 398 | 407 | 465 | 434 | 678 | 740 | 520 | 871 |
| **533** | 408 | 418 | 470 | 440 | 701 | 750 | 533 | 873 |
| **537** | 417 | 419 | 472 | 445 | 770 | 762 | 533 | 874 |
| **539** | 439 | 433 | 482 | 446 | 804 | 846 | 538 | 998 |
| **565** | 451 | 435 | 491 | 448 | 833 | 974 | 541 | 1004 |
| **587** | 455 | 443 | 496 | 454 | 868 | 1109 | 577 | 1080 |
| **602** | 475 | 460 | 509 | 457 | 878 | 1195 | 604 | 1132 |
| **619** | 487 | 513 | 523 | 469 | 943 | 1215 | 612 | 1142 |
| **625** | 487 | 523 | 560 | 505 | 970 | 1318 | 625 | 1182 |
| **679** | 609 | 564 | 569 | 537 | 1010 | 1354 | 660 | 1381 |
| **714** | 627 | 769 | 588 | 548 | 1326 | 2012 | 682 | 1794 |
| | | | | | | | | |
| **374,84** | 350,2 | 331,62 | 343,06 | 319,46 | 492,54 | 619,86 | 450,82 | 622,3 |

| | **34/3-1 S** | | | | | | | | | | | | |
|---|---|---|---|---|---|---|---|---|---|---|---|---|---|
| **3868,79** | **3868,87** | **3870,35** | **3873,30** | **3874,18** | **3880,56** | **3885,70** | **3886,27** | **3887,35** | **3899,97** | **3900,01** | **3901,13** | **3915,60** | **3927,81** |
| **116** | 65 | 58 | 220 | 103 | 121 | 140 | 125 | 117 | 111 | 110 | 104 | 182 | 152 |
| **125** | 99 | 93 | 232 | 168 | 160 | 146 | 140 | 125 | 153 | 140 | 113 | 186 | 165 |
| **140** | 104 | 94 | 236 | 191 | 160 | 147 | 186 | 142 | 164 | 151 | 121 | 187 | 167 |
| **140** | 109 | 102 | 240 | 197 | 191 | 150 | 188 | 145 | 165 | 157 | 121 | 187 | 173 |
| **142** | 115 | 103 | 244 | 207 | 194 | 154 | 189 | 146 | 170 | 182 | 121 | 189 | 180 |

| | | | | | | | | | | | | | |
|---|---|---|---|---|---|---|---|---|---|---|---|---|---|
| **144** | 127 | 106 | 247 | 217 | 201 | 169 | 194 | 151 | 171 | 187 | 126 | 190 | 183 |
| **148** | 127 | 106 | 249 | 245 | 221 | 169 | 208 | 169 | 172 | 190 | 132 | 199 | 189 |
| **153** | 129 | 108 | 255 | 247 | 226 | 178 | 208 | 177 | 177 | 197 | 146 | 214 | 193 |
| **156** | 142 | 110 | 256 | 270 | 231 | 192 | 213 | 177 | 184 | 206 | 152 | 217 | 195 |
| **171** | 143 | 114 | 258 | 278 | 239 | 192 | 220 | 179 | 185 | 225 | 164 | 218 | 195 |
| **173** | 149 | 115 | 262 | 280 | 241 | 196 | 220 | 187 | 196 | 238 | 165 | 218 | 199 |
| **179** | 161 | 118 | 263 | 281 | 247 | 197 | 233 | 211 | 196 | 239 | 166 | 223 | 204 |
| **185** | 162 | 119 | 275 | 286 | 251 | 206 | 234 | 213 | 214 | 240 | 175 | 226 | 212 |
| **185** | 163 | 120 | 280 | 289 | 256 | 209 | 237 | 216 | 230 | 242 | 181 | 236 | 218 |
| **189** | 165 | 124 | 287 | 289 | 259 | 209 | 253 | 218 | 230 | 244 | 188 | 237 | 219 |
| **189** | 166 | 125 | 290 | 291 | 267 | 213 | 253 | 224 | 238 | 247 | 205 | 238 | 223 |
| **191** | 168 | 127 | 295 | 291 | 274 | 225 | 265 | 228 | 243 | 250 | 208 | 240 | 226 |
| **192** | 169 | 128 | 308 | 309 | 283 | 229 | 267 | 230 | 244 | 254 | 209 | 242 | 235 |
| **203** | 175 | 132 | 313 | 322 | 307 | 230 | 272 | 232 | 257 | 260 | 214 | 246 | 236 |
| **206** | 177 | 135 | 315 | 333 | 315 | 230 | 275 | 233 | 260 | 270 | 216 | 251 | 243 |
| **206** | 177 | 137 | 315 | 339 | 316 | 231 | 276 | 240 | 261 | 276 | 219 | 258 | 245 |
| **207** | 182 | 140 | 323 | 351 | 320 | 241 | 305 | 249 | 264 | 278 | 221 | 260 | 246 |
| **215** | 184 | 143 | 340 | 359 | 320 | 242 | 312 | 257 | 271 | 283 | 222 | 265 | 247 |
| **225** | 194 | 145 | 348 | 360 | 329 | 250 | 312 | 261 | 276 | 284 | 229 | 272 | 252 |
| **226** | 197 | 155 | 349 | 369 | 329 | 252 | 315 | 265 | 277 | 286 | 234 | 275 | 253 |
| **233** | 197 | 156 | 356 | 383 | 336 | 258 | 318 | 273 | 278 | 287 | 237 | 279 | 254 |
| **234** | 197 | 163 | 358 | 387 | 338 | 268 | 324 | 275 | 279 | 289 | 250 | 281 | 255 |
| **242** | 203 | 170 | 364 | 390 | 358 | 271 | 335 | 280 | 280 | 295 | 270 | 289 | 258 |
| **243** | 204 | 176 | 371 | 402 | 358 | 275 | 339 | 289 | 280 | 304 | 275 | 292 | 261 |
| **244** | 204 | 186 | 372 | 404 | 359 | 279 | 352 | 290 | 300 | 310 | 276 | 293 | 269 |
| **244** | 221 | 203 | 373 | 429 | 363 | 283 | 353 | 314 | 307 | 314 | 277 | 300 | 270 |
| **252** | 222 | 210 | 388 | 431 | 365 | 285 | 354 | 315 | 308 | 314 | 278 | 317 | 271 |
| **254** | 232 | 211 | 392 | 435 | 397 | 295 | 356 | 328 | 310 | 317 | 298 | 321 | 276 |
| **272** | 232 | 217 | 395 | 436 | 400 | 300 | 375 | 329 | 311 | 321 | 298 | 357 | 277 |
| **295** | 232 | 217 | 405 | 439 | 406 | 303 | 381 | 331 | 313 | 325 | 300 | 357 | 284 |
| **296** | 234 | 220 | 414 | 440 | 408 | 304 | 387 | 335 | 322 | 346 | 309 | 357 | 290 |
| **297** | 239 | 221 | 414 | 446 | 409 | 313 | 390 | 343 | 324 | 348 | 310 | 361 | 297 |
| **298** | 240 | 226 | 415 | 448 | 410 | 321 | 391 | 354 | 332 | 356 | 317 | 364 | 298 |
| **304** | 244 | 228 | 425 | 453 | 414 | 326 | 397 | 357 | 333 | 361 | 323 | 392 | 299 |
| **312** | 255 | 232 | 425 | 464 | 414 | 347 | 398 | 367 | 339 | 371 | 330 | 400 | 299 |
| **317** | 258 | 241 | 429 | 486 | 430 | 354 | 405 | 369 | 352 | 372 | 332 | 401 | 301 |
| **334** | 264 | 260 | 430 | 499 | 446 | 362 | 412 | 370 | 363 | 373 | 344 | 411 | 302 |
| **336** | 271 | 272 | 436 | 517 | 449 | 380 | 415 | 373 | 377 | 384 | 357 | 425 | 302 |
| **337** | 301 | 276 | 442 | 525 | 461 | 389 | 422 | 378 | 378 | 412 | 364 | 445 | 314 |
| **347** | 311 | 326 | 452 | 541 | 492 | 412 | 429 | 383 | 391 | 431 | 375 | 465 | 316 |
| **353** | 337 | 341 | 469 | 557 | 506 | 415 | 444 | 390 | 403 | 432 | 390 | 465 | 354 |
| **355** | 369 | 342 | 473 | 565 | 553 | 428 | 448 | 410 | 417 | 440 | 395 | 486 | 359 |
| **362** | 390 | 356 | 492 | 592 | 575 | 456 | 451 | 414 | 424 | 488 | 437 | 499 | 372 |

| | | | | | | | | | | | | | |
|---|---|---|---|---|---|---|---|---|---|---|---|---|---|
| **447** | 393 | 399 | 556 | 643 | 587 | 456 | 455 | 512 | 425 | 528 | 441 | 529 | 393 |
| **503** | 515 | 429 | 607 | 803 | 633 | 487 | 593 | 780 | 448 | 552 | 504 | 579 | 396 |
| | | | | | | | | | | | | | |
| **242,34** | 210,28 | 184,7 | 353,06 | 379,74 | 342,5 | 271,28 | 316,48 | 283,02 | 278,06 | 298,12 | 252,78 | 306,42 | 256,34 |

# *Appendix III*

## Petrography – *Thin section* analysis of selected samples

### 34/3-2_4057,75

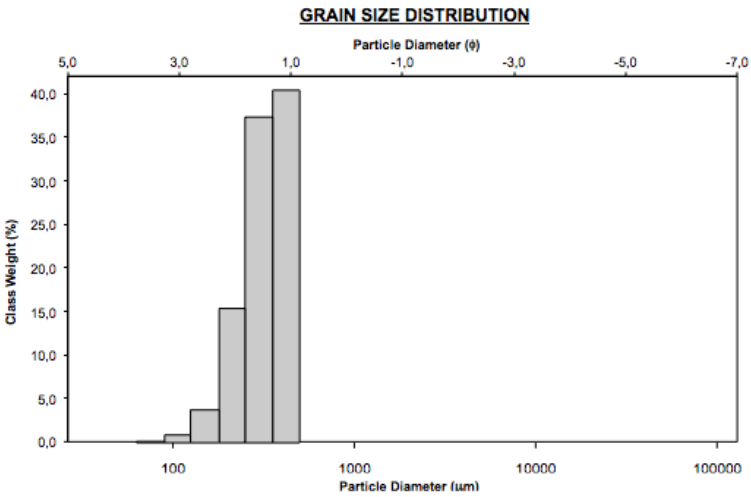


**SAMPLE STATISTICS**

SAMPLE IDENTITY:

SAMPLE TYPE: Unimodal, Well Sorted
SEDIMENT NAME: Well Sorted Medium Sand

ANALYST & DATE: ,

TEXTURAL GROUP: Sand

| | µm | ϕ |
|---|---|---|
| MODE 1: | 427,5 | 1,247 |
| MODE 2: | | |
| MODE 3: | | |
| $D_{10}$: | 200,5 | 1,120 |
| MEDIAN or $D_{50}$: | 327,5 | 1,610 |
| $D_{90}$: | 460,0 | 2,318 |
| ($D_{90}$ / $D_{10}$): | 2,294 | 2,069 |
| ($D_{90}$ - $D_{10}$): | 259,5 | 1,198 |
| ($D_{75}$ / $D_{25}$): | 1,553 | 1,488 |
| ($D_{75}$ - $D_{25}$): | 144,6 | 0,635 |

GRAIN SIZE DISTRIBUTION

| | | | |
|---|---|---|---|
| GRAVEL: | 0,0% | COARSE SAND: | 0,0% |
| SAND: | 100,0% | MEDIUM SAND: | 79,9% |
| MUD: | 0,0% | FINE SAND: | 19,1% |
| | | V FINE SAND: | 1,0% |
| V COARSE GRAVEL: | 0,0% | V COARSE SILT: | 0,0% |
| COARSE GRAVEL: | 0,0% | COARSE SILT: | 0,0% |
| MEDIUM GRAVEL: | 0,0% | MEDIUM SILT: | 0,0% |
| FINE GRAVEL: | 0,0% | FINE SILT: | 0,0% |
| V FINE GRAVEL: | 0,0% | V FINE SILT: | 0,0% |
| V COARSE SAND: | 0,0% | CLAY: | 0,0% |

| | METHOD OF MOMENTS | | | FOLK & WARD METHOD | | |
|---|---|---|---|---|---|---|
| | Arithmetic µm | Geometric µm | Logarithmic ϕ | Geometric µm | Logarithmic ϕ | Description |
| MEAN ($\bar{x}$): | 332,6 | 314,0 | 1,671 | 320,0 | 1,644 | Medium Sand |
| SORTING ($\sigma$): | 89,33 | 1,361 | 0,445 | 1,366 | 0,450 | Well Sorted |
| SKEWNESS ($Sk$): | -0,371 | -1,037 | 1,037 | -0,167 | 0,167 | Fine Skewed |
| KURTOSIS ($K$): | 2,099 | 4,078 | 4,078 | 0,919 | 0,919 | Mesokurtic |

The sample is dominated by medium sand that is well sorted. The calculated porosity is 9,1% due to carbonate cement. The IGV is calculated to be 36,9%.

**34_3-2_4061,75**

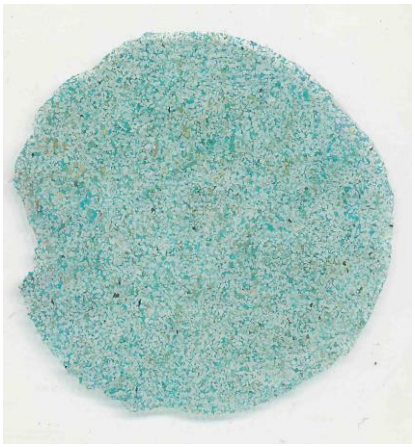

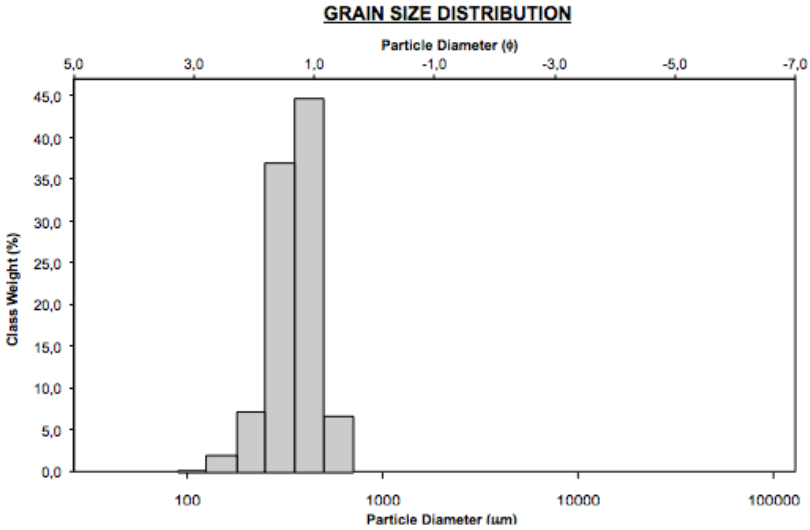


## SAMPLE STATISTICS

SAMPLE IDENTITY:

ANALYST & DATE: ,

SAMPLE TYPE: Unimodal, Well Sorted

TEXTURAL GROUP: Sand

SEDIMENT NAME: Well Sorted Medium Sand

| | µm | ϕ |
|---|---|---|
| MODE 1: | 427,5 | 1,247 |
| MODE 2: | | |
| MODE 3: | | |
| $D_{10}$: | 251,2 | 1,033 |
| MEDIAN or $D_{50}$: | 361,0 | 1,470 |
| $D_{90}$: | 488,7 | 1,993 |
| ($D_{90}$ / $D_{10}$): | 1,945 | 1,929 |
| ($D_{90}$ - $D_{10}$): | 237,4 | 0,960 |
| ($D_{75}$ / $D_{25}$): | 1,514 | 1,500 |
| ($D_{75}$ - $D_{25}$): | 148,0 | 0,598 |

GRAIN SIZE DISTRIBUTION

| | | | |
|---|---|---|---|
| GRAVEL: | 0,0% | COARSE SAND: | 7,0% |
| SAND: | 100,0% | MEDIUM SAND: | 83,6% |
| MUD: | 0,0% | FINE SAND: | 9,3% |
| | | V FINE SAND: | 0,2% |
| V COARSE GRAVEL: | 0,0% | V COARSE SILT: | 0,0% |
| COARSE GRAVEL: | 0,0% | COARSE SILT: | 0,0% |
| MEDIUM GRAVEL: | 0,0% | MEDIUM SILT: | 0,0% |
| FINE GRAVEL: | 0,0% | FINE SILT: | 0,0% |
| V FINE GRAVEL: | 0,0% | V FINE SILT: | 0,0% |
| V COARSE SAND: | 0,0% | CLAY: | 0,0% |

| | METHOD OF MOMENTS | | | FOLK & WARD METHOD | | |
|---|---|---|---|---|---|---|
| | Arithmetic µm | Geometric µm | Logarithmic ϕ | Geometric µm | Logarithmic ϕ | Description |
| MEAN ($\bar{x}$) | 370,2 | 350,9 | 1,511 | 355,0 | 1,494 | Medium Sand |
| SORTING ($\sigma$): | 99,90 | 1,331 | 0,413 | 1,340 | 0,423 | Well Sorted |
| SKEWNESS ($Sk$): | 0,337 | -0,636 | 0,636 | -0,120 | 0,120 | Fine Skewed |
| KURTOSIS ($K$): | 3,271 | 4,000 | 4,000 | 0,990 | 0,990 | Mesokurtic |

The sample is dominated by medium sand witch is well sorted. The calculated porosity is 18,8%, and the IGV is calculated to be 36,3%.

## 34_3-2_4073,25

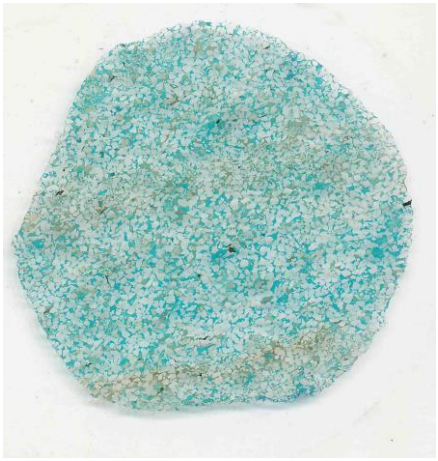

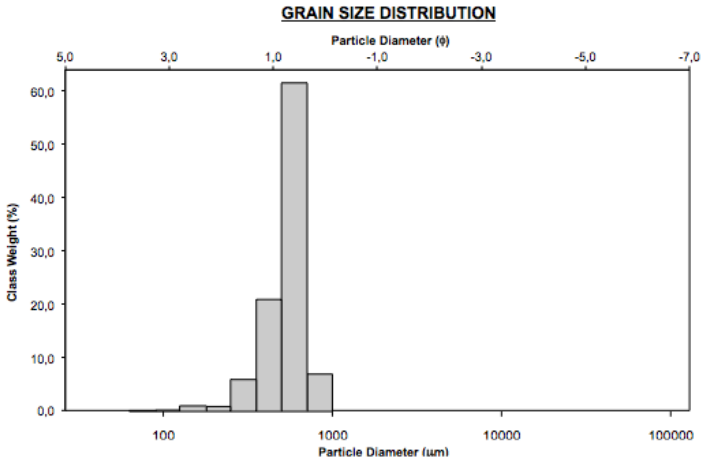


### SAMPLE STATISTICS

SAMPLE IDENTITY:

ANALYST & DATE: ,

SAMPLE TYPE: Unimodal, Well Sorted

TEXTURAL GROUP: Sand

SEDIMENT NAME: Well Sorted Coarse Sand

| | µm | ϕ |
|---|---|---|
| MODE 1: | 605,0 | 0,747 |
| MODE 2: | | |
| MODE 3: | | |
| $D_{10}$: | 363,4 | 0,518 |
| MEDIAN or $D_{50}$: | 559,7 | 0,837 |
| $D_{90}$: | 698,4 | 1,460 |
| ($D_{90}$ / $D_{10}$): | 1,922 | 2,820 |
| ($D_{90}$ - $D_{10}$): | 335,0 | 0,942 |
| ($D_{75}$ / $D_{25}$): | 1,386 | 1,739 |
| ($D_{75}$ - $D_{25}$): | 179,0 | 0,471 |

GRAIN SIZE DISTRIBUTION

| | | | |
|---|---|---|---|
| GRAVEL: | 0,0% | COARSE SAND: | 70,4% |
| SAND: | 100,0% | MEDIUM SAND: | 27,2% |
| MUD: | 0,0% | FINE SAND: | 2,0% |
| | | V FINE SAND: | 0,4% |
| V COARSE GRAVEL: | 0,0% | V COARSE SILT: | 0,0% |
| COARSE GRAVEL: | 0,0% | COARSE SILT: | 0,0% |
| MEDIUM GRAVEL: | 0,0% | MEDIUM SILT: | 0,0% |
| FINE GRAVEL: | 0,0% | FINE SILT: | 0,0% |
| V FINE GRAVEL: | 0,0% | V FINE SILT: | 0,0% |
| V COARSE SAND: | 0,0% | CLAY: | 0,0% |

| | METHOD OF MOMENTS | | | FOLK & WARD METHOD | | |
|---|---|---|---|---|---|---|
| | Arithmetic µm | Geometric µm | Logarithmic ϕ | Geometric µm | Logarithmic ϕ | Description |
| MEAN ($\bar{x}$): | 556,0 | 526,7 | 0,925 | 533,1 | 0,908 | Coarse Sand |
| SORTING ($\sigma$): | 137,6 | 1,356 | 0,439 | 1,325 | 0,406 | Well Sorted |
| SKEWNESS ($Sk$): | -0,373 | -1,971 | 1,971 | -0,301 | 0,301 | Very Fine Skewed |
| KURTOSIS ($K$): | 4,110 | 9,688 | 9,688 | 1,248 | 1,248 | Leptokurtic |

The sample is dominated by coarse sand and is well sorted. The calculated porosity 16,8%, and the IGV is calculated to be 33,9%.

**34_3-2_4079,5**

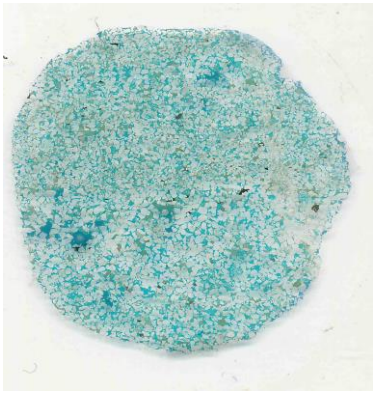

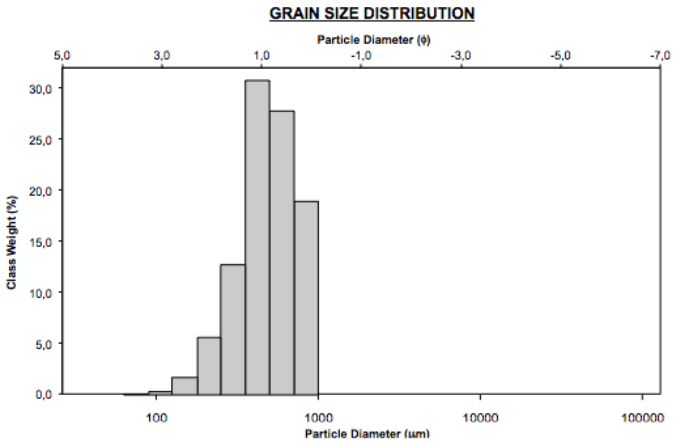


## SAMPLE STATISTICS

SAMPLE IDENTITY: ANALYST & DATE: ,

SAMPLE TYPE: Unimodal, Moderately Well Sorted TEXTURAL GROUP: Sand

SEDIMENT NAME: Moderately Well Sorted Coarse Sand

| | µm | ϕ |
|---|---|---|
| MODE 1: | 427,5 | 1,247 |
| MODE 2: | | |
| MODE 3: | | |
| $D_{10}$: | 266,0 | 0,258 |
| MEDIAN or $D_{50}$: | 489,0 | 1,032 |
| $D_{90}$: | 836,4 | 1,911 |
| ($D_{90}$ / $D_{10}$): | 3,145 | 7,414 |
| ($D_{90}$ - $D_{10}$): | 570,4 | 1,653 |
| ($D_{75}$ / $D_{25}$): | 1,780 | 2,395 |
| ($D_{75}$ - $D_{25}$): | 289,9 | 0,832 |

GRAIN SIZE DISTRIBUTION

| | | | |
|---|---|---|---|
| GRAVEL: | 0,0% | COARSE SAND: | 48,0% |
| SAND: | 100,0% | MEDIUM SAND: | 44,4% |
| MUD: | 0,0% | FINE SAND: | 7,3% |
| | | V FINE SAND: | 0,4% |
| V COARSE GRAVEL: | 0,0% | V COARSE SILT: | 0,0% |
| COARSE GRAVEL: | 0,0% | COARSE SILT: | 0,0% |
| MEDIUM GRAVEL: | 0,0% | MEDIUM SILT: | 0,0% |
| FINE GRAVEL: | 0,0% | FINE SILT: | 0,0% |
| V FINE GRAVEL: | 0,0% | V FINE SILT: | 0,0% |
| V COARSE SAND: | 0,0% | CLAY: | 0,0% |

| | METHOD OF MOMENTS | | | FOLK & WARD METHOD | | |
|---|---|---|---|---|---|---|
| | Arithmetic µm | Geometric µm | Logarithmic ϕ | Geometric µm | Logarithmic ϕ | Description |
| MEAN ($\bar{x}$): | 526,2 | 477,5 | 1,067 | 485,8 | 1,042 | Medium Sand |
| SORTING ($\sigma$): | 201,7 | 1,529 | 0,612 | 1,554 | 0,636 | Moderately Well Sorted |
| SKEWNESS ($Sk$): | 0,278 | -0,639 | 0,639 | -0,082 | 0,082 | Symmetrical |
| KURTOSIS ($K$): | 2,178 | 3,335 | 3,335 | 1,036 | 1,036 | Mesokurtic |

The sample is divided between medium and coarse sand. From the scan of the thin section it looks like the sample is divided in two. Upper half consists of medium grains, the lower half coarse grains. The sorting is moderately well sorted. The calculated porosity is 15%, and the IGV is calculated to be 35%.

## 34_3-3_3925,12

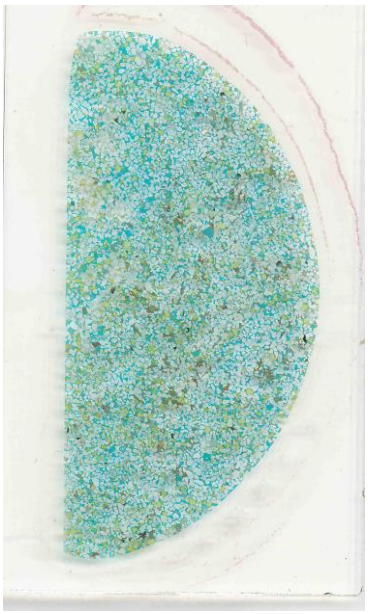

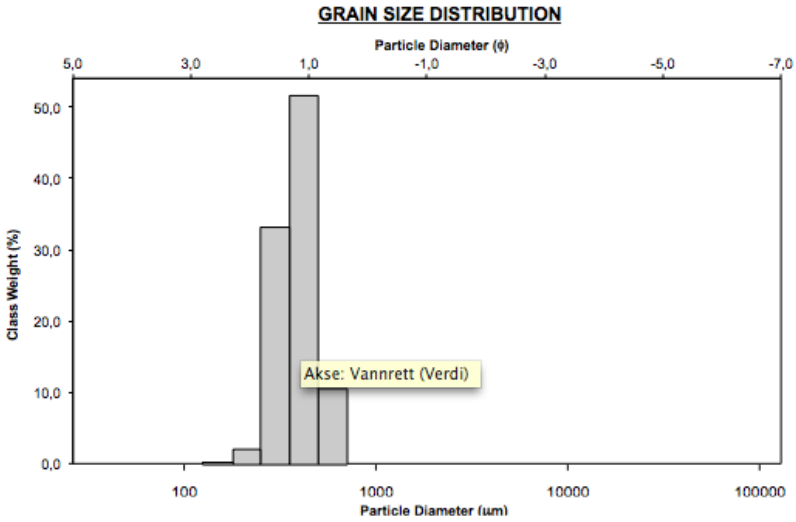


**SAMPLE STATISTICS**

SAMPLE IDENTITY:

ANALYST & DATE: ,

SAMPLE TYPE: Unimodal, Well Sorted

TEXTURAL GROUP: Sand

SEDIMENT NAME: Well Sorted Medium Sand

| | µm | ϕ |
|---|---|---|
| MODE 1: | 427,5 | 1,247 |
| MODE 2: | | |
| MODE 3: | | |
| $D_{10}$: | 270,1 | 0,954 |
| MEDIAN or $D_{50}$: | 387,1 | 1,369 |
| $D_{90}$: | 516,2 | 1,889 |
| ($D_{90}$ / $D_{10}$): | 1,912 | 1,980 |
| ($D_{90}$ - $D_{10}$): | 246,2 | 0,935 |
| ($D_{75}$ / $D_{25}$): | 1,449 | 1,473 |
| ($D_{75}$ - $D_{25}$): | 141,4 | 0,535 |

GRAIN SIZE DISTRIBUTION

| | | | |
|---|---|---|---|
| GRAVEL: | 0,0% | COARSE SAND: | 11,0% |
| SAND: | 100,0% | MEDIUM SAND: | 86,6% |
| MUD: | 0,0% | FINE SAND: | 2,4% |
| | | V FINE SAND: | 0,0% |
| V COARSE GRAVEL: | 0,0% | V COARSE SILT: | 0,0% |
| COARSE GRAVEL: | 0,0% | COARSE SILT: | 0,0% |
| MEDIUM GRAVEL: | 0,0% | MEDIUM SILT: | 0,0% |
| FINE GRAVEL: | 0,0% | FINE SILT: | 0,0% |
| V FINE GRAVEL: | 0,0% | V FINE SILT: | 0,0% |
| V COARSE SAND: | 0,0% | CLAY: | 0,0% |

| | METHOD OF MOMENTS | | | FOLK & WARD METHOD | | |
|---|---|---|---|---|---|---|
| | Arithmetic µm | Geometric µm | Logarithmic ϕ | Geometric µm | Logarithmic ϕ | Description |
| MEAN ($\bar{x}$) | 398,7 | 381,6 | 1,390 | 377,4 | 1,406 | Medium Sand |
| SORTING ($\sigma$): | 95,98 | 1,273 | 0,348 | 1,298 | 0,376 | Well Sorted |
| SKEWNESS ($Sk$): | 0,556 | -0,146 | 0,146 | -0,051 | 0,051 | Symmetrical |
| KURTOSIS ($K$): | 3,131 | 3,185 | 3,185 | 0,948 | 0,948 | Mesokurtic |

The sample is dominated by medium sand, which is well sorted. The calculated porosity is 14,6%, and the IGV is calculated to be 32,3%. There is a high content of clay mix in the sample.

**34_3-3_3949,06**

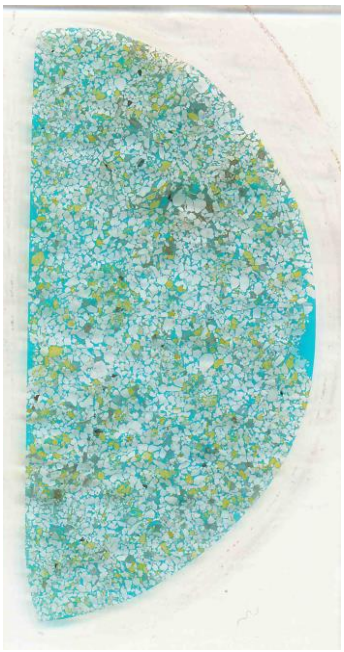

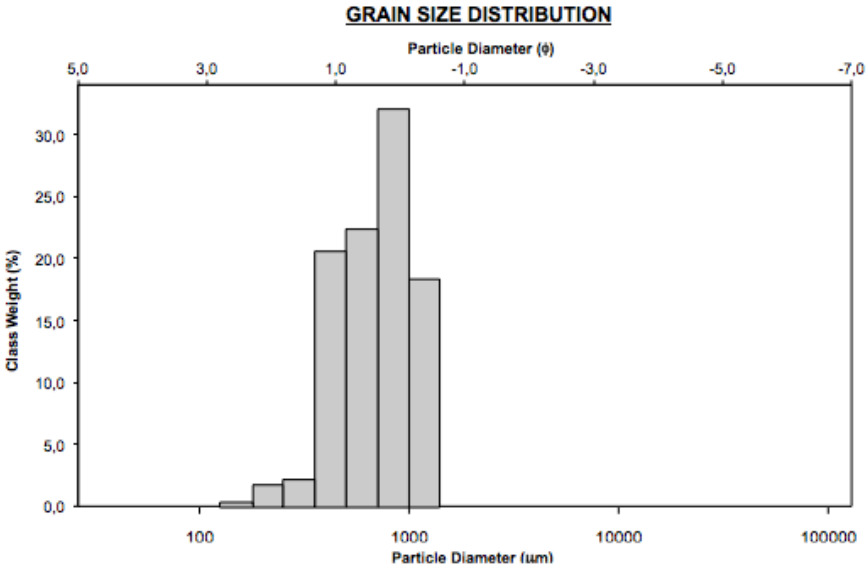


## SAMPLE STATISTICS

SAMPLE IDENTITY:

ANALYST & DATE: ,

SAMPLE TYPE: Unimodal, Moderately Well Sorted

TEXTURAL GROUP: Sand

SEDIMENT NAME: Moderately Well Sorted Coarse Sand

| | µm | ϕ |
|---|---|---|
| MODE 1: | 855,0 | 0,247 |
| MODE 2: | | |
| MODE 3: | | |
| $D_{10}$: | 388,0 | -0,221 |
| MEDIAN or $D_{50}$: | 718,0 | 0,478 |
| $D_{90}$: | 1165,9 | 1,366 |
| ($D_{90}$ / $D_{10}$): | 3,005 | -6,168 |
| ($D_{90}$ - $D_{10}$): | 778,0 | 1,587 |
| ($D_{75}$ / $D_{25}$): | 1,883 | 10,14 |
| ($D_{75}$ - $D_{25}$): | 437,6 | 0,913 |

GRAIN SIZE DISTRIBUTION

| | | | |
|---|---|---|---|
| GRAVEL: | 0,0% | COARSE SAND: | 56,0% |
| SAND: | 100,0% | MEDIUM SAND: | 23,3% |
| MUD: | 0,0% | FINE SAND: | 2,2% |
| | | V FINE SAND: | 0,0% |
| V COARSE GRAVEL: | 0,0% | V COARSE SILT: | 0,0% |
| COARSE GRAVEL: | 0,0% | COARSE SILT: | 0,0% |
| MEDIUM GRAVEL: | 0,0% | MEDIUM SILT: | 0,0% |
| FINE GRAVEL: | 0,0% | FINE SILT: | 0,0% |
| V FINE GRAVEL: | 0,0% | V FINE SILT: | 0,0% |
| V COARSE SAND: | 18,4% | CLAY: | 0,0% |

| | METHOD OF MOMENTS | | | FOLK & WARD METHOD | | |
|---|---|---|---|---|---|---|
| | Arithmetic µm | Geometric µm | Logarithmic ϕ | Geometric µm | Logarithmic ϕ | Description |
| MEAN ($\bar{x}$) | 742,8 | 675,8 | 0,565 | 684,6 | 0,547 | Coarse Sand |
| SORTING ($\sigma$): | 280,9 | 1,517 | 0,601 | 1,516 | 0,600 | Moderately Well Sorted |
| SKEWNESS ($Sk$): | 0,240 | -0,586 | 0,586 | -0,127 | 0,127 | Fine Skewed |
| KURTOSIS ($K$): | 2,095 | 3,137 | 3,137 | 0,824 | 0,824 | Platykurtic |

The sample is dominated by coarse sand, but there are moderate amounts of very coarse and medium sand as well. The sorting s moderately well sorted. The calculated porosity is 14,9%, and the IGV is calculated to be 31%.

**34_3-3_3975,06**

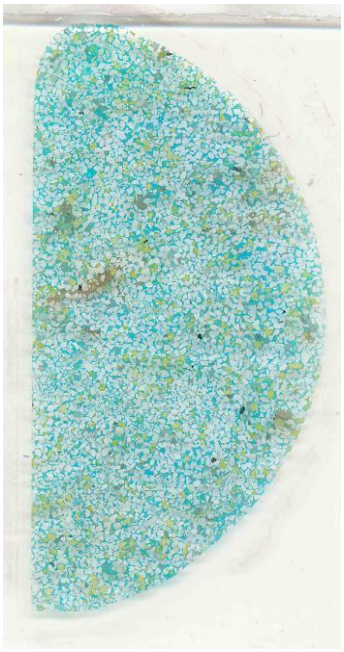

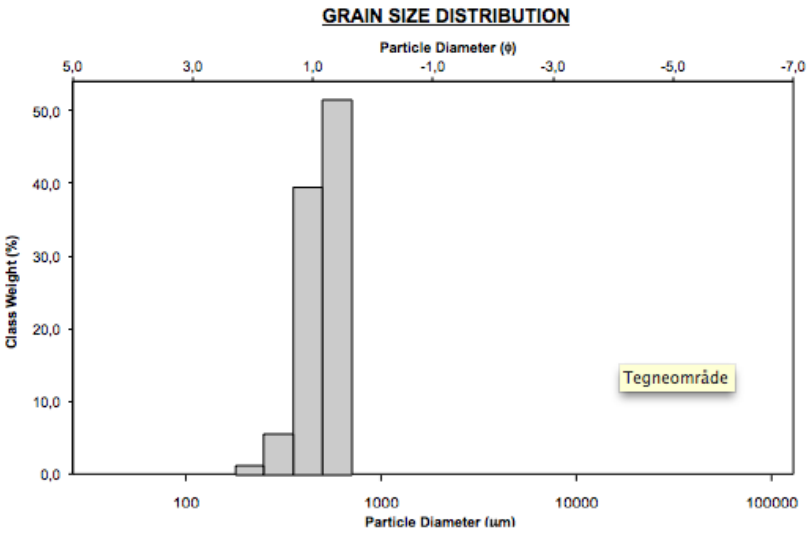


## SAMPLE STATISTICS

SAMPLE IDENTITY:

ANALYST & DATE: ,

SAMPLE TYPE: Unimodal, Well Sorted

TEXTURAL GROUP: Sand

SEDIMENT NAME: Well Sorted Coarse Sand

| | µm | ϕ |
|---|---|---|
| MODE 1: | 605,0 | 0,747 |
| MODE 2: | | |
| MODE 3: | | |
| $D_{10}$: | 364,1 | 0,589 |
| MEDIAN or $D_{50}$: | 510,5 | 0,970 |
| $D_{90}$: | 664,7 | 1,458 |
| ($D_{90}$ / $D_{10}$): | 1,826 | 2,474 |
| ($D_{90}$ - $D_{10}$): | 300,6 | 0,868 |
| ($D_{75}$ / $D_{25}$): | 1,453 | 1,737 |
| ($D_{75}$ - $D_{25}$): | 187,8 | 0,539 |

GRAIN SIZE DISTRIBUTION

| | | | |
|---|---|---|---|
| GRAVEL: | 0,0% | COARSE SAND: | 53,1% |
| SAND: | 100,0% | MEDIUM SAND: | 45,6% |
| MUD: | 0,0% | FINE SAND: | 1,3% |
| | | V FINE SAND: | 0,0% |
| V COARSE GRAVEL: | 0,0% | V COARSE SILT: | 0,0% |
| COARSE GRAVEL: | 0,0% | COARSE SILT: | 0,0% |
| MEDIUM GRAVEL: | 0,0% | MEDIUM SILT: | 0,0% |
| FINE GRAVEL: | 0,0% | FINE SILT: | 0,0% |
| V FINE GRAVEL: | 0,0% | V FINE SILT: | 0,0% |
| V COARSE SAND: | 0,0% | CLAY: | 0,0% |

| | METHOD OF MOMENTS | | | FOLK & WARD METHOD | | |
|---|---|---|---|---|---|---|
| | Arithmetic µm | Geometric µm | Logarithmic ϕ | Geometric µm | Logarithmic ϕ | Description |
| MEAN ($\bar{x}$): | 511,9 | 492,1 | 1,023 | 500,0 | 1,000 | Coarse Sand |
| SORTING ($\sigma$): | 105,3 | 1,258 | 0,331 | 1,280 | 0,356 | Well Sorted |
| SKEWNESS ($Sk$): | -0,575 | -1,047 | 1,047 | -0,182 | 0,182 | Fine Skewed |
| KURTOSIS ($K$): | 2,189 | 3,957 | 3,957 | 0,861 | 0,861 | Platykurtic |

The sample is dominated by medium to coarse sand, which is well sorted. The calculated porosity is 11,4, and the IGV is calculated to be 36%.

**34_3-3_3984,06**

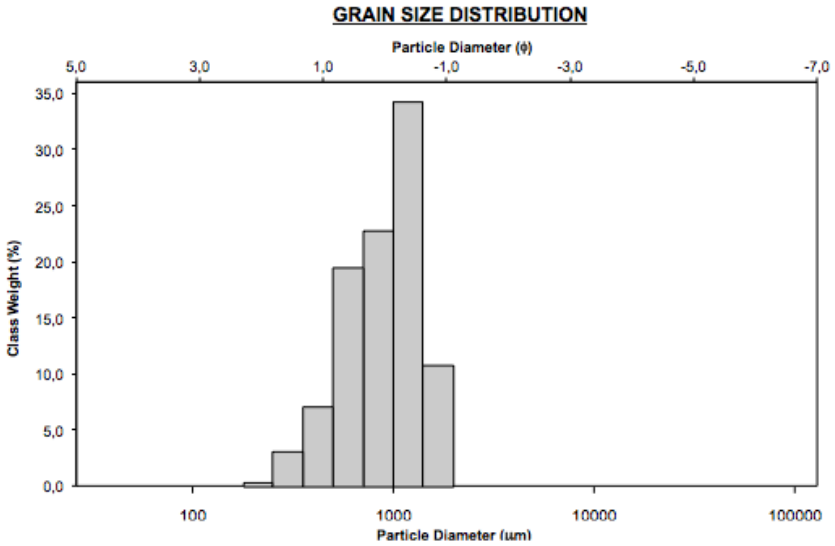


## SAMPLE STATISTICS

SAMPLE IDENTITY: ANALYST & DATE: ,

SAMPLE TYPE: Unimodal, Moderately Well Sorted TEXTURAL GROUP: Sand

SEDIMENT NAME: Moderately Well Sorted Very Coarse Sand

| | µm | ϕ |
|---|---|---|
| MODE 1: | 1200,0 | -0,243 |
| MODE 2: | | |
| MODE 3: | | |
| $D_{10}$: | 479,9 | -0,550 |
| MEDIAN or $D_{50}$: | 938,0 | 0,092 |
| $D_{90}$: | 1464,6 | 1,059 |
| ($D_{90}$ / $D_{10}$): | 3,052 | -1,924 |
| ($D_{90}$ - $D_{10}$): | 984,7 | 1,610 |
| ($D_{75}$ / $D_{25}$): | 1,920 | -2,209 |
| ($D_{75}$ - $D_{25}$): | 587,1 | 0,941 |

GRAIN SIZE DISTRIBUTION

| | | | |
|---|---|---|---|
| GRAVEL: | 0,0% | COARSE SAND: | 43,5% |
| SAND: | 100,0% | MEDIUM SAND: | 10,5% |
| MUD: | 0,0% | FINE SAND: | 0,4% |
| | | V FINE SAND: | 0,0% |
| V COARSE GRAVEL: | 0,0% | V COARSE SILT: | 0,0% |
| COARSE GRAVEL: | 0,0% | COARSE SILT: | 0,0% |
| MEDIUM GRAVEL: | 0,0% | MEDIUM SILT: | 0,0% |
| FINE GRAVEL: | 0,0% | FINE SILT: | 0,0% |
| V FINE GRAVEL: | 0,0% | V FINE SILT: | 0,0% |
| V COARSE SAND: | 45,7% | CLAY: | 0,0% |

| | METHOD OF MOMENTS | | | FOLK & WARD METHOD | | |
|---|---|---|---|---|---|---|
| | Arithmetic µm | Geometric µm | Logarithmic ϕ | Geometric µm | Logarithmic ϕ | Description |
| MEAN ($\bar{x}$): | 967,7 | 872,8 | 0,196 | 882,0 | 0,181 | Coarse Sand |
| SORTING ($\sigma$): | 383,6 | 1,552 | 0,635 | 1,572 | 0,653 | Moderately Well Sorted |
| SKEWNESS ($Sk$): | 0,295 | -0,575 | 0,575 | -0,204 | 0,204 | Fine Skewed |
| KURTOSIS ($K$): | 2,365 | 2,842 | 2,842 | 0,948 | 0,948 | Mesokurtic |

The sample is dominated by coarse and very coarse sand, which is moderately well sorted. The calculated porosity is 8,7%, and the IGV is calculated to be 38,8%.

## 34_3-1_3885,70

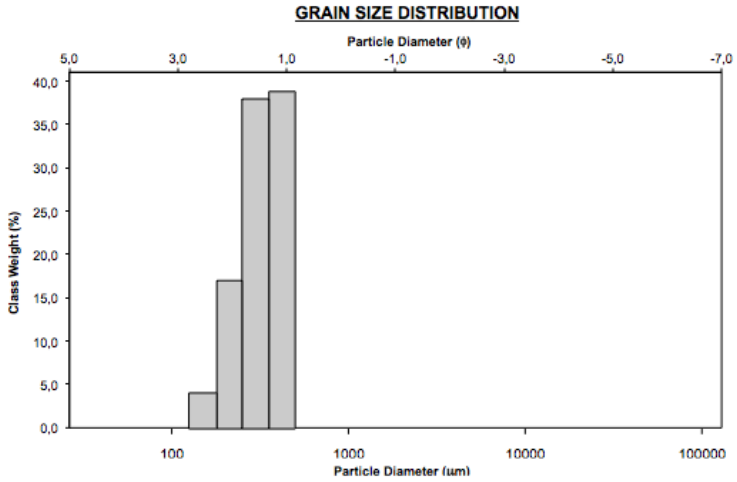


### SAMPLE STATISTICS

SAMPLE IDENTITY:

ANALYST & DATE: ,

SAMPLE TYPE: Unimodal, Well Sorted

TEXTURAL GROUP: Sand

SEDIMENT NAME: Well Sorted Medium Sand

| | µm | ϕ |
|---|---|---|
| MODE 1: | 427,5 | 1,247 |
| MODE 2: | | |
| MODE 3: | | |
| $D_{10}$: | 200,8 | 1,125 |
| MEDIAN or $D_{50}$: | 323,2 | 1,630 |
| $D_{90}$: | 458,4 | 2,316 |
| ($D_{90}$ / $D_{10}$): | 2,283 | 2,058 |
| ($D_{90}$ - $D_{10}$): | 257,6 | 1,191 |
| ($D_{75}$ / $D_{25}$): | 1,555 | 1,485 |
| ($D_{75}$ - $D_{25}$): | 143,6 | 0,637 |

GRAIN SIZE DISTRIBUTION

| | | | |
|---|---|---|---|
| GRAVEL: | 0,0% | COARSE SAND: | 0,0% |
| SAND: | 100,0% | MEDIUM SAND: | 78,9% |
| MUD: | 0,0% | FINE SAND: | 21,1% |
| | | V FINE SAND: | 0,0% |
| V COARSE GRAVEL: | 0,0% | V COARSE SILT: | 0,0% |
| COARSE GRAVEL: | 0,0% | COARSE SILT: | 0,0% |
| MEDIUM GRAVEL: | 0,0% | MEDIUM SILT: | 0,0% |
| FINE GRAVEL: | 0,0% | FINE SILT: | 0,0% |
| V FINE GRAVEL: | 0,0% | V FINE SILT: | 0,0% |
| V COARSE SAND: | 0,0% | CLAY: | 0,0% |

| | METHOD OF MOMENTS | | | FOLK & WARD METHOD | | |
|---|---|---|---|---|---|---|
| | Arithmetic µm | Geometric µm | Logarithmic ϕ | Geometric µm | Logarithmic ϕ | Description |
| MEAN ($\bar{x}$) | 330,6 | 313,1 | 1,675 | 316,8 | 1,658 | Medium Sand |
| SORTING ($\sigma$): | 87,47 | 1,339 | 0,421 | 1,364 | 0,448 | Well Sorted |
| SKEWNESS ($Sk$): | -0,236 | -0,697 | 0,697 | -0,140 | 0,140 | Fine Skewed |
| KURTOSIS ($K$): | 1,872 | 2,757 | 2,757 | 0,899 | 0,899 | Platykurtic |

The sample is dominated by medium sand, but there are moderate amounts of fine sand as well. The sorting is well sorted. The calculated porosity is 17,9%, and the IGV is calculated to be 32,9%.

**34_3-1_3901,13**

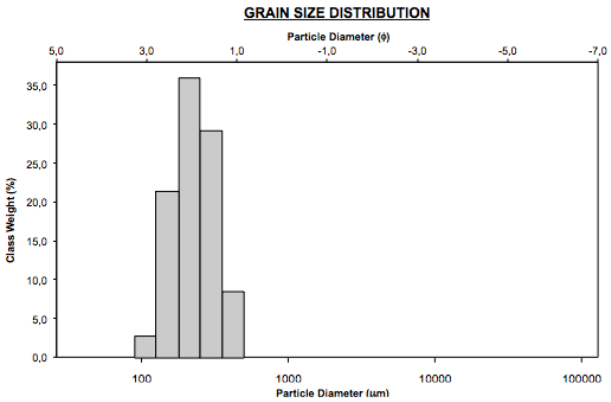


## SAMPLE STATISTICS

SAMPLE IDENTITY: ANALYST & DATE: ,

SAMPLE TYPE: Unimodal, Moderately Well Sorted TEXTURAL GROUP: Sand

SEDIMENT NAME: Moderately Well Sorted Fine Sand

| | µm | ϕ |
|---|---|---|
| MODE 1: | 215,0 | 2,237 |
| MODE 2: | | |
| MODE 3: | | |
| $D_{10}$: | 140,1 | 1,516 |
| MEDIAN or $D_{50}$: | 225,6 | 2,148 |
| $D_{90}$: | 349,6 | 2,835 |
| ($D_{90}$ / $D_{10}$): | 2,494 | 1,870 |
| ($D_{90}$ - $D_{10}$): | 209,4 | 1,319 |
| ($D_{75}$ / $D_{25}$): | 1,656 | 1,412 |
| ($D_{75}$ - $D_{25}$): | 116,5 | 0,728 |

GRAIN SIZE DISTRIBUTION

| | | | |
|---|---|---|---|
| GRAVEL: | 0,0% | COARSE SAND: | 0,0% |
| SAND: | 100,0% | MEDIUM SAND: | 39,0% |
| MUD: | 0,0% | FINE SAND: | 58,2% |
| | | V FINE SAND: | 2,7% |
| V COARSE GRAVEL: | 0,0% | V COARSE SILT: | 0,0% |
| COARSE GRAVEL: | 0,0% | COARSE SILT: | 0,0% |
| MEDIUM GRAVEL: | 0,0% | MEDIUM SILT: | 0,0% |
| FINE GRAVEL: | 0,0% | FINE SILT: | 0,0% |
| V FINE GRAVEL: | 0,0% | V FINE SILT: | 0,0% |
| V COARSE SAND: | 0,0% | CLAY: | 0,0% |

| | METHOD OF MOMENTS | | | FOLK & WARD METHOD | | |
|---|---|---|---|---|---|---|
| | Arithmetic µm | Geometric µm | Logarithmic ϕ | Geometric µm | Logarithmic ϕ | Description |
| MEAN ($\bar{x}$) | 242,6 | 226,0 | 2,146 | 224,6 | 2,154 | Fine Sand |
| SORTING ($\sigma$): | 81,85 | 1,399 | 0,485 | 1,437 | 0,523 | Moderately Well Sorted |
| SKEWNESS ($Sk$): | 0,674 | -0,015 | 0,015 | 0,010 | -0,010 | Symmetrical |
| KURTOSIS ($K$): | 2,893 | 2,384 | 2,384 | 0,936 | 0,936 | Mesokurtic |

The sample is dominated by fine sand, but there is also moderates amounts of medium sand. The sample contain quit much clay mix. The sorting is moderately well sorted. The calculated porosity is 12,6%, and the IGV is calculated to be 32,9%.

**34_3-1_3915,60**

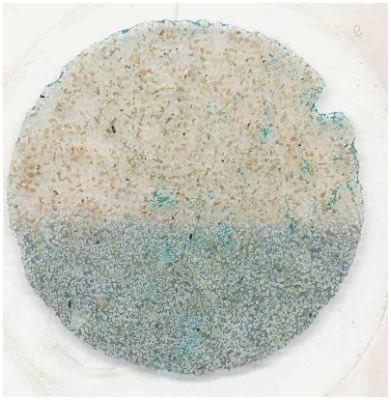

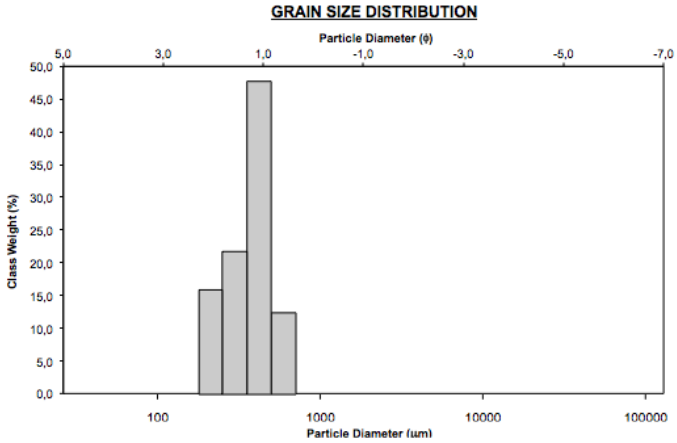


## SAMPLE STATISTICS

SAMPLE IDENTITY:

ANALYST & DATE: ,

SAMPLE TYPE: Unimodal, Well Sorted

TEXTURAL GROUP: Sand

SEDIMENT NAME: Well Sorted Medium Sand

| | µm | ϕ |
|---|---|---|
| MODE 1: | 427,5 | 1,247 |
| MODE 2: | | |
| MODE 3: | | |
| $D_{10}$: | 222,2 | 0,883 |
| MEDIAN or $D_{50}$: | 385,4 | 1,376 |
| $D_{90}$: | 542,1 | 2,170 |
| ($D_{90}$ / $D_{10}$): | 2,440 | 2,456 |
| ($D_{90}$ - $D_{10}$): | 319,9 | 1,287 |
| ($D_{75}$ / $D_{25}$): | 1,590 | 1,596 |
| ($D_{75}$ - $D_{25}$): | 170,5 | 0,669 |

GRAIN SIZE DISTRIBUTION

| | | | |
|---|---|---|---|
| GRAVEL: | 0,0% | COARSE SAND: | 13,0% |
| SAND: | 100,0% | MEDIUM SAND: | 71,4% |
| MUD: | 0,0% | FINE SAND: | 15,6% |
| | | V FINE SAND: | 0,0% |
| V COARSE GRAVEL: | 0,0% | V COARSE SILT: | 0,0% |
| COARSE GRAVEL: | 0,0% | COARSE SILT: | 0,0% |
| MEDIUM GRAVEL: | 0,0% | MEDIUM SILT: | 0,0% |
| FINE GRAVEL: | 0,0% | FINE SILT: | 0,0% |
| V FINE GRAVEL: | 0,0% | V FINE SILT: | 0,0% |
| V COARSE SAND: | 0,0% | CLAY: | 0,0% |

| | METHOD OF MOMENTS | | | FOLK & WARD METHOD | | |
|---|---|---|---|---|---|---|
| | Arithmetic µm | Geometric µm | Logarithmic ϕ | Geometric µm | Logarithmic ϕ | Description |
| MEAN ($\bar{x}$) | 389,0 | 366,0 | 1,450 | 362,1 | 1,466 | Medium Sand |
| SORTING ($\sigma$): | 114,9 | 1,364 | 0,448 | 1,402 | 0,488 | Well Sorted |
| SKEWNESS ($Sk$): | 0,243 | -0,363 | 0,363 | -0,220 | 0,220 | Fine Skewed |
| KURTOSIS ($K$): | 2,520 | 2,332 | 2,332 | 1,001 | 1,001 | Mesokurtic |

This sample is dominated by medium sand. The sorting is well sorted. The sample contains about 30% carbonate cement. The calculated porosity is 3,2%, and the IGV is calculated to be 44,6%, due to the carbonate cement. The thin section is divided in two by the color. The purple – blue color is the staining of the carbonate cement, and the other half has no staining.

**34_3-1_3927,81**

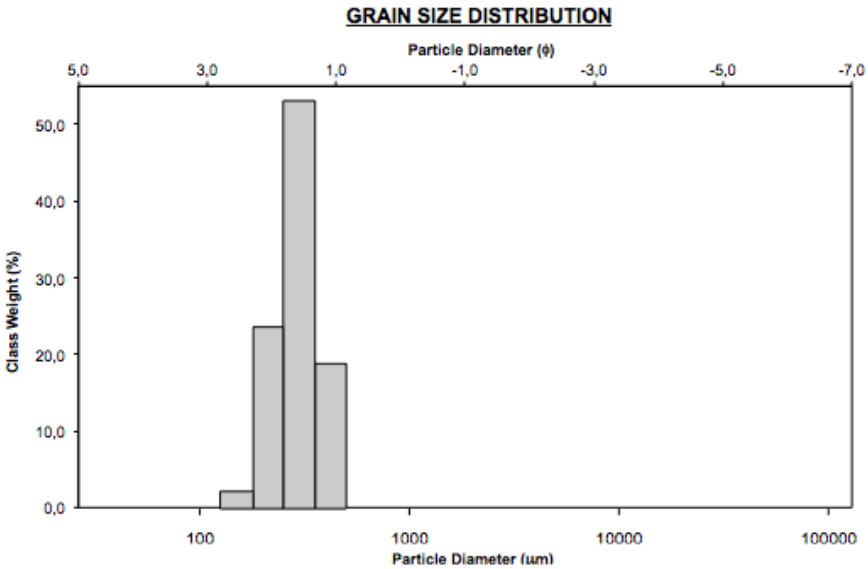


## SAMPLE STATISTICS

SAMPLE IDENTITY:

ANALYST & DATE: ,

SAMPLE TYPE: Unimodal, Well Sorted

TEXTURAL GROUP: Sand

SEDIMENT NAME: Well Sorted Medium Sand

| | µm | ϕ |
|---|---|---|
| MODE 1: | 302,5 | 1,747 |
| MODE 2: | | |
| MODE 3: | | |
| $D_{10}$: | 200,4 | 1,257 |
| MEDIAN or $D_{50}$: | 292,0 | 1,776 |
| $D_{90}$: | 418,3 | 2,319 |
| ($D_{90}$ / $D_{10}$): | 2,087 | 1,844 |
| ($D_{90}$ - $D_{10}$): | 217,9 | 1,061 |
| ($D_{75}$ / $D_{25}$): | 1,379 | 1,300 |
| ($D_{75}$ - $D_{25}$): | 94,00 | 0,463 |

GRAIN SIZE DISTRIBUTION

| | | | |
|---|---|---|---|
| GRAVEL: | 0,0% | COARSE SAND: | 0,0% |
| SAND: | 100,0% | MEDIUM SAND: | 74,5% |
| MUD: | 0,0% | FINE SAND: | 25,5% |
| | | V FINE SAND: | 0,0% |
| V COARSE GRAVEL: | 0,0% | V COARSE SILT: | 0,0% |
| COARSE GRAVEL: | 0,0% | COARSE SILT: | 0,0% |
| MEDIUM GRAVEL: | 0,0% | MEDIUM SILT: | 0,0% |
| FINE GRAVEL: | 0,0% | FINE SILT: | 0,0% |
| V FINE GRAVEL: | 0,0% | V FINE SILT: | 0,0% |
| V COARSE SAND: | 0,0% | CLAY: | 0,0% |

| | METHOD OF MOMENTS | | | FOLK & WARD METHOD | | |
|---|---|---|---|---|---|---|
| | Arithmetic µm | Geometric µm | Logarithmic ϕ | Geometric µm | Logarithmic ϕ | Description |
| MEAN ($\bar{x}$) | 302,7 | 269,5 | 1,788 | 288,3 | 1,794 | Medium Sand |
| SORTING ($\sigma$): | 72,91 | 1,278 | 0,354 | 1,312 | 0,392 | Well Sorted |
| SKEWNESS ($Sk$): | 0,350 | -0,252 | 0,252 | -0,035 | 0,035 | Symmetrical |
| KURTOSIS ($K$): | 2,572 | 2,891 | 2,891 | 1,143 | 1,143 | Leptokurtic |

The sample is dominated by medium sand, but has moderate amounts of fine sand. The sorting is well sorted. The calculated porosity is 19,3%, and the IGV is calculated to be 37,2%.

**34_5-1_3645,75**

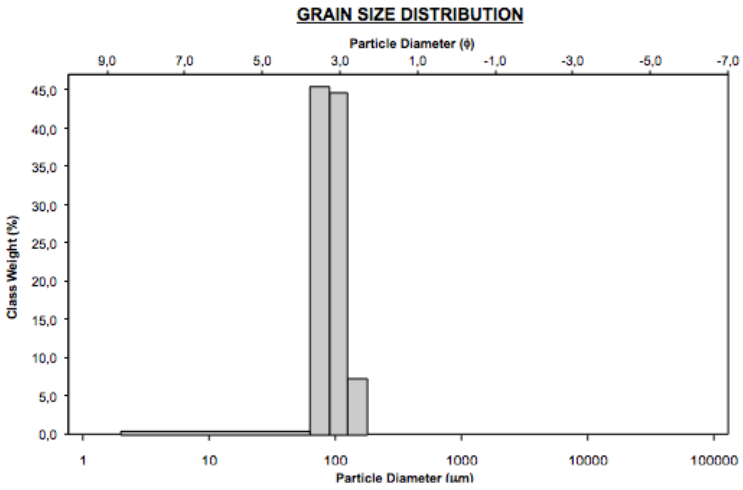


## SAMPLE STATISTICS

SAMPLE IDENTITY:

ANALYST & DATE: ,

SAMPLE TYPE: Unimodal, Well Sorted

TEXTURAL GROUP: Sand

SEDIMENT NAME: Well Sorted Very Fine Sand

| | µm | ϕ |
|---|---|---|
| MODE 1: | 76,50 | 3,731 |
| MODE 2: | | |
| MODE 3: | | |
| $D_{10}$: | 65,57 | 3,027 |
| MEDIAN or $D_{50}$: | 89,45 | 3,483 |
| $D_{90}$: | 122,7 | 3,931 |
| ($D_{90}$ / $D_{10}$): | 1,871 | 1,298 |
| ($D_{90}$ - $D_{10}$): | 57,09 | 0,903 |
| ($D_{75}$ / $D_{25}$): | 1,479 | 1,177 |
| ($D_{75}$ - $D_{25}$): | 35,29 | 0,565 |

GRAIN SIZE DISTRIBUTION

| | | | |
|---|---|---|---|
| GRAVEL: | 0,0% | COARSE SAND: | 0,0% |
| SAND: | 95,2% | MEDIUM SAND: | 0,0% |
| MUD: | 4,8% | FINE SAND: | 7,6% |
| | | V FINE SAND: | 87,6% |
| V COARSE GRAVEL: | 0,0% | V COARSE SILT: | 1,0% |
| COARSE GRAVEL: | 0,0% | COARSE SILT: | 1,0% |
| MEDIUM GRAVEL: | 0,0% | MEDIUM SILT: | 1,0% |
| FINE GRAVEL: | 0,0% | FINE SILT: | 1,0% |
| V FINE GRAVEL: | 0,0% | V FINE SILT: | 0,9% |
| V COARSE SAND: | 0,0% | CLAY: | 0,0% |

| | METHOD OF MOMENTS | | | FOLK & WARD METHOD | | |
|---|---|---|---|---|---|---|
| | Arithmetic µm | Geometric µm | Logarithmic ϕ | Geometric µm | Logarithmic ϕ | Description |
| MEAN ($\bar{x}$): | 93,05 | 83,46 | 3,583 | 89,58 | 3,481 | Very Fine Sand |
| SORTING ($\sigma$): | 25,67 | 1,648 | 0,721 | 1,291 | 0,369 | Well Sorted |
| SKEWNESS ($Sk$): | 0,261 | -2,967 | 2,967 | 0,073 | -0,073 | Symmetrical |
| KURTOSIS ($K$): | 3,807 | 12,74 | 12,74 | 0,847 | 0,847 | Platykurtic |

The sample is dominated by very fine sand. There is a clear stratifying in the thin section. The sorting is well sorted. The calculated porosity is 14,9%, and the IGV is calculated to be 33,7%.

**34_5-1_3677,73**

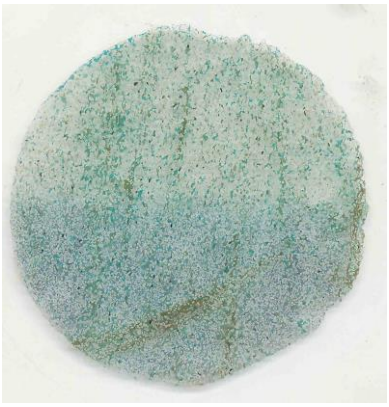

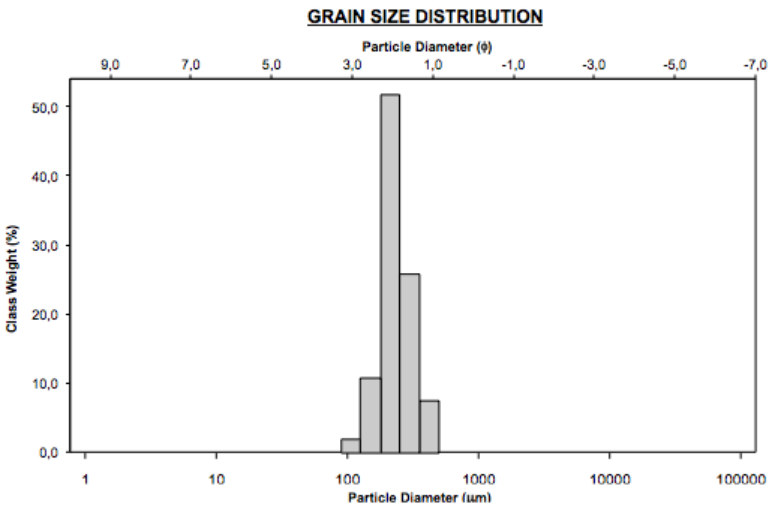


## SAMPLE STATISTICS

SAMPLE IDENTITY:

ANALYST & DATE: ,

SAMPLE TYPE: Unimodal, Well Sorted

TEXTURAL GROUP: Sand

SEDIMENT NAME: Well Sorted Fine Sand

| | µm | ϕ |
|---|---|---|
| MODE 1: | 215,0 | 2,237 |
| MODE 2: | | |
| MODE 3: | | |
| $D_{10}$: | 160,0 | 1,535 |
| MEDIAN or $D_{50}$: | 227,1 | 2,139 |
| $D_{90}$: | 345,0 | 2,644 |
| ($D_{90}$ / $D_{10}$): | 2,156 | 1,722 |
| ($D_{90}$ - $D_{10}$): | 185,0 | 1,109 |
| ($D_{75}$ / $D_{25}$): | 1,471 | 1,307 |
| ($D_{75}$ - $D_{25}$): | 91,05 | 0,557 |

GRAIN SIZE DISTRIBUTION

| | | | |
|---|---|---|---|
| GRAVEL: | 0,0% | COARSE SAND: | 0,0% |
| SAND: | 100,0% | MEDIUM SAND: | 35,0% |
| MUD: | 0,0% | FINE SAND: | 63,0% |
| | | V FINE SAND: | 2,0% |
| V COARSE GRAVEL: | 0,0% | V COARSE SILT: | 0,0% |
| COARSE GRAVEL: | 0,0% | COARSE SILT: | 0,0% |
| MEDIUM GRAVEL: | 0,0% | MEDIUM SILT: | 0,0% |
| FINE GRAVEL: | 0,0% | FINE SILT: | 0,0% |
| V FINE GRAVEL: | 0,0% | V FINE SILT: | 0,0% |
| V COARSE SAND: | 0,0% | CLAY: | 0,0% |

| | METHOD OF MOMENTS | | | FOLK & WARD METHOD | | |
|---|---|---|---|---|---|---|
| | Arithmetic µm | Geometric µm | Logarithmic ϕ | Geometric µm | Logarithmic ϕ | Description |
| MEAN ($\bar{x}$) | 245,8 | 232,4 | 2,106 | 236,5 | 2,080 | Fine Sand |
| SORTING ($\sigma$): | 73,06 | 1,335 | 0,417 | 1,353 | 0,436 | Well Sorted |
| SKEWNESS ($Sk$): | 0,903 | 0,030 | -0,030 | 0,140 | -0,140 | Coarse Skewed |
| KURTOSIS ($K$): | 3,656 | 3,249 | 3,249 | 1,140 | 1,140 | Leptokurtic |

The sample is dominated by fine sand, but there are also moderate amounts of medium sand. The sorting is well sorted. The calculated porosity is 2,9%, due to high amounts of carbonate cement. The IGV is calculated to be 27,1%. The thin section is divided in two. The lower half, purple – blue color, is the staining of the carbonate cement. The upper half, white-ish color, is grains without staining.

**34_5-1_3686,32**

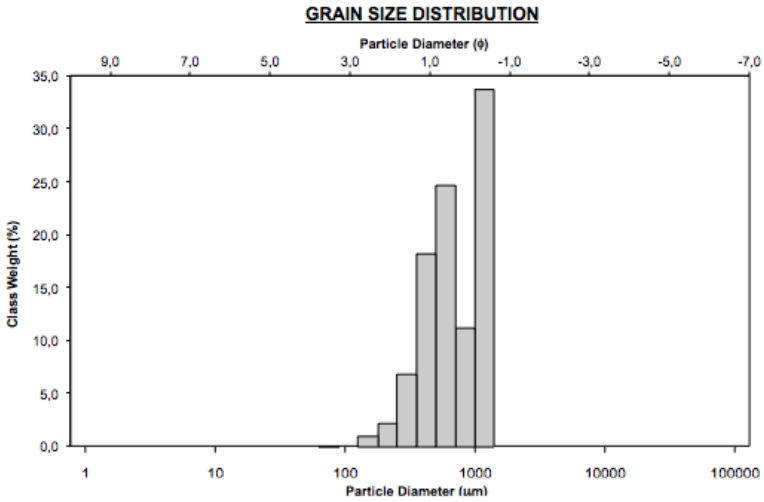


## SAMPLE STATISTICS

SAMPLE IDENTITY: ANALYST & DATE: ,

SAMPLE TYPE: Bimodal, Moderately Sorted TEXTURAL GROUP: Sand

SEDIMENT NAME: Moderately Sorted Coarse Sand

| | µm | ϕ |
|---|---|---|
| MODE 1: | 1200,0 | -0,243 |
| MODE 2: | 605,0 | 0,747 |
| MODE 3: | | |
| $D_{10}$: | 347,1 | -0,342 |
| MEDIAN or $D_{50}$: | 665,2 | 0,588 |
| $D_{90}$: | 1267,3 | 1,527 |
| ($D_{90}$ / $D_{10}$): | 3,651 | -4,468 |
| ($D_{90}$ - $D_{10}$): | 920,2 | 1,868 |
| ($D_{75}$ / $D_{25}$): | 2,351 | -8,779 |
| ($D_{75}$ - $D_{25}$): | 627,2 | 1,233 |

GRAIN SIZE DISTRIBUTION

| | | | |
|---|---|---|---|
| GRAVEL: | 0,0% | COARSE SAND: | 37,2% |
| SAND: | 100,0% | MEDIUM SAND: | 25,7% |
| MUD: | 0,0% | FINE SAND: | 3,3% |
| | | V FINE SAND: | 0,0% |
| V COARSE GRAVEL: | 0,0% | V COARSE SILT: | 0,0% |
| COARSE GRAVEL: | 0,0% | COARSE SILT: | 0,0% |
| MEDIUM GRAVEL: | 0,0% | MEDIUM SILT: | 0,0% |
| FINE GRAVEL: | 0,0% | FINE SILT: | 0,0% |
| V FINE GRAVEL: | 0,0% | V FINE SILT: | 0,0% |
| V COARSE SAND: | 33,8% | CLAY: | 0,0% |

| | METHOD OF MOMENTS | | | FOLK & WARD METHOD | | |
|---|---|---|---|---|---|---|
| | Arithmetic µm | Geometric µm | Logarithmic ϕ | Geometric µm | Logarithmic ϕ | Description |
| MEAN ($\bar{x}$) | 766,3 | 671,1 | 0,575 | 678,4 | 0,560 | Coarse Sand |
| SORTING ($\sigma$): | 344,6 | 1,667 | 0,737 | 1,680 | 0,748 | Moderately Sorted |
| SKEWNESS ($Sk$): | 0,144 | -0,519 | 0,519 | -0,037 | 0,037 | Symmetrical |
| KURTOSIS ($K$): | 1,527 | 2,622 | 2,622 | 0,762 | 0,762 | Platykurtic |

The sample is a grain size mix, from very coarse to medium sand. The sorting is moderately. The calculated porosity is 16,9%, and the IGV is calculated to be 36,3%. This sample has high percentage (8,5%) of chlorite coating.

**34_5-1_3688,5**

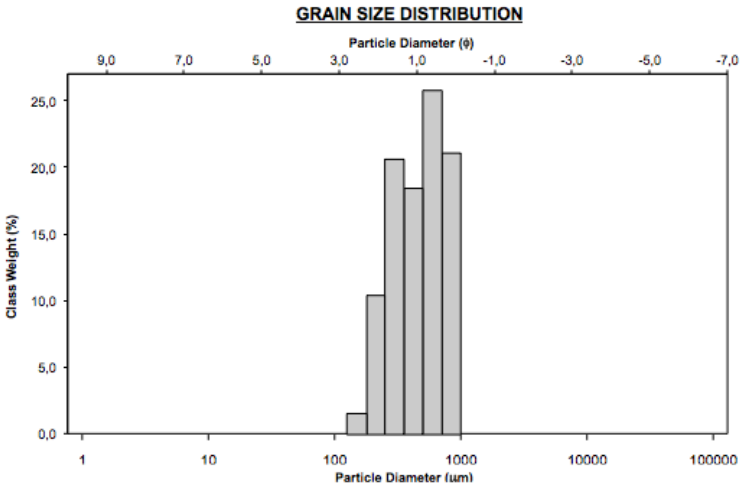


## SAMPLE STATISTICS

SAMPLE IDENTITY:

ANALYST & DATE: ,

SAMPLE TYPE: Bimodal, Moderately Sorted

TEXTURAL GROUP: Sand

SEDIMENT NAME: Moderately Sorted Coarse Sand

| | µm | ϕ |
|---|---|---|
| MODE 1: | 605,0 | 0,747 |
| MODE 2: | 302,5 | 1,747 |
| MODE 3: | | |
| $D_{10}$: | 235,6 | 0,231 |
| MEDIAN or $D_{50}$: | 482,8 | 1,050 |
| $D_{90}$: | 851,8 | 2,086 |
| ($D_{90}$ / $D_{10}$): | 3,615 | 9,015 |
| ($D_{90}$ - $D_{10}$): | 616,2 | 1,854 |
| ($D_{75}$ / $D_{25}$): | 2,182 | 2,999 |
| ($D_{75}$ - $D_{25}$): | 366,6 | 1,125 |

GRAIN SIZE DISTRIBUTION

| | | | |
|---|---|---|---|
| GRAVEL: | 0,0% | COARSE SAND: | 48,1% |
| SAND: | 100,0% | MEDIUM SAND: | 40,1% |
| MUD: | 0,0% | FINE SAND: | 11,8% |
| | | V FINE SAND: | 0,0% |
| V COARSE GRAVEL: | 0,0% | V COARSE SILT: | 0,0% |
| COARSE GRAVEL: | 0,0% | COARSE SILT: | 0,0% |
| MEDIUM GRAVEL: | 0,0% | MEDIUM SILT: | 0,0% |
| FINE GRAVEL: | 0,0% | FINE SILT: | 0,0% |
| V FINE GRAVEL: | 0,0% | V FINE SILT: | 0,0% |
| V COARSE SAND: | 0,0% | CLAY: | 0,0% |

| | METHOD OF MOMENTS | | | FOLK & WARD METHOD | | |
|---|---|---|---|---|---|---|
| | Arithmetic µm | Geometric µm | Logarithmic ϕ | Geometric µm | Logarithmic ϕ | Description |
| MEAN ($\bar{x}$): | 513,3 | 456,2 | 1,132 | 464,2 | 1,107 | Medium Sand |
| SORTING ($\sigma$): | 222,0 | 1,598 | 0,677 | 1,643 | 0,717 | Moderately Sorted |
| SKEWNESS ($Sk$): | 0,285 | -0,301 | 0,301 | -0,132 | 0,132 | Fine Skewed |
| KURTOSIS ($K$): | 1,833 | 2,058 | 2,058 | 0,803 | 0,803 | Platykurtic |

The sample is a grain size mix between coarse and medium sand. The sorting is moderately sorted. The calculated porosity is 11%, and the IGV is calculated to be 34,5%. There are high amounts of clay mix in the sample that are not included in the interpretation.

# *Appendix IV*

**Facies percentage**

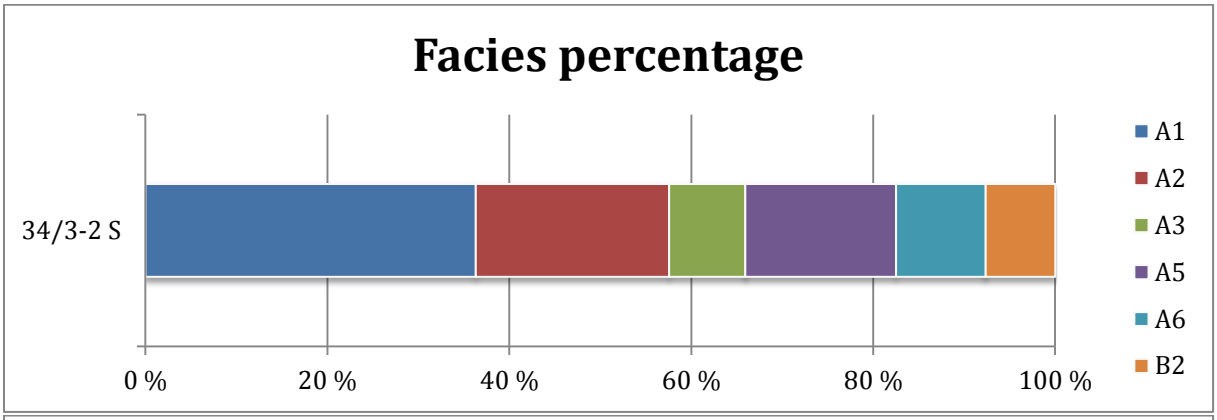


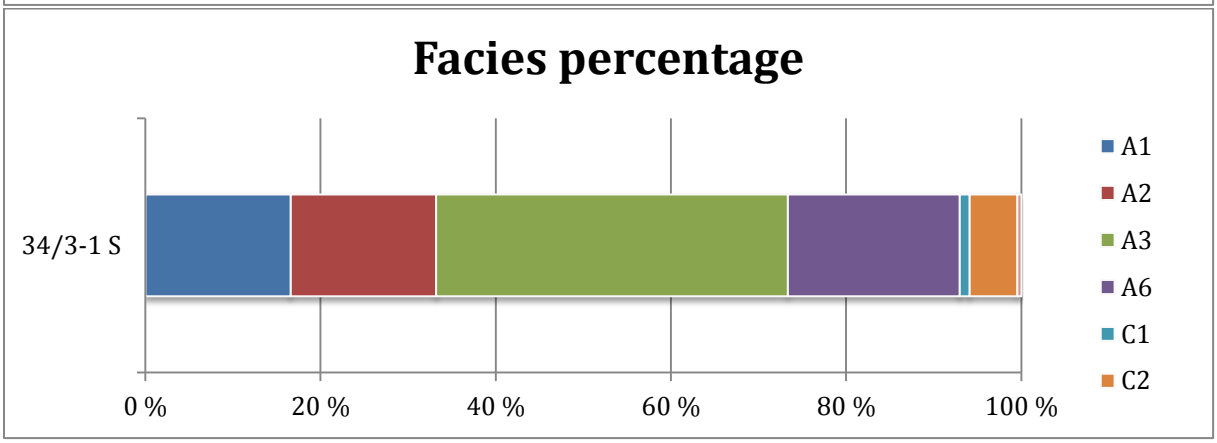


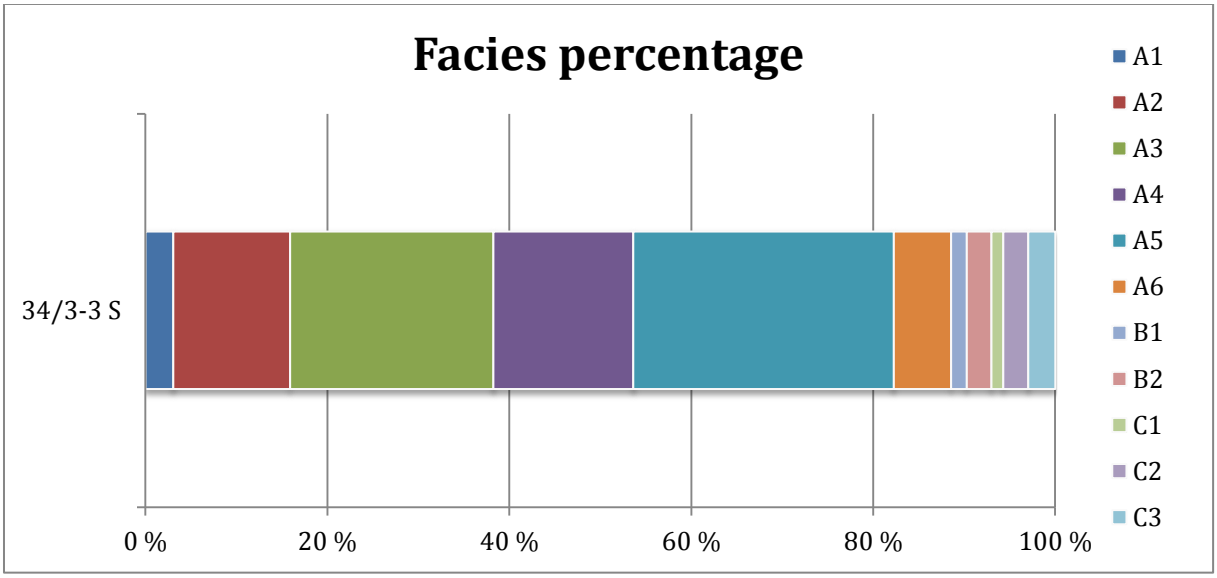

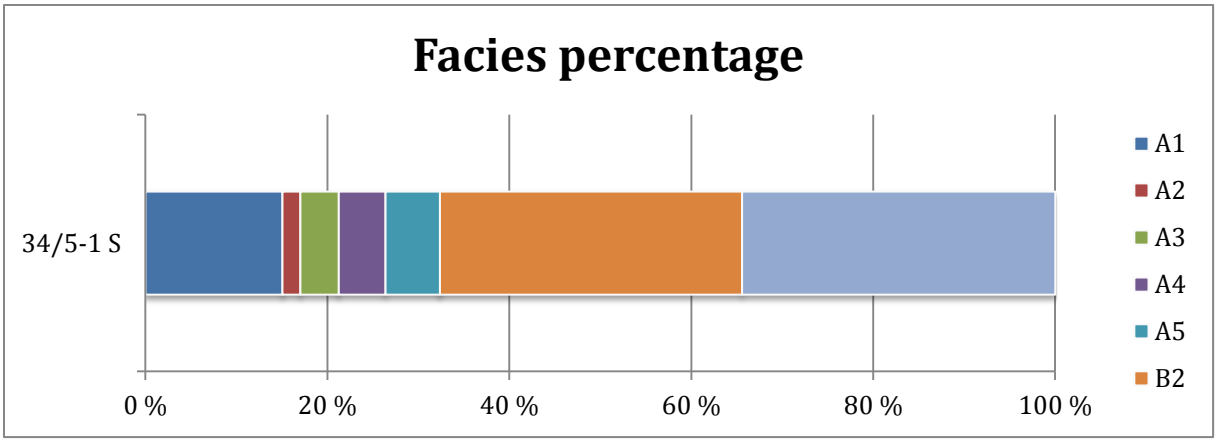
Facies percentage
34/5-1 S
0 %
20 %
40 %
60 %
80 %
100 %
A1
A2
A3
A4
A5
B2

# *Appendix V*

Illustration of the digitalized cored intervals from all the wells.

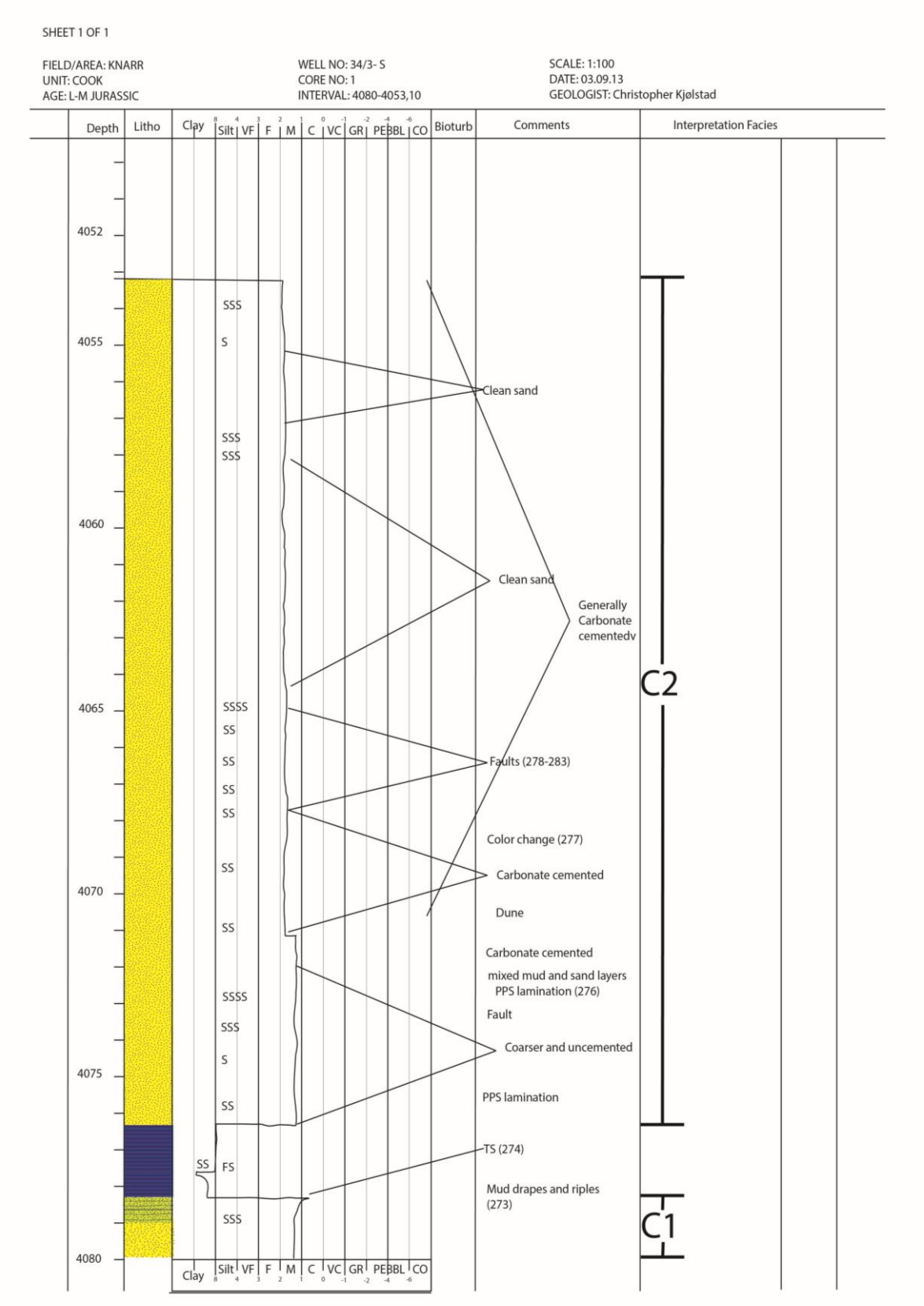

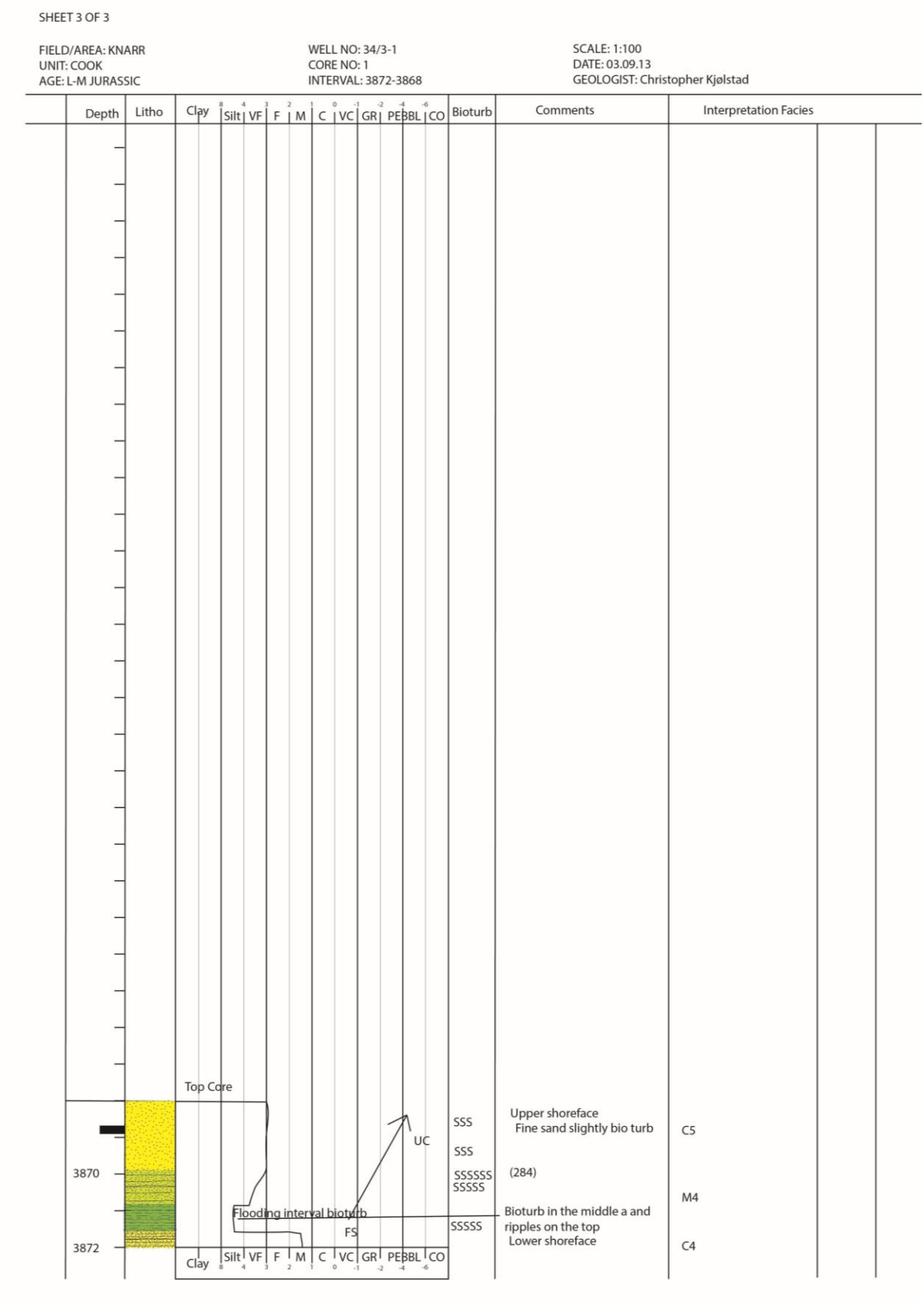
SHEET 3 OF 3
FIELD/AREA: KNARR
UNIT: COOK
AGE: L-M JURASSIC
WELL NO: 34/3-1
CORE NO: 1
INTERVAL: 3872-3868
SCALE: 1:100
DATE: 03.09.13
GEOLOGIST: Christopher Kjølstad
Depth
Litho
Clay
Silt
VF
F
M
C
VC
GR
PEBBL
CO
Bioturb
Comments
Interpretation Facies
Top Core
3870
3872
UC
FS
Flooding interval bioturb
SSS
SSS
SSSSSS
SSSSS
SSSSS
Upper shoreface
Fine sand slightly bio turb
(284)
Bioturb in the middle a and
ripples on the top
Lower shoreface
C5
M4
C4

Appendix

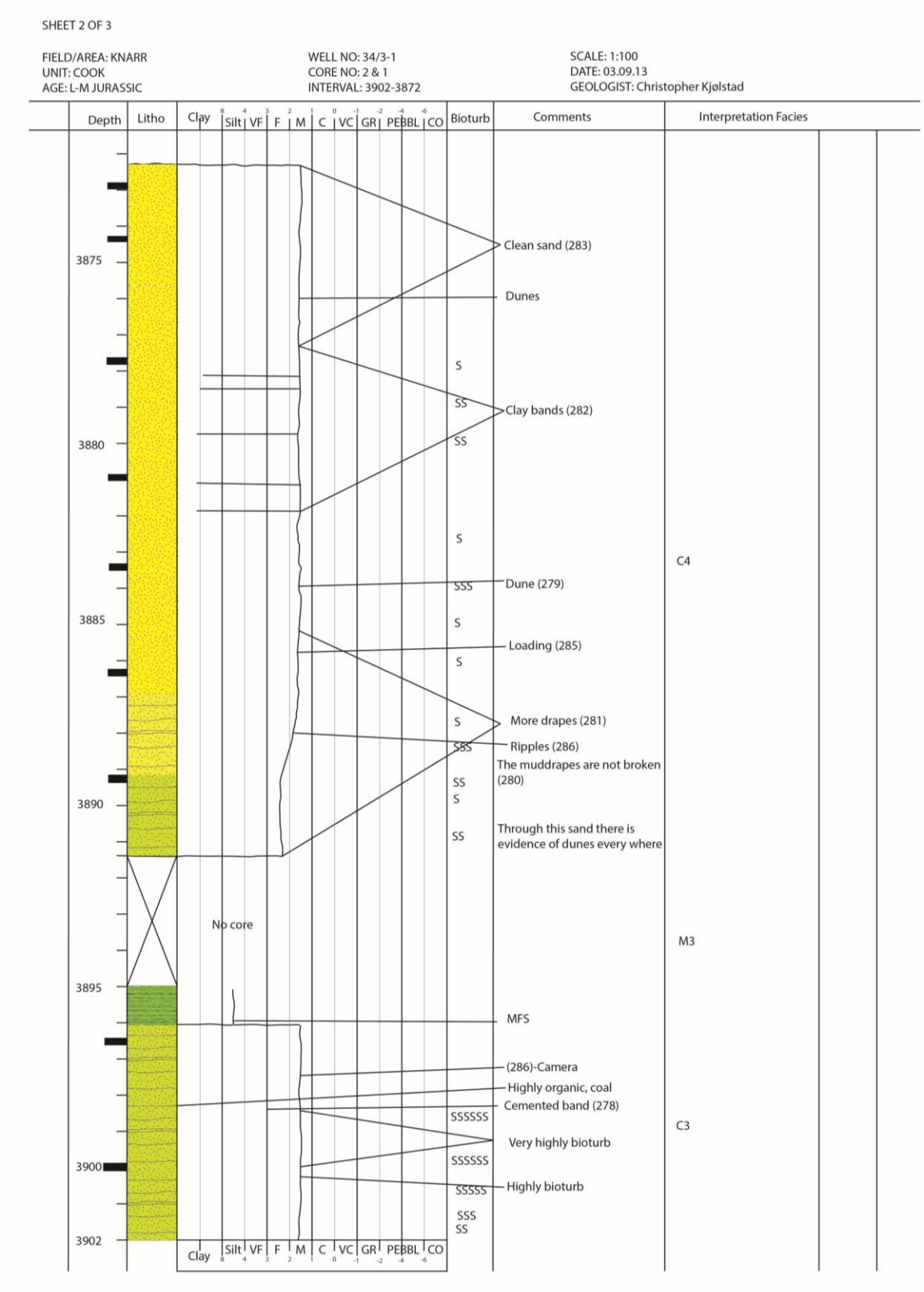
SHEET 2 OF 3
FIELD/AREA: KNARR
UNIT: COOK
AGE: L-M JURASSIC
WELL NO: 34/3-1
CORE NO: 2 & 1
INTERVAL: 3902-3872
SCALE: 1:100
DATE: 03.09.13
GEOLOGIST: Christopher Kjølstad
Depth
Litho
Clay
Silt
VF
F
M
C
VC
GR
PEBBL
CO
Bioturb
Comments
Interpretation Facies
3875
3880
3885
3890
3895
3900
3902
Clean sand (283)
Dunes
Clay bands (282)
Dune (279)
Loading (285)
More drapes (281)
Ripples (286)
The muddrapes are not broken (280)
Through this sand there is evidence of dunes every where
No core
MFS
(286)-Camera
Highly organic, coal
Cemented band (278)
Very highly bioturb
Highly bioturb
C4
M3
C3

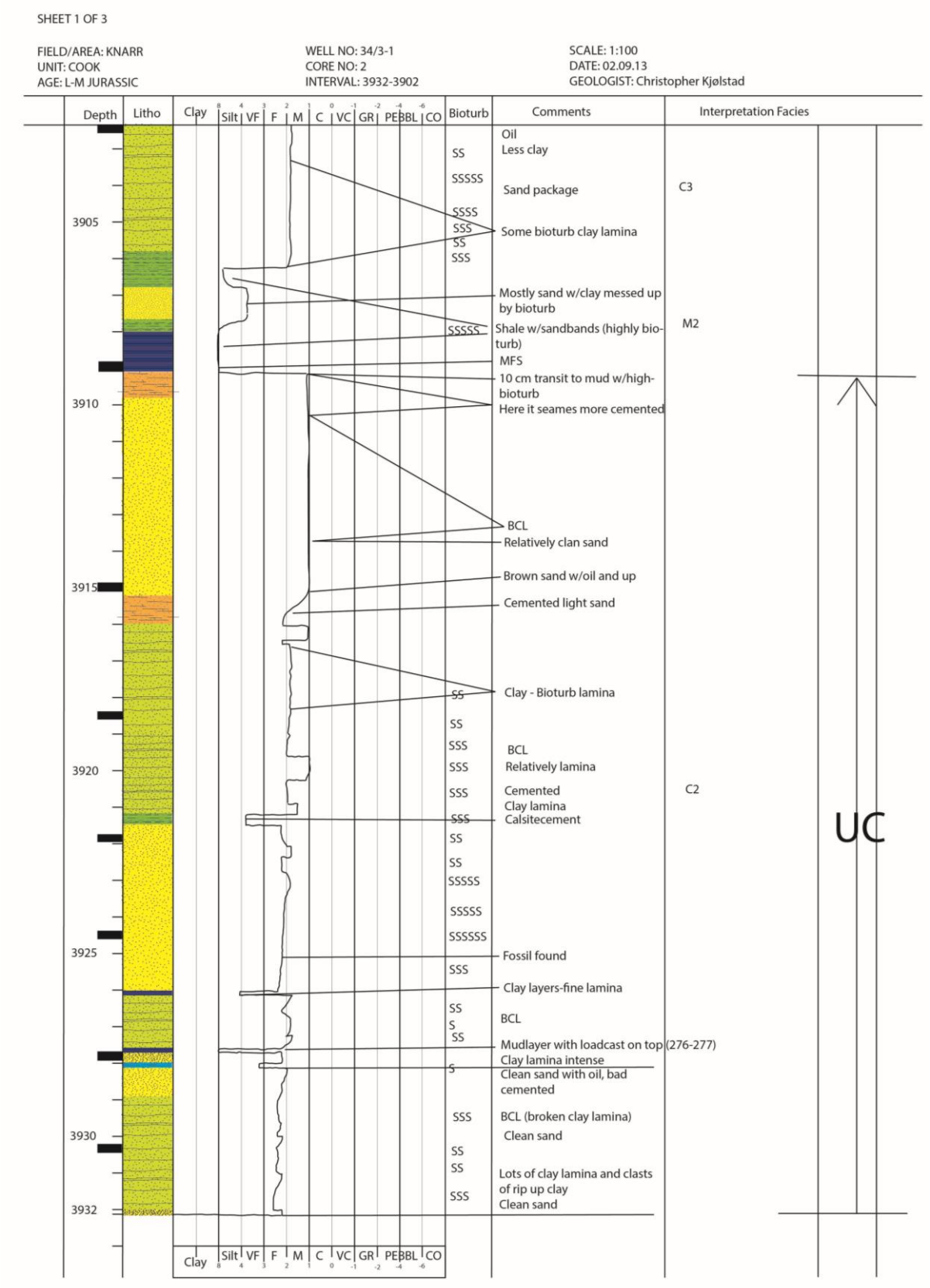
SHEET 1 OF 3
FIELD/AREA: KNARR
UNIT: COOK
AGE: L-M JURASSIC
WELL NO: 34/3-1
CORE NO: 2
INTERVAL: 3932-3902
SCALE: 1:100
DATE: 02.09.13
GEOLOGIST: Christopher Kjølstad
Depth
Litho
Clay
Silt
VF
F
M
C
VC
GR
PEBBL
CO
Bioturb
Comments
Interpretation Facies
3905
3910
3915
3920
3925
3930
3932
Oil
Less clay
Sand package
C3
Some bioturb clay lamina
Mostly sand w/clay messed up by bioturb
Shale w/sandbands (highly bio-turb)
M2
MFS
10 cm transit to mud w/high-bioturb
Here it seames more cemented
BCL
Relatively clan sand
Brown sand w/oil and up
Cemented light sand
Clay - Bioturb lamina
BCL
Relatively lamina
Cemented
Clay lamina
Calsitecement
C2
UC
Fossil found
Clay layers-fine lamina
BCL
Mudlayer with loadcast on top (276-277)
Clay lamina intense
Clean sand with oil, bad cemented
BCL (broken clay lamina)
Clean sand
Lots of clay lamina and clasts of rip up clay
Clean sand

Appendix

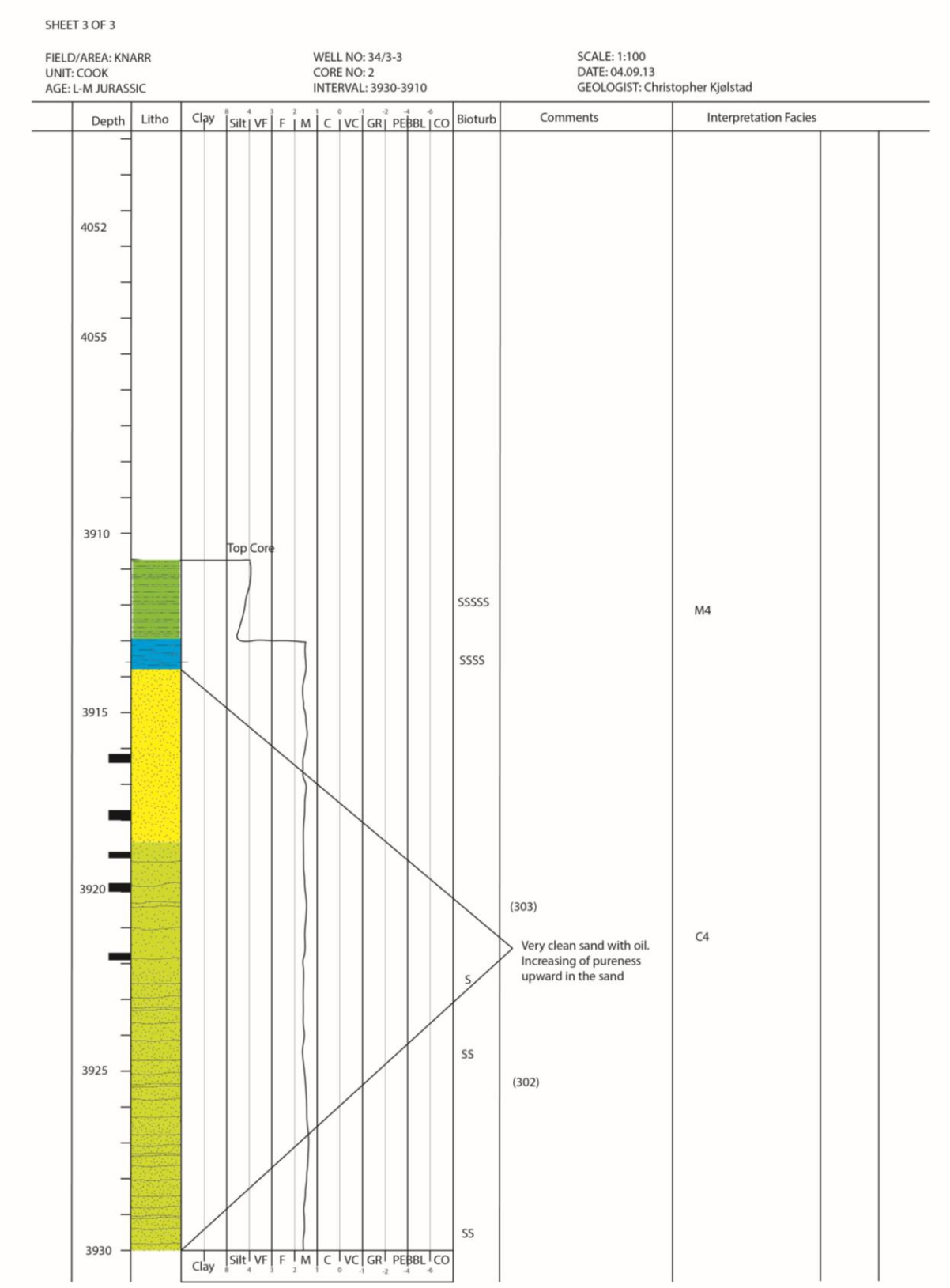
SHEET 3 OF 3
FIELD/AREA: KNARR
UNIT: COOK
AGE: L-M JURASSIC
WELL NO: 34/3-3
CORE NO: 2
INTERVAL: 3930-3910
SCALE: 1:100
DATE: 04.09.13
GEOLOGIST: Christopher Kjølstad
Depth
Litho
Clay
Silt
VF
F
M
C
VC
GR
PEBBL
CO
Bioturb
Comments
Interpretation Facies
4052
4055
3910
3915
3920
3925
3930
Top Core
SSSSS
SSSS
S
SS
SS
(303)
Very clean sand with oil.
Increasing of pureness
upward in the sand
(302)
M4
C4

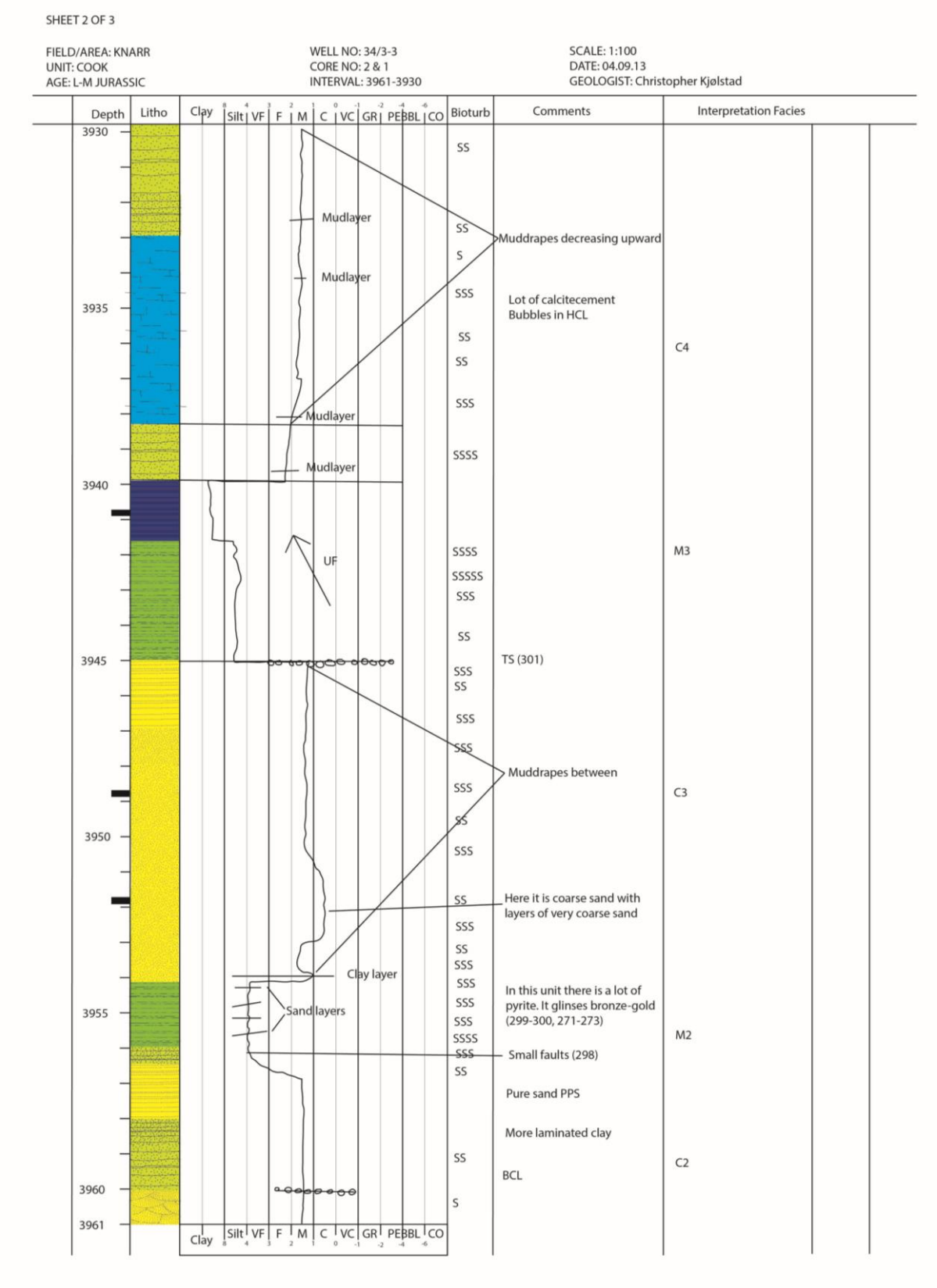
SHEET 2 OF 3
FIELD/AREA: KNARR
UNIT: COOK
AGE: L-M JURASSIC
WELL NO: 34/3-3
CORE NO: 2 & 1
INTERVAL: 3961-3930
SCALE: 1:100
DATE: 04.09.13
GEOLOGIST: Christopher Kjølstad
Depth
Litho
Clay
Silt
VF
F
M
C
VC
GR
PEBBL
CO
Bioturb
Comments
Interpretation Facies
3930
3935
3940
3945
3950
3955
3960
3961
Mudlayer
Mudlayer
Mudlayer
Mudlayer
UF
Clay layer
Sand layers
Muddrapes decreasing upward
Lot of calcitecement
Bubbles in HCL
TS (301)
Muddrapes between
Here it is coarse sand with
layers of very coarse sand
In this unit there is a lot of
pyrite. It glinses bronze-gold
(299-300, 271-273)
Small faults (298)
Pure sand PPS
More laminated clay
BCL
C4
M3
C3
M2
C2

Appendix

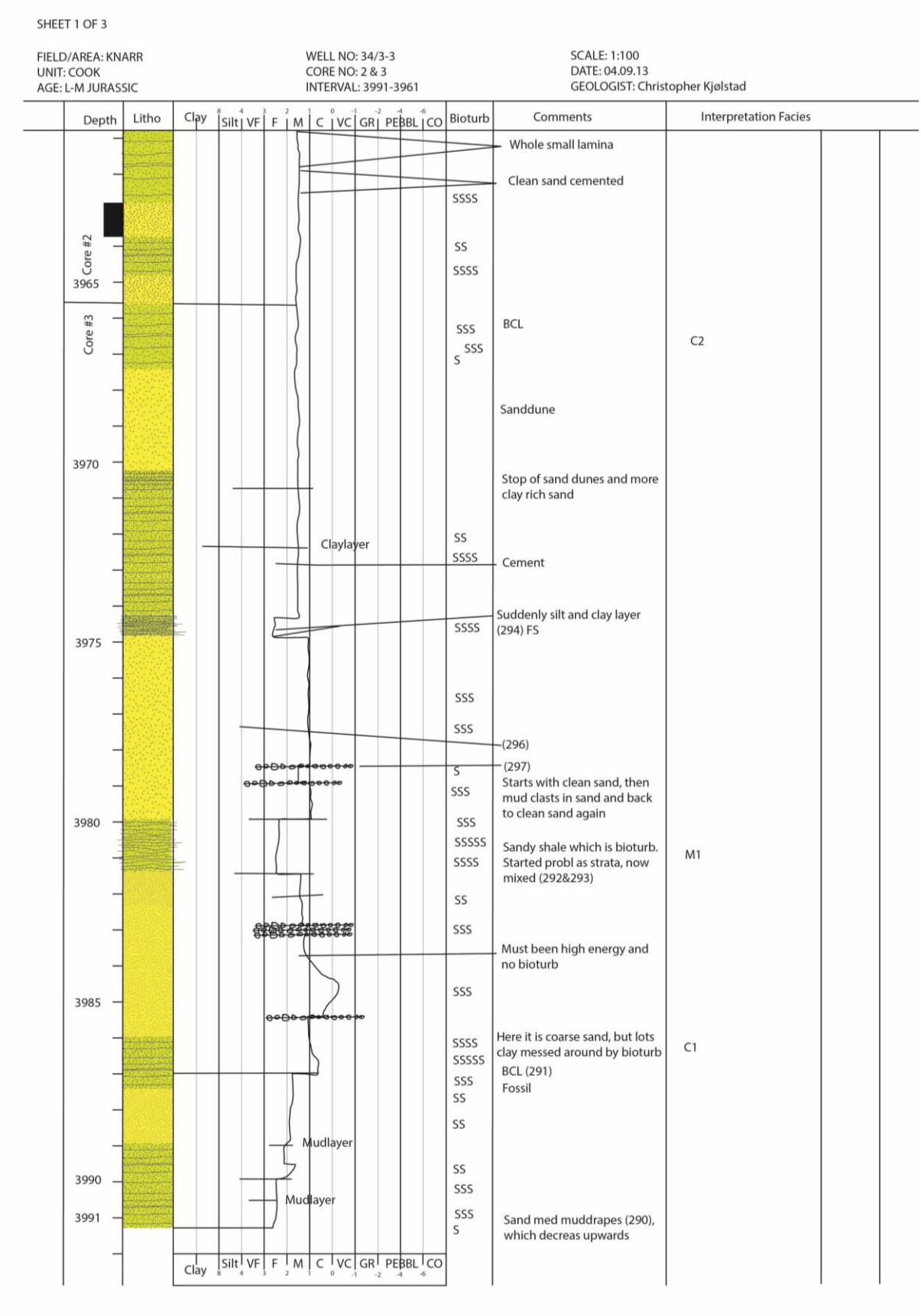
SHEET 1 OF 3
FIELD/AREA: KNARR
UNIT: COOK
AGE: L-M JURASSIC
WELL NO: 34/3-3
CORE NO: 2 & 3
INTERVAL: 3991-3961
SCALE: 1:100
DATE: 04.09.13
GEOLOGIST: Christopher Kjølstad
Depth
Litho
Clay
Silt
VF
F
M
C
VC
GR
PEBBL
CO
Bioturb
Comments
Interpretation Facies
Core #2
Core #3
3965
3970
3975
3980
3985
3990
3991
Whole small lamina
Clean sand cemented
BCL
Sanddune
Stop of sand dunes and more clay rich sand
Claylayer
Cement
Suddenly silt and clay layer (294) FS
(296)
(297)
Starts with clean sand, then mud clasts in sand and back to clean sand again
Sandy shale which is bioturb. Started probl as strata, now mixed (292&293)
Must been high energy and no bioturb
Here it is coarse sand, but lots clay messed around by bioturb
BCL (291)
Fossil
Mudlayer
Mudlayer
Sand med muddrapes (290), which decreas upwards
C2
M1
C1

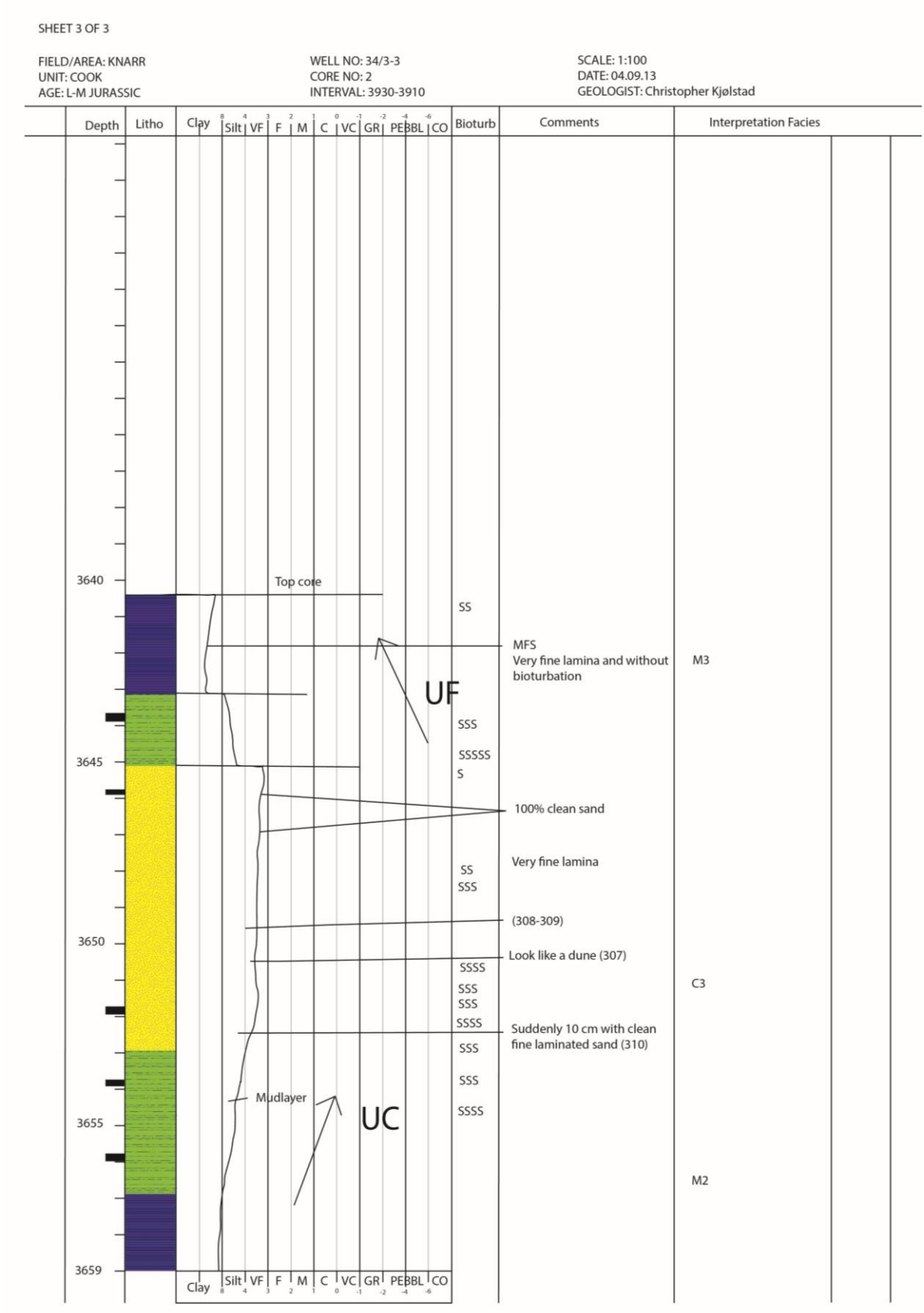
SHEET 3 OF 3
FIELD/AREA: KNARR
UNIT: COOK
AGE: L-M JURASSIC
WELL NO: 34/3-3
CORE NO: 2
INTERVAL: 3930-3910
SCALE: 1:100
DATE: 04.09.13
GEOLOGIST: Christopher Kjølstad
Depth
Litho
Clay
Silt
VF
F
M
C
VC
GR
PEBBL
CO
Bioturb
Comments
Interpretation Facies
3640
3645
3650
3655
3659
Top core
SS
MFS
Very fine lamina and without bioturbation
M3
UF
SSS
SSSSS
S
100% clean sand
Very fine lamina
SS
SSS
(308-309)
Look like a dune (307)
SSSS
SSS
C3
SSS
SSSS
Suddenly 10 cm with clean fine laminated sand (310)
SSS
SSS
Mudlayer
UC
SSSS
M2

Appendix

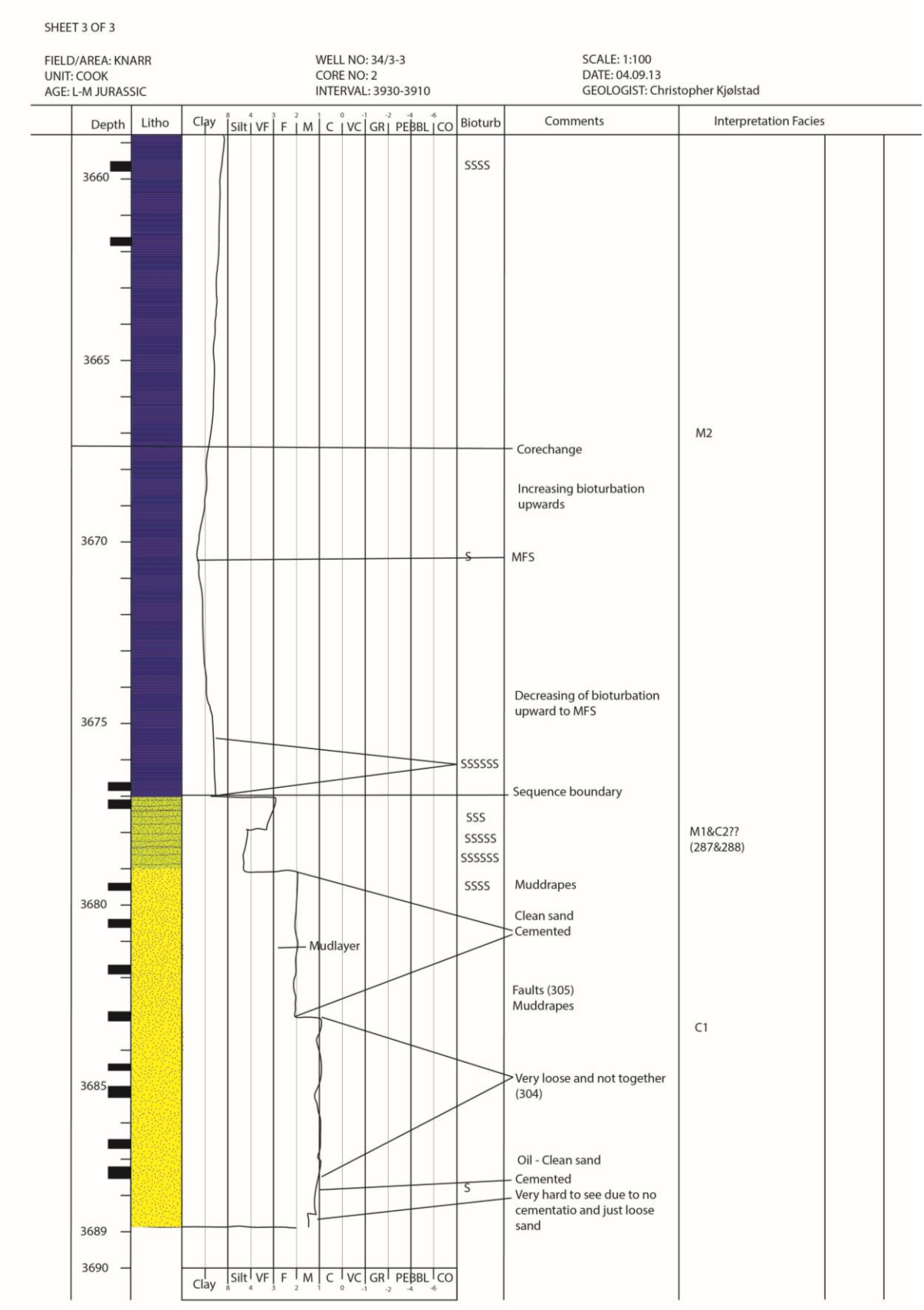
SHEET 3 OF 3
FIELD/AREA: KNARR
UNIT: COOK
AGE: L-M JURASSIC
WELL NO: 34/3-3
CORE NO: 2
INTERVAL: 3930-3910
SCALE: 1:100
DATE: 04.09.13
GEOLOGIST: Christopher Kjølstad
Depth
Litho
Clay
Silt
VF
F
M
C
VC
GR
PEBBL
CO
Bioturb
Comments
Interpretation Facies
3660
3665
3670
3675
3680
3685
3689
3690
SSSS
Corechange
M2
Increasing bioturbation upwards
S
MFS
Decreasing of bioturbation upward to MFS
SSSSSS
Sequence boundary
SSS
SSSSS
SSSSSS
M1&C2??
(287&288)
SSSS
Muddrapes
Clean sand
Cemented
Mudlayer
Faults (305)
Muddrapes
C1
Very loose and not together (304)
Oil - Clean sand
Cemented
S
Very hard to see due to no cementatio and just loose sand

# *Appendix VI*

## Values of point counting

| Sands | 34-3-3 | 34-3-3 | Qz_Detrial | Q_Cement | K-feldspar | Porosity | Kaolinite | Illite | Mica | Rock fragment | Carbonate | Clay mix | Carbonat cement | Chl_coat | Tot prosent | IGV |
|---|---|---|---|---|---|---|---|---|---|---|---|---|---|---|---|---|
| C4 | 3921,12 | 3455,25 | 45,7 | 0,0 | 11,6 | 14,1 | 10,0 | 2,5 | 2,8 | 0,9 | 2,5 | 4,3 | 0,0 | 5,6 | 100,0 | 36,5 |
| C4 | 3925,12 | 3459,15 | 45,4 | 0,9 | 10,9 | 14,6 | 1,2 | 0,0 | 6,5 | 2,5 | 2,5 | 9,6 | 0,0 | 5,9 | 100,0 | 32,3 |
| C4 | 3929,12 | 3463,10 | 40,3 | 0,0 | 8,0 | 1,7 | 0,7 | 0,0 | 5,3 | 0,0 | 7,0 | 15,3 | 21,7 | 0,0 | 100,0 | 39,3 |
| C4 | 3933,12 | 3467,00 | 58,7 | 0,0 | 9,7 | 6,0 | 0,0 | 0,0 | 7,7 | 0,7 | 1,3 | 9,7 | 3,0 | 3,3 | 100,0 | 22,0 |
| C3 | 3946,06 | 3479,65 | 48,3 | 0,0 | 15,7 | 12,3 | 0,0 | 0,0 | 4,0 | 0,3 | 0,7 | 5,0 | 1,3 | 12,3 | 100,0 | 31,0 |
| C3 | 3949,06 | 3482,60 | 50,7 | 0,0 | 13,7 | 12,3 | 0,0 | 0,7 | 4,0 | 0,0 | 0,7 | 6,0 | 0,7 | 11,3 | 100,0 | 31,0 |
| C3 | 3952,06 | 3485,55 | 46,0 | 0,0 | 8,1 | 12,1 | 0,0 | 0,0 | 2,0 | 6,9 | 3,2 | 9,8 | 0,0 | 11,9 | 100,0 | 33,8 |
| C2 | 3975,06 | 3508,05 | 53,4 | 0,0 | 6,7 | 11,4 | 0,0 | 4,2 | 1,4 | 1,1 | 1,4 | 4,9 | 0,0 | 15,6 | 100,0 | 36,0 |
| C1 | 3984,06 | 3516,90 | 50,3 | 0,3 | 7,7 | 9,3 | 0,0 | 0,0 | 3,0 | 0,0 | 0,7 | 18,3 | 0,0 | 10,3 | 100,0 | 38,3 |

| Sands | 34-5-1 | 34-5-1 | Qz_Detrial | Q_Cement | K-feldspar | Porosity | Kaolinite | Illite | Mica | Rock fragment | Carbonate | Clay mix | Carbonat cement | Chl_coat | Tot prosent | IGV |
|---|---|---|---|---|---|---|---|---|---|---|---|---|---|---|---|---|
| C4 | 3638,00 | 3067,10 | 41,9 | 2,7 | 5,0 | 0,7 | 0,3 | 4,3 | 14,0 | 0,0 | 3,7 | 27,2 | 0,3 | 0,0 | 100,0 | 35,5 |
| C4 | 3640,00 | 3069,05 | 36,9 | 1,0 | 2,3 | 0,0 | 0,3 | 3,0 | 19,6 | 0,0 | 5,0 | 31,2 | 0,7 | 0,0 | 100,0 | 36,2 |
| C3 | 3645,75 | 3074,65 | 55,0 | 0,0 | 4,0 | 20,0 | 0,0 | 0,0 | 5,3 | 0,0 | 2,0 | 11,3 | 0,3 | 2,0 | 100,0 | 33,7 |
| C3 | 3646,50 | 3075,35 | 32,3 | 0,0 | 9,7 | 0,7 | 0,0 | 0,0 | 17,7 | 0,0 | 7,3 | 11,7 | 20,7 | 0,0 | 100,0 | 33,0 |
| C3 | 3649,25 | 3078,00 | 53,0 | 0,0 | 8,0 | 12,0 | 1,0 | 0,0 | 11,3 | 0,0 | 1,7 | 12,0 | 0,3 | 0,7 | 100,0 | 26,0 |
| C3 | 3650,25 | 3079,00 | 54,3 | 0,0 | 6,7 | 14,7 | 0,7 | 0,0 | 7,0 | 0,0 | 1,7 | 14,0 | 1,0 | 0,0 | 100,0 | 30,3 |
| C1 | 3677,73 | 3105,60 | 45,5 | 1,0 | 3,9 | 2,9 | 6,4 | 0,0 | 16,1 | 0,0 | 7,4 | 2,3 | 11,6 | 2,9 | 100,0 | 27,1 |
| C1 | 3678,50 | 3106,30 | 36,3 | 0,0 | 12,7 | 2,0 | 1,7 | 0,0 | 8,0 | 0,0 | 0,7 | 38,7 | 0,0 | 0,0 | 100,0 | 42,3 |
| C1 | 3679,25 | 3107,05 | 30,2 | 0,0 | 4,7 | 5,3 | 17,9 | 6,6 | 12,6 | 3,7 | 2,7 | 15,0 | 1,3 | 0,0 | 100,0 | 46,2 |
| C1 | 3684,90 | 3112,50 | 58,7 | 0,3 | 6,9 | 9,9 | 3,3 | 1,2 | 2,4 | 3,0 | 1,5 | 3,3 | 0,0 | 9,6 | 100,0 | 27,5 |
| C1 | 3686,32 | 3114,90 | 44,7 | 0,0 | 15,3 | 13,3 | 4,0 | 0,0 | 3,0 | 0,0 | 0,7 | 7,7 | 0,0 | 11,3 | 100,0 | 36,3 |
| C1 | 3688,50 | 3116,00 | 51,3 | 0,0 | 7,2 | 11,0 | 8,5 | 0,0 | 4,1 | 0,3 | 2,5 | 9,9 | 0,3 | 4,7 | 100,0 | 34,5 |

| Sands | 34-3-2 | 34-3-2 | Qz_Detrial | Q_Cement | K-feldspar | Porosity | Kaolinite | Illite | Mica | Rock fragment | Carbonate | Clay mix | Carbonat cement | Chl_coat | Tot prosent | IGV |
|---|---|---|---|---|---|---|---|---|---|---|---|---|---|---|---|---|
| C2 | 4053,00 | 3610,30 | 44,3 | 0,0 | 15,7 | 1,7 | 0,0 | 0,0 | 7,3 | 0,0 | 0,7 | 3,7 | 22,3 | 4,3 | 100,0 | 32,0 |
| C2 | 4053,75 | 3611,05 | 52,3 | 0,0 | 3,8 | 18,5 | 6,2 | 0,0 | 5,9 | 0,0 | 0,9 | 1,0 | 0,0 | 11,5 | 100,0 | 37,1 |
| C2 | 4057,75 | 3615,05 | 47,0 | 0,3 | 5,1 | 9,1 | 0,8 | 0,0 | 7,9 | 0,8 | 2,3 | 0,9 | 11,0 | 14,7 | 100,0 | 36,9 |
| C2 | 4059,50 | 3616,80 | 44,0 | 0,0 | 14,3 | 1,3 | 3,3 | 0,0 | 5,7 | 0,0 | 0,0 | 23,7 | 1,7 | 6,0 | 100,0 | 36,0 |
| C2 | 4061,75 | 3619,05 | 46,3 | 0,0 | 13,7 | 8,7 | 6,7 | 0,0 | 3,7 | 0,0 | 0,0 | 14,0 | 0,3 | 6,7 | 100,0 | 36,3 |
| C2 | 4069,25 | 3626,50 | 43,0 | 0,0 | 7,7 | 0,3 | 0,0 | 0,0 | 3,7 | 0,0 | 6,0 | 2,7 | 36,7 | 0,0 | 100,0 | 39,7 |
| C2 | 4071,00 | 3628,25 | 61,3 | 0,0 | 4,7 | 15,7 | 0,0 | 0,0 | 3,0 | 0,7 | 1,3 | 8,0 | 0,3 | 5,0 | 100,0 | 29,0 |
| C2 | 4073,25 | 3630,50 | 50,8 | 0,0 | 7,6 | 16,8 | 1,2 | 0,0 | 4,0 | 2,1 | 1,5 | 8,6 | 0,0 | 7,3 | 100,0 | 33,9 |
| C1 | 4079,50 | 3636,80 | 54,8 | 0,0 | 4,0 | 15,0 | 0,3 | 0,0 | 2,8 | 1,4 | 2,0 | 4,9 | 0,9 | 13,9 | 100,0 | 35,0 |
| C1 | 4086,00 | 3643,30 | 51,7 | 0,0 | 5,3 | 0,7 | 0,0 | 0,0 | 3,7 | 0,0 | 1,3 | 32,7 | 0,7 | 4,0 | 100,0 | 38,0 |

# Appendix

| Sands | 34-3-1 | 34-3-1 | Qz_Detrial | Q_Cement | K-feldspar | Porosity | Kaolinite | Illite | Mica | Rock fragment | Carbonate | Clay mix | Carbonat cement | Chl_coat | Tot prosent | IGV |
|---|---|---|---|---|---|---|---|---|---|---|---|---|---|---|---|---|
| C5 | 3868,79 | 3322,80 | 45,8 | 1,7 | 8,3 | 2,3 | 6,3 | 2,7 | 10,0 | 0,0 | 15,9 | 7,0 | 0,0 | 0,0 | 100,0 | 19,9 |
| C5 | 3868,87 | 3322,90 | 45,5 | 3,0 | 4,3 | 4,7 | 5,6 | 1,7 | 6,3 | 0,0 | 20,3 | 8,6 | 0,0 | 0,0 | 100,0 | 23,6 |
| C5 | 3870,35 | 3324,20 | 34,0 | 0,0 | 6,0 | 0,0 | 0,0 | 0,0 | 7,7 | 0,0 | 1,3 | 1,0 | 50,0 | 0,0 | 100,0 | 51,0 |
| C4 | 3873,30 | 3326,90 | 65,8 | 0,7 | 3,0 | 12,0 | 6,0 | 0,0 | 2,0 | 0,0 | 4,0 | 4,7 | 2,0 | 0,0 | 100,0 | 25,2 |
| C4 | 3874,18 | 3327,70 | 42,3 | 4,3 | 14,3 | 7,7 | 0,3 | 0,3 | 1,3 | 0,3 | 0,0 | 14,7 | 14,3 | 0,0 | 100,0 | 41,7 |
| C4 | 3880,56 | 3333,50 | 59,1 | 1,0 | 7,6 | 9,0 | 3,3 | 1,0 | 4,0 | 0,0 | 2,7 | 1,7 | 10,6 | 0,0 | 100,0 | 26,6 |
| C4 | 3885,70 | 3338,20 | 59,5 | 2,0 | 0,7 | 17,9 | 2,7 | 2,3 | 3,7 | 0,3 | 3,0 | 3,3 | 4,7 | 0,0 | 100,0 | 32,9 |
| C4 | 3886,27 | 3338,70 | 38,0 | 0,0 | 12,3 | 0,0 | 0,3 | 0,0 | 2,7 | 0,0 | 0,0 | 1,7 | 45,0 | 0,0 | 100,0 | 47,0 |
| C4 | 3887,35 | 3339,70 | 50,8 | 3,3 | 1,7 | 11,0 | 4,0 | 4,7 | 8,3 | 0,0 | 2,3 | 9,3 | 4,7 | 0,0 | 100,0 | 36,9 |
| C3 | 3899,97 | 3351,31 | 50,8 | 0,7 | 11,0 | 19,6 | 5,0 | 0,0 | 5,6 | 1,0 | 1,7 | 3,7 | 1,0 | 0,0 | 100,0 | 29,9 |
| C3 | 3900,01 | 3351,33 | 50,2 | 0,0 | 11,3 | 19,6 | 3,0 | 0,0 | 5,3 | 0,0 | 4,7 | 4,3 | 1,7 | 0,0 | 100,0 | 28,6 |
| C3 | 3901,13 | 3352,35 | 52,8 | 0,7 | 1,3 | 12,6 | 3,7 | 7,0 | 5,6 | 0,0 | 7,3 | 7,0 | 2,0 | 0,0 | 100,0 | 32,9 |
| C2 | 3915,60 | 3365,65 | 39,0 | 0,0 | 11,3 | 2,7 | 1,0 | 0,0 | 4,0 | 0,0 | 1,0 | 7,7 | 33,3 | 0,0 | 100,0 | 44,7 |
| C2 | 3927,81 | 3376,85 | 47,2 | 0,3 | 12,0 | 19,3 | 7,0 | 0,0 | 2,0 | 0,0 | 1,7 | 5,0 | 5,6 | 0,0 | 100,0 | 37,2 |